Radio galaxies and feedback from AGN jets

M.J. Hardcastle[1] and J.H. Croston[2]

[1]*Centre for Astrophysics Research, University of Hertfordshire, College Lane, Hatfield AL10 9AB*
[2]*School of Physical Sciences, The Open University, Walton Hall, Milton Keynes, MK7 6AA, UK*

Abstract

We review current understanding of the population of radio galaxies and radio-loud quasars from an observational perspective, focusing on their large-scale structures and dynamics. We discuss the physical conditions in radio galaxies, their fuelling and accretion modes, host galaxies and large-scale environments, and the role(s) they play as engines of feedback in the process of galaxy evolution. Finally we briefly summarise other astrophysical uses of radio galaxy populations, including the study of cosmic magnetism and cosmological applications, and discuss future prospects for advancing our understanding of the physics and feedback behaviour of radio galaxies.

Keywords:

1. Introduction

Radio galaxies and radio-loud quasars (collectively radio-loud AGN, or RLAGN in this article) are active galaxies characterized by radio emission driven by jets on scales from pc to Mpc. The characteristic radio emission is synchrotron emission: that is, it indicates the presence of magnetic fields and highly relativistic electrons and/or positrons. Synchrotron emission may be seen in other wavebands, and this enabled the detection of the first radio galaxy jet before the advent of radio astronomy (Curtis, 1918) but it was only with the capabilities of radio interferometry (Ryle, 1952) that it became possible to detect and image these objects in detail and in large numbers. As we will discuss in more detail below, radio observations remain key to an understanding of their origin, dynamics and energetics.

Radio images of some characteristic large-angular-scale nearby RLAGN are shown in Fig. 1. These show the large-scale jets and lobes that are the defining feature of this type of object. The first observations capable of showing the radio jets (e.g., Northover, 1973) motivated the development of the now standard 'beam model', in which collimated outflows from the active nucleus drive the extended structures (Longair et al., 1973; Scheuer, 1974; Blandford and Rees, 1974). Some authors have used 'beam' to refer to the outflows themselves and 'jet' to refer to their observational manifestations, but in this review we use 'jet' interchangeably for both, relying on context to make the distinction clear where it is needed.

Key historical developments in observational RLAGN studies after the first surveys and optical identifications included the development in the 1970s of high-resolution interferometers such as the 5-km telescope and the NRAO Very Large Array (VLA), which allowed detailed study of radio structures as well as optical identifications for the first time; progress in very long baseline interferometry (VLBI), which has given increasingly detailed views of the inner parts of the jets; the advent of sensitive optical telescopes, including the *Hubble Space Telescope*, which allowed detailed studies of RLAGN host galaxies and environments in the optical, as well as the study of optical synchrotron radiation; a greatly improved understanding of the nature of the active nuclei themselves, driven by a combination of broad-band photometry and spectroscopy; and the development of X-ray telescopes with the sensitivity needed to image both the hot gas environments of RLAGN and the X-ray synchrotron and inverse-Compton emission from the large-scale radio structures. Some of the understanding derived from those observational advances is discussed in later sections of this review. However, perhaps the most important development has been the realization that the energetic input of RLAGN can have a profound effect on both the galaxies that they inhabit and their large-scale environment, heating the hot gas that surrounds them and preventing it from cooling and forming stars; this process is an important member of a family of processes that have come to be called 'AGN
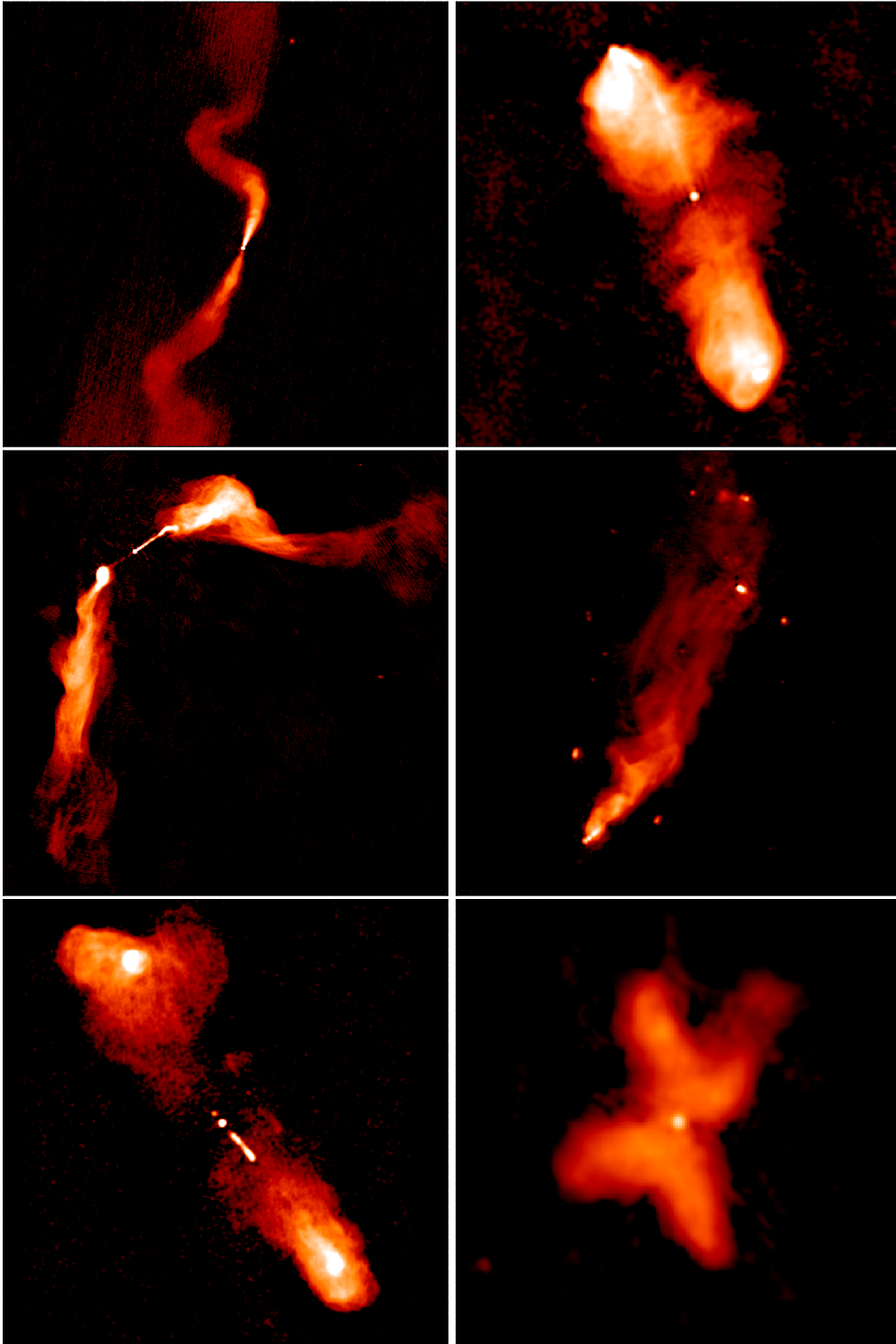
Figure 1: Radio images of nearby radio galaxies showing a range of morphologies: top row are the Fanaroff-Riley class I source 3C 31 (left) and the Fanaroff-Riley class II source 3C 98; middle row are the wide-angle tail source 3C 465 (left) and narrow-angle tail / head-tail source NGC 6109 (right); and bottom row are double-double radio galaxy 3C 219 (left), and core-restarting radio galaxy 3C 315 (right). Compact 'cores' may be seen in all images, well-collimated jets are visible in 3C 31, 3C 98 and 3C 465, and hotspots in 3C 98, 3C 465 and 3C 219. 3C 31 image kindly provided by Robert Laing; 3C 98 image from the online 'Atlas of DRAGNS' at http://www.jb.man.ac.uk/atlas/; 3C 465 image courtesy of Emmanuel Bempong-Manful; 3C 219 image from Clarke et al. (1992); NGC 6109 and 3C 315 from unpublished LOFAR data.

feedback'. This understanding of the importance of RLAGN in galaxy formation and evolution, derived both from X-ray observations and from numerical modelling of the formation and evolution of galaxies, has moved RLAGN studies into the mainstream of extragalactic astrophysics. In this chapter we will therefore also discuss how observations and models of RLAGN constrain the 'feedback' processes that may be operating.

Throughout the review we adopt the convention that γ represents the (random) Lorentz factor of an individual electron and Γ represents the bulk Lorentz factor due to directed motion. Luminosities and physical sizes quoted are based on a standard concordance cosmology with $H_0 = 70$ km s^{-1} Mpc^{-1}.

2. Observational approaches

In this section we provide an overview of the observational methods that provide us with constraints on radio galaxy physics.

2.1. Radio

The fact that the radio emission is synchrotron emission was realised early on from its polarization and spectrum (Baade, 1956; Burbidge, 1956) and, together with the optical identification of these objects with relatively distant galaxies (see Section 2.2), turned out to imply very large energies stored in the extended structures. The details of the radiation mechanisms can be found in e.g., Longair (2010) or Rybicki and Lightman (1979). The point that we wish to emphasise here is that the energy density in the radiating electrons and field, U, can be written in terms of the volume emissivity $J(\nu)$ and the magnetic field strength B: for a power-law distribution of electron energies with energy index p, we find

$$U = kJ(\nu)B^{-\frac{p+1}{2}} + \frac{B^2}{2\mu_0} \qquad (1)$$

where k is a constant incorporating physical constants, the observing frequency, and the integral over electron energies. Clearly eq. 1 has a *minimum* at some value of B, and by solving for the minimum and computing the minimum energy density, we can get both an estimate of a characteristic field strength and a lower limit on the energy responsible for a given region of a radio source. The minimum-energy condition turns out to be close to the *equipartition* energy, $U_e = U_B$, but the important conclusion is that the minimum-energy field strengths for 100-kpc-scale lobes such as those shown

in Fig. 1 are of order 1 nT for a powerful source, leading to energy densities of order a few $\times 10^{-13}$ J m^{-1} and total energies of order 10^{54} J or more — which would require the direct conversion to energy of millions of solar masses of matter. If there is any departure from the minimum-energy assumptions, these numbers will be larger — and possibly very much larger if, e.g., there are large departures from equipartition or if the energy density in the lobes is dominated by non-radiating particles.

It can be seen that estimates of the energetics of the radio-emitting structures depend strongly on the characteristic magnetic field strength. This cannot be estimated directly from observations of synchrotron intensity. Synchrotron emission is strongly polarized — the fractional polarization can be $\sim 70\%$ for a uniform-field region with a power-law spectrum, and even higher where the spectrum is exponentially cutting off — but the polarization does not tell us about the field strength either, although it does give an emission-weighted estimate of the magnetic field *direction* along a particular line of sight, if Faraday rotation effects may be neglected (see below). For optically thin radio emission, the only way of directly estimating the magnetic field strength is to use additional observations, for example observations of inverse-Compton emission, discussed below (Section 2.4).

Faraday rotation is an effect caused by the propagation of electromagnetic radiation through a magnetised, ionized medium. The polarization angle rotates due to a difference in propagation speed for the two circularly polarized components of the electromagnetic wave. The change in angle is dependent on frequency, and the rotation measure — the strength of the rotation effect — depends on the magnetic field strength and electron density of the intervening material (e.g. Cioffi and Jones, 1980). For a single line of sight through a Faraday-active medium towards a background polarized source the measured polarization angle χ is given by (Burn, 1966):

$$\chi = \chi_0 + \phi\lambda^2 \qquad (2)$$

where χ_0 is the intrinsic polarization angle and ϕ is given by

$$\phi = K \int_0^d n_e \mathbf{B} \cdot d\mathbf{S} \qquad (3)$$

in which K is a constant with value (in SI units) 2.63×10^{-13} T^{-1}. Clearly in general different lines of sight, even within a given telescope beam, will have different values of ϕ. However, observationally, it is often the case that the rotation measure $RM = d\chi/d\lambda^2$ shows smooth behaviour across a source, and in this

case rotation measure observations can be used to estimate magnetic field strength *external* to the source along the line of sight in situations where the density of intervening plasma is known or can be estimated. Frequency-dependent depolarization also provides information about the magnetic field strength and/or the density of thermal plasma internal and external to the radio lobes (e.g. Burn, 1966; Laing, 1988), although disentengling the contributions of different components can be challenging.

Although RLAGN are now detected at many other wavebands, radio observations continue to provide the most efficient method of *selecting* them. Early surveys such as the 3C or Parkes surveys (Bennett, 1962; Bolton et al., 1964), and the optically identified catalogues derived from them (e.g., 3CRR, Laing et al., 1983), have been the background for many of the detailed studies of the physics of individual AGN or small samples. Because RLAGN are a comparatively rare population, wide sky areas are necessary to get a representative view of the local population, and so historically low-frequency radio telescopes, with their large fields of view but comparatively low sensitivity, were the survey instruments of choice. Low-frequency selection has the advantage that the low-frequency emission of RLAGN is dominated by the steep-spectrum emission from the lobes, presumed to be more or less isotropic. More recently surveys at GHz frequencies, especially with the Very Large Array (VLA), have been used to generate large samples. Wide-area surveys can be used to find many objects in the local universe (Best and Heckman, 2012) while deep surveys with a narrow field of view probe the RLAGN population at high redshift (e.g., Smolčić et al., 2017). In these sensitive surveys, separating the radio emission from RLAGN from that due to star formation in the host galaxy becomes a major concern. Forthcoming wide and/or deep surveys with LOFAR (Shimwell et al., 2017), ASKAP (Norris et al., 2011), and MeerKAT (Jarvis et al., 2016) will provide still larger samples of the AGN population without the limitations in *uv* plane coverage imposed by the design of the VLA.

Historically, RLAGN would be selected from a survey and then followed up with pointed radio observations for detailed study. Here, as with study at other wavebands, the very large range of angular scales spanned by RLAGN can be problematic. The closest radio galaxy, Centaurus A, has scales of interest ranging from tens of degrees to microarcseconds, and to study even a fraction of that range requires the combination of data from multiple telescopes (Feain et al., 2011). For objects at more typical distances the largest angular scales might be arcminutes, corresponding to hundreds of kpc to Mpc. A correspondingly large range of interferometer baselines is needed to study the whole radio structure.

Radio observations at GHz frequencies with sub-arcsecond to arcminute resolution, as provided by instruments such as the (Jansky) VLA, ATCA and e-MERLIN, typically correspond to scales of kpc to hundreds of kpc and are used to study the large-scale structures such as kpc-scale jets, lobes and hotspots, either in individual objects (e.g., Carilli et al., 1991; Laing and Bridle, 2002) or large samples (e.g., Black et al., 1992; Fernini et al., 1993; Bridle et al., 1994; Fernini et al., 1997; Leahy et al., 1997; Hardcastle et al., 1997; Gilbert et al., 2004; Mullin et al., 2006). The review of Bridle and Perley (1984) still provides a good summary of many of the early observational discoveries. Resolved broad-band spectral mapping gives (model-dependent) information about the age of the radio-emitting plasma, so-called 'spectral ageing' (Burch, 1977; Myers and Spangler, 1985; Alexander and Leahy, 1987; Harwood et al., 2013) based on the different radiation timescales for electrons of different energies (see Section 4.4, below). Polarization imaging at GHz frequencies tell us about the configuration of the magnetic fields in the large-scale lobes, jets and hotspots (Laing, 1980; Bridle and Perley, 1984; Laing, 1989; Hardcastle et al., 1998) but, because Faraday rotation effects become dominant at low frequencies, broad-band polarization studies can also tell us about the thermal material immediately around or even inside the lobes, both for individual sources or on a statistical basis (Dreher et al., 1987; Laing, 1988; Garrington et al., 1988; Taylor and Perley, 1993; Laing et al., 2008; Hardcastle et al., 2012; Anderson et al., 2018).

VLBI observations with milliarcsec resolution, corresponding to physical scales of pc, allow the study of the regions where the jets are formed and accelerated. Time-resolved studies of jet dynamics are generally only possible on these scales, and both studies of individual objects and systematic total intensity studies of large samples (Lister et al., 2016) provide our best constraints on bulk speeds of jets on these scales. Multi-frequency studies exploiting self-absorption at lower frequencies can probe magnetic field strengths (O'Sullivan and Gabuzda, 2009) while polarization studies constrain the magnetic field configuration in the jets (Gabuzda et al., 2004).

A good deal of work has been done on the 21-cm line of neutral hydrogen, either in emission or in absorption against the synchrotron continuum, in the host galaxies of RLAGN. A key result is that a number of RLAGN

show outflowing neutral hydrogen, presumably associated with the interaction between the jets/lobes and their environment, as well as having small-scale nuclear HI components plausibly associated with the fuel supply. See Morganti and Oosterloo (2018) for a recent review.

2.2. Optical/IR

Matching a radio source with an optical counterpart, known as optical identification, is crucial to any kind of physical interpretation. The identification of powerful radio sources such as Cygnus A, M87 and Centaurus A with peculiar galaxies by Baade and Minkowski (1954a,b) marked the beginning of the study of the physics of these objects, leading, as already noted, directly to an understanding of the large energies involved, and thence, through the discovery of quasars (Schmidt, 1963) to the idea that RLAGN must be powered by accretion onto supermassive galactic-centre black holes (Lynden-Bell, 1969).

Optical identification requires the combination of a good radio image (with resolution sufficient to distinguish between different possible optical counterparts) and a good optical image, and so it has always been a significant limitation on the exploitation of radio surveys — the final optical identification of the 3CRR sample, for example, came in 1996 (Rawlings et al., 1996), decades after the initial radio observations. Deep optical images are required to find the counterparts of high-redshift radio sources, and these are not easily available over wide sky areas. This continues to be an issue for current and next-generation sky surveys, mitigated to some extent by the fact that the more recent surveys are carried out at an angular resolution that allows optical identification without requiring followup radio observations.

Optical counterparts ('host galaxies') of RLAGN have a number of interesting properties. An important minority are quasars: in other words, we have a direct view of radiatively efficient nuclear accretion. Almost all the rest are early-type galaxies, implying a relationship between RLAGN activity and the most massive systems; but of those galaxies some, particularly those associated with the most powerful radio galaxies, are peculiar, showing strong narrow emission lines similar to those of Seyfert 2 galaxies in optical spectra. The interpretation of these peculiarities as due to galaxy collision dates back to the earliest optical identifications (Baade and Minkowski, 1954a), and indeed for these powerful objects there is a higher than average fraction of disturbed or merger-like hosts (Heckman et al., 1986; Ramos Almeida et al., 2012). However, other radio galaxy hosts show no evidence of peculiarities that

cannot be attributed to the jet. We will return to the implications of these observations for accretion in Section 6.3, while the relationship between radio properties, stellar mass and star formation will be discussed in more detail in Section 7.

Optical observations are important in a number of other areas. Optical synchrotron emission can be identified readily by its polarization, and it was in fact optical polarimetry that provided early confirmation of the synchrotron nature of the continuum radiation from RLAGN (Baade, 1956), though radio polarimetry soon followed. The realization that optically-emitting electrons had short lifetimes, necessitating continuous energy supply, was influential in the development of jet models for RLAGN. Optical observations of extended emission-line nebulae around the radio lobes provided early evidence for the impact of the RLAGN on their environments, e.g., McCarthy et al. (1987); O'Dea et al. (2002). Optical studies also provide constraints on the environments of RLAGN — see Section 7.

2.3. mm/sub-mm/FIR

RLAGN synchrotron emission persists through to frequencies of 100 GHz and above and shows little difference from what is seen at lower radio frequencies (e.g., Hardcastle and Looney, 2008). The sub-mm region is important for studies of molecular gas in radio-galaxy environments, fuelling and the interaction of jets with this material. Sub-mm observations demonstrate the presence of molecular gas in the hosts of many nearby radio galaxies (e.g. Prandoni et al., 2010; Hamer et al., 2014; Rose et al., 2019; North et al., 2019; Ruffa et al., 2019). In some cases the molecular gas appears mainly located in a rotating disk, while in other cases it may be infalling. As with the neutral hydrogen discussed above, there is also strong evidence in some cases that the molecular material is influenced by the radio lobes (e.g., Russell et al., 2017; Tremblay et al., 2018). These observations are discussed further in Section 8. Far-IR observations, probing the component of dust heated by star formation rather than the AGN, have shown that nearby normal AGN tend to have low star formation rates, but the details depend on the type of galaxy (e.g., Hardcastle et al., 2013) while individual RLAGN associated with very high dust luminosities and hence, presumably, star-formation rates have been discovered (e.g., Barthel et al., 2012; Seymour et al., 2012).

2.4. X-ray

X-ray observations provide information on the accretion state and obscuration of the active nucleus, the

large-scale components of the radio source (jets, lobes and hotspots) and the galaxy-to-cluster-scale hot-gas environment.

Radiatively efficient AGN are strong X-ray sources, and so in many quasars the X-ray emission is dominated by the active nucleus; however, at soft X-ray energies this emission is strongly suppressed by even moderate levels of obscuration, which has the useful effect that other components of RLAGN can be studied well at these energies. (We discuss nuclear X-ray emission further in Section 6.1.)

X-ray radiation from the jets, hotspots and lobes is non-thermal and gives us information about the particle populations responsible for the emission. A key emission mechanism in this band is inverse-Compton scattering, where the relativistic electrons responsible for the synchrotron emission also scatter a photon field to high energies. Possible photon fields include the CMB, which is always present, but also synchrotron photons ('synchrotron self-Compton'), starlight from the host galaxy, radiation from the central AGN itself, or the extragalactic background light. Where the X-ray emission mechanism is inverse-Compton scattering, as in the case of lobes (Croston et al., 2005) and some hotspots (Hardcastle et al., 2004), its luminosity depends on the photon field and on the number of relatively low-energy relativistic electrons ($\gamma \sim 1000$ for scattering of $z = 0$ CMB photons into the soft X-ray) and so it gives a good constraint on the electron energetics and therefore, indirectly, on magnetic field strengths and source dynamics (see Section 4). Where instead the non-thermal X-ray emission mechanism is synchrotron emission, as in other hotspots and the jets of low-luminosity sources (Hardcastle et al., 2001), it points to a very energetic population of electrons (dependent on assumed magnetic field strength, $\gamma \sim 10^8$ or more) which generally implies local (*in situ*) particle acceleration. The prominent jets seen in some high-luminosity objects, such as 3C 273 (Harris and Stern, 1987), PKS 0637−752 (Schwartz et al., 2000) or Pictor A (Wilson et al., 2001) are still the subject of debate; the original proposal that they represent inverse-Compton emission from the highly boosted CMB from jets with $\Gamma \sim 10$ (Tavecchio et al., 2000; Celotti et al., 2001), while attractive, has a number of problems (Stawarz et al., 2004; Hardcastle, 2006; Cara et al., 2013; Meyer et al., 2015) and it seems likely that at least some of these powerful jets have a synchrotron origin, with electron spectra extending through the optical emission region to the X-ray (Hardcastle et al., 2016). Jet X-ray properties are reviewed in much more detail by Worrall (2009).

The thermal X-ray radiation from the hot phase of the ambient medium of the RLAGN has been of huge importance to constraining dynamical models of these sources since its first discovery (Longair and Willmore, 1974; Hardcastle and Worrall, 2000b). More recently, sensitive X-ray imaging has revealed deficits of X-ray emission ('cavities') associated with the kpc-scale lobes of many RLAGN (e.g., Bîrzan et al., 2004), and also found a small number of unambiguous shock features, demonstrating supersonic bulk motion of the lobes through the medium (e.g., Kraft et al., 2003; Croston et al., 2009, 2011). The implications of these observations are discussed in Sections 4 and 5.

2.5. γ-ray

Most γ-ray-emitting RLAGN are blazars, discussed elsewhere in this volume; in these systems the nuclear γ rays are thought to be Doppler-boosted inverse-Compton scattering of either the synchrotron continuum itself or of other photon fields (radiation from the AGN or torus where present — see Section 6.1). The numbers of non-blazar or so-called misaligned RLAGN that are known GeV γ-ray emitters has greatly increased due to the sky survey of the *Fermi* satellite, and now stands at some tens of objects (Ackermann et al., 2015) including well-known nearby radio galaxies such as Cen A, M87, NGC 1275 and NGC 6251. Of particular interest are the detections of extended lobes in Cen A and Fornax A (Abdo et al., 2010; Ackermann et al., 2016). In a leptonic model for the γ-ray emission, this can constrain magnetic field strengths just as X-ray inverse-Compton emission can, but also demonstrates the presence of high-energy electrons in the lobes. Only a small number of non-blazar RLAGN (6 at the time of writing: Rieger and Levinson 2018) are detected at TeV energies. These again include the nearest powerful radio galaxies, Cen A and M87. M87's TeV emission is highly variable at high energies on timescales of days, and appears to be associated with the sub-pc scale jet (Hada et al., 2015). By contrast, Cen A's emission seems steady over long time periods (H. E. S. S. Collaboration et al., 2018) and so an origin of part or all of it in the large-scale components of the source remain possible. Inverse-Compton scattering of starlight by the known population of TeV electrons that produce the X-ray jet is a required process; if this dominates at high energies then the forthcoming Cerenkov Telescope Array should able to resolve the jet in Cen A at TeV energies and permit the first direct magnetic field measurement in a low-power jet (Hardcastle and Croston, 2011).

3. Radio-galaxy populations

From the first double radio sources in the 3C catalogue to current low-frequency radio-galaxy samples, our understanding of the diversity of radio-galaxy populations has evolved dramatically over the last seventy years. In Fig. 2 we summarize the radio luminosity and size ranges spanned by particular sub-populations of RLAGN, as discussed in this Section. We note that the samples plotted in this 'P-D' diagram are all subject to a range of selection effects, so that gaps between sub-categories do not indicate sharp delineations between separate populations. The main conclusion to be drawn from Fig. 2 is that AGN-driven jet structures occur over a very wide span in radio luminosity (nearly ten orders of magnitude) and source size (six orders of magnitude).

In this section we discuss the main classes of radio galaxy that can be categorised primarily from radio observations. We make some reference to host-galaxy and multi-wavelength properties in this section, but we defer full discussion of these topics, and of classification based on nuclear properties, to later sections. We also defer discussion of the cosmic evolution of RLAGN populations to Section 7.

3.1. The Fanaroff-Riley dichotomy

The Fanaroff-Riley (Fanaroff and Riley, 1974) morphological distinction between centre-brightened and edge-brightened radio galaxies (e.g. Fig. 1), found to be linked to radio luminosity, has since been widely adopted and applied to many radio catalogues in the past four decades. While there remains debate about the link between accretion mode and jet morphology (e.g., Best and Heckman, 2012; Gendre et al., 2013; Mingo et al., 2014; Ineson et al., 2015; Tadhunter, 2016; Hardcastle et al., 2007a, 2009; Hardcastle, 2018a, and see Section 6.1), the FR morphological divide is thought to be fundamentally linked to jet dynamics: the edge-brightened FRII radio galaxies are thought to have jets that remain relativistic throughout, terminating in a hotspot (internal shock), while the centre-brightened FRIs are known to have initially relativistic jets that decelerate on kpc scales (e.g., Bicknell, 1995; Laing and Bridle, 2002; Tchekhovskoy and Bromberg, 2016). This structural difference must necessarily result not purely from properties of the central engine, but rather from the interplay of jet power and environmental density, so that jets of the same power might in a poor (host-scale) environment remain relativistic and well-collimated, but in a richer environment decelerate, entrain ISM gas, and expand to form turbulent FRI plumes. Such an explanation seemed to find support in the discovery by Ledlow and Owen (1996) that the FRI/II luminosity break is dependent on host-galaxy magnitude, so that FRIs are found to have higher radio luminosities in brighter host galaxies (where the density of the interstellar medium is assumed to be higher). However, this result was based on strongly flux-limited samples, with different redshift distributions and environments for the FRIs and FRIIs, and so serious selection effects mean that there is now some uncertainty as to whether this relation in fact holds across the full population of radio galaxies (Best, 2009; Lin et al., 2010; Wing and Blanton, 2011; Singal and Rajpurohit, 2014; Capetti et al., 2017; Shabala, 2018).

As radio surveys have reached lower flux limits, evidence has also emerged that the FR morphological division is less closely tied to radio luminosity than was previously thought, with the emergence of an unexpected population of low-luminosity sources with edge-brightened FRII morphology (Best, 2009; Miraghaei and Best, 2017; Capetti et al., 2017; Mingo et al., 2019). Using a large sample from the LOFAR Two-Metre Sky Survey (LoTSS), Mingo et al. (2019) have shown that these 'FRII-low' radio galaxies form a substantial fraction of the FRIIs at $z < 0.8$ (see also Fig. 2). This population was absent from early studies as they are rare in the very local Universe, and hence have fluxes below the limits of early surveys such as 3CRR (Mingo et al., 2019). The substantial overlap in luminosity range for FRIs and FRIIs found in modern samples does not necessarily break the jet disruption paradigm for the morphological distinction. Firstly, the conversion from jet power to radio luminosity has very large scatter and systematic biases, as discussed in Section 4.5 (Hardcastle, 2018b; Croston et al., 2018). Secondly, there does appear to be a link between morphology and host brightness (Mingo et al., 2019) so that the low-luminosity FRIIs may occupy particularly poor local environments, consistent with their remaining undisrupted despite their (presumably) comparatively low jet power.

3.2. Blazars

Blazars are a sub-category of radio-loud AGN with distinct properties, including bright variable emission at a range of wavelengths, thought to reflect relativistic effects in a jet oriented at a small angle to the line of sight. Blazars show a diverse range of radio structures (e.g., Rector and Stocke, 2001; Giroletti et al., 2004). It is thought that sub-classes of blazars can be unified with radio galaxies and quasars, with apparent difference in properties explained by orientation effects (Section 6.1). We do not discuss blazars or the consequences of their properties for source models in detail in this work, deferring to the dedicated Chapter in this volume.
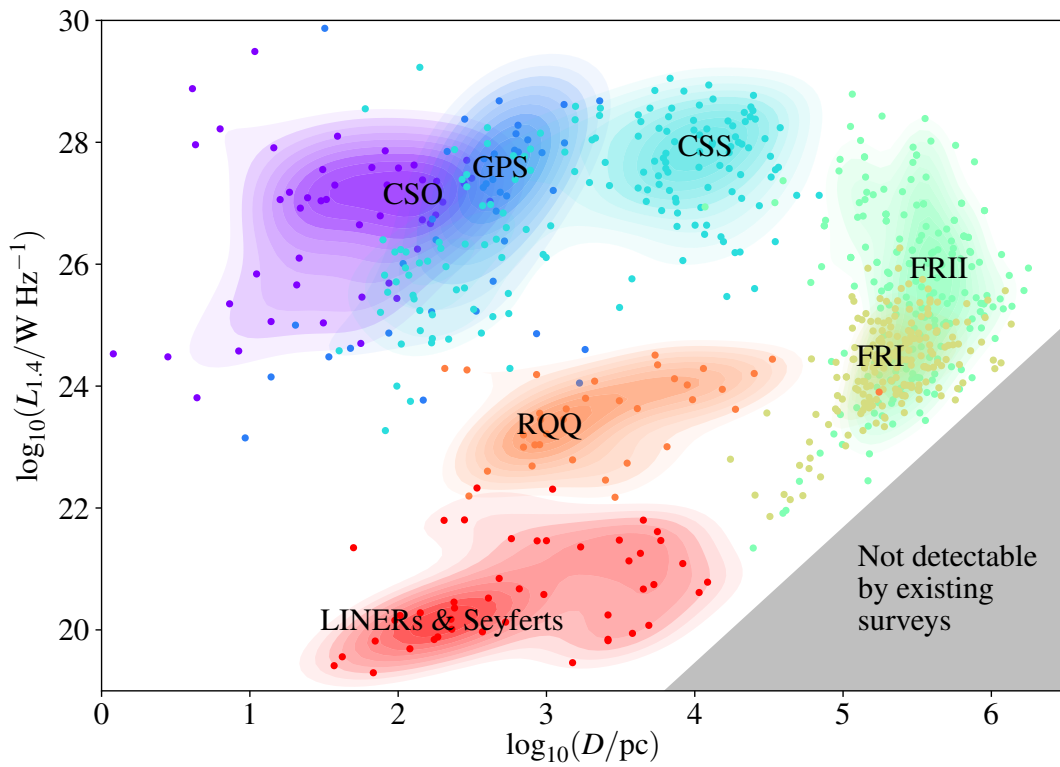
Figure 2: Power/linear-size plot (Baldwin, 1982) for different types of radio-loud and radio-quiet AGN, adapted from plots presented by An and Baan (2012) and Jarvis et al. (2019). Points show individual objects and coloured contours represent a smoothed estimator of source density. The different categories of source shown are: CSO, GPS, CSS, all objects so classed by An and Baan; FRI, FRII, all objects so classed by either An and Baan or Mingo et al. (2019) (points are representative); RQQ, objects from Jarvis et al. (2019) and Kukula et al. (1998); Seyferts and LINERS, objects from Gallimore et al. (2006); and Baldi et al. (2018a). The shaded bottom-right corner shows the effect of surface-brightness limitations.

3.3. Cluster radio-galaxy populations

The large-scale environments of radio galaxies are discussed in Section 7. The majority of radio galaxies do not live in rich cluster environments; however, those radio galaxies that do inhabit the richest environments show a range of characteristic morphological features, likely to be caused by their dense surrounding medium (e.g., Owen and Ledlow, 1997).

While there are examples of cluster-centre radio galaxies with morphologies typical of the FRI or FRII class (e.g., Cygnus A), many cluster-centre radio galaxies, including the most famous cluster-centre radio galaxy Perseus A (3C 84), show amorphous radio structure with no evidence for collimated jets on scales of tens of kpc (e.g., Miley and Perola, 1975; Burns, 1990; Owen and Ledlow, 1997). Another radio-galaxy subpopulation that is strongly associated with galaxy clusters are the bent-tail sources, which can be further separated into the head-tail / narrow-angle (NAT) and wide-angle tail (WAT) sources (Owen and Rudnick, 1976; O'Dea and Owen, 1985). The bent jets and plumes/tails of these sources are thought to be left behind as the host galaxy moves with respect to the intracluster medium, and have been the subject of extensive dynamical studies. In Section 7 we comment on their relation with their — typically cluster — environments, and in Section 9 discuss their use as probes of dense environments in the more distant Universe.

As lower-frequency radio observations have become increasingly sensitive, it has become clear that another common feature of cluster centre radio sources is the presence of low surface brightness extended lobes permeating a larger volume than the currently active source, and likely to indicate previous episodes of activity — in some cases linked to the presence of outer 'cavities' (surface brightness depressions) in the X-ray emission from the intracluster medium. The nearby radio galaxy M87 is an example of a cluster source with a very extended low-surface brightness halo pervading the intracluster medium (Owen et al., 2000; de Gasperin et al., 2012). Galaxy clusters also frequently possess diffuse radio emission that is not directly associated with current radio jet activity (haloes and relics) (Feretti and Giovannini, 1996). The links between past and current radio galaxy activity and cluster diffuse radio emission are an interesting topic of current research, which is discussed further in Section 9.

3.4. Restarting and remnant radio galaxies

Double-double radio galaxies (Schoenmakers et al., 2000) and other restarting radio galaxies (e.g., Clarke and Burns, 1991; Bridle et al., 1989; Jamrozy et al., 2007) are further populations that provide important insights into radio-galaxy life cycles and triggering. Spectral and morphological studies have also been used to identify 'dying' radio galaxies (e.g., Murgia et al., 1999), now commonly known as remnant radio galaxies (we avoid the term 'relic' radio galaxy in this context, to avoid confusion with cluster radio relics). Double-double radio galaxies (DDRGs) are systems in which an inner pair of radio lobes propagate along the same axis as outer lobes. Typically, both sets of structure have edge-brightened, FRII-like morphology. Samples of tens of DDRGs now exist, from investigations with the FIRST, NVSS, and most recently LoTSS surveys (Nandi and Saikia, 2012; Kuźmicz et al., 2017; Mahatma et al., 2019). Mahatma et al. (2019) investigated the host galaxies of a sample of DDRGs, finding no significant differences to a control sample of similar luminosity ordinary radio galaxies. It appears that DDRG structure is not caused by specific host galaxy conditions, but is likely to relate to accretion conditions being interrupted and restarting. There have also been detailed studies of other types of candidate restarting objects, in which small-scale sources are surrounded by extended halos and/or misaligned outer lobes (e.g., Jamrozy et al., 2007; Jetha et al., 2008; Brienza et al., 2018). The recent LoTSS study of Mingo et al. (2019) suggests that there may be a moderate sized population of newly restarted jets embedded in extended radio emission, but follow-up work is needed to investigate this population further. Larger statistical samples and spectral modelling are needed to draw firm conclusions about the prevalence and duty cycle of recurrent activity, but it is clear that objects with visible signatures of recurrent activity are rare in the radio-loud AGN population.

Remnant radio galaxies can be difficult to identify due to their low surface brightness, and until recently relatively few were known (e.g., Parma et al., 2007; Murgia et al., 2011; Saripalli et al., 2012). Sensitive low-frequency surveys were expected to turn up larger numbers of these sources, expected to be dominated by steep-spectrum aged plasma. Brienza et al. (2017) identified 23 candidate remnant sources in the Lockman Hole survey area, while Mahatma et al. (2018) searched for radio cores in a low-frequency selected sample, finding that only 11/33 candidate remnant sources showed no radio core, indicating a true remnant (note that some sources with a radio core may be restarting radio galaxies). Population modelling and theoretical work indicate that the observed remnant fraction should be low, as lobes will fade through radiative losses on a short timescale after the jet turns off (Godfrey et al., 2017;

Hardcastle, 2018a).

3.5. Compact and unresolved radio-loud AGN

In addition to the extended radio galaxy populations, populations of compact radio galaxies, including luminous populations of compact symmetric objects (CSOs), gigahertz-peaked spectrum (GPS) sources, and compact steep spectrum (CSS) sources have been studied for many decades (e.g., O'Dea and Baum, 1997; O'Dea, 1998). More recently fainter populations of compact sources have been shown to constitute a very large AGN population (e.g., Sadler et al., 2014; Baldi et al., 2015; Gürkan et al., 2018; Hardcastle et al., 2019b), thought to possess low-power small-scale jet activity. These compact radio-loud AGN are of importance for understanding radio-galaxy triggering and life cycles. We briefly discuss the main subclasses before commenting on current understanding of their relationship(s) to the large-scale radio galaxy population.

Compact steep-spectrum and gigahertz peaked spectrum sources are powerful radio-loud AGN ($L_{1.4\mathrm{GHz}} > 10^{25}$ W Hz^{-1}) smaller than $1 - 2$ arcsec (e.g., O'Dea, 1998; Orienti, 2016). The CSS sources have typical physical sizes extending to $\sim$ 20 kpc, while the GPS sources are smaller, typically < 1 kpc. Compact symmetric objects (CSOs) are the smallest sources, with sizes of less than a few hundred pc. The radio spectra of CSS sources peak at MHz frequencies, while the higher-frequency GHz turnover in GPS sources is traditionally thought to indicate self-absorption due to high densities in very compact synchrotron-emitting regions, although free-free emission is another possible mechanism to explain the observations. CSS sources possess interesting features in optical emission line and molecular gas, indicative of jet/environment interaction on small scales. Recently, Callingham et al. (2017) have presented the largest sample to data of such systems, obtained with the MWA GLEAM survey. There have been two competing hypotheses for these populations: that they are 'young' sources that will evolve to become traditional FRI or FRII radio galaxies (O'Dea, 1998), or that they are 'frustrated' jets occurring in dense environments and unable to grow to a large size (e.g., van Breugel et al., 1984). It is likely that both scenarios are relevant for a subset of objects, since small, young objects will necessarily probe the densest possible parts of a particular environment. In principle, low-frequency spectral information may be able to distinguish the influence of synchrotron self-absorption and free-free absorption, expected in a dense environment — Callingham et al. (2017) found a small sample of potential candidates in which free-free absorption may be important. Observations of X-ray absorption can also be used to search for a dense medium around compact sources (Sobolewska et al., 2019).

As shown in Fig. 2, the CSO, GPS and CSS categories have historically applied to objects of high luminosity, due to the high flux limits of early radio surveys. However, in addition to the peaked spectrum and luminous compact AGN populations, there is a large population of low-luminosity radio sources with evidence for small-scale jets. Radio nuclei in ordinary elliptical galaxies have been known for many years (e.g., Ho, 1999), and have recently been investigated systematically at high resolution (Baldi et al., 2018b). Low-luminosity kpc-scale jet structures have been studied extensively in Seyfert galaxies (e.g., Gallimore et al., 2006; Hota and Saikia, 2006; Croston et al., 2008b; Mingo et al., 2011; Jones et al., 2011; Mingo et al., 2012; Williams et al., 2017), and examples of small-scale jets are emerging in radio-quiet quasars (e.g., Jarvis et al., 2019).

Recently the 'FR0' nomenclature has been introduced to describe the population of unresolved low-luminosity radio-loud AGN (e.g., Sadler et al., 2014; Baldi et al., 2015; Hardcastle et al., 2019b). We do not favour this terminology: as stated by Fanaroff and Riley (1974), the FRI/FRII classification is a morphological one, and as such it relies on observations capable of resolving the source (i.e. the source must be at least a factor of a few larger than the beam size of the radio observations before a classification can be made). If these observations do not exist, the FR class of the source is unknown — this gives rise to the large fraction of sources classed as 'C' ('compact') in early catalogues such as the 3CRR catalogue of Laing et al. (1983). When higher-resolution observations become available, as is now the case for the 3CRR objects, the sources can be classified. A classification based on a source's unresolved nature in a particular survey (with a particular resolution and surface brightness limit) can never be physical, and indeed some evidence exists that objects selected this way are a heterogeneous population (Baldi et al., 2019). Nevertheless, it is certain that this dominant population of compact radio-loud AGN in the nearby Universe — however they are designated — are of great importance for our understanding of radio-galaxy life cycles and AGN feedback, and are in need of further study.

4. Physical conditions

A great deal of observational work has gone into measurement of the physical conditions in various components of the radio sources and in the external medium. Below we summarize some of the current understanding on this topic.

4.1. Jet speeds

VLBI observations of pc-scale jets measure apparent superluminal motions, $v_{app} > c$. These imply highly relativistic jet bulk motions on pc scales: superluminal apparent speeds as high as $50c$ have been observed (Lister et al., 2016), which on standard assumptions (in particular equating the pattern speed, or the speed of motion of structures in the jet, with the bulk flow speed) would imply bulk Lorentz factors $\Gamma > 50$. These very high values may represent the extremes of a dispersion of bulk speeds within a given source, in which case we would expect internal dissipation to reduce the effective bulk speed on scales of hundreds of pc. However, it seems clear that the jet may leave the inner parts of the radio source with highly relativistic bulk speeds.

These speeds are in contrast to those estimated using Doppler boosting arguments from unified models of RLAGN (see Section 6.1). Constraints derived from luminosity functions of blazars and their presumed parent population of radio galaxies (Urry et al., 1991; Hardcastle et al., 2002) imply bulk beaming speeds of $\Gamma \sim 3$–5. More problematically, all estimates of the kpc-scale jet speeds in powerful FRII RLAGN tend to give $\beta \approx 0.5$ – 0.7 (Wardle and Aaron, 1997; Hardcastle et al., 1999; Arshakian and Longair, 2004; Mullin and Hardcastle, 2009); these estimates rely on the demonstration using polarization statistics in quasars (Laing, 1988; Garrington et al., 1988) that the one-sidedness of kpc-scale jets is indeed due to beaming. With the debatable exception of the beamed inverse-Compton model for powerful jets (Section 2.4) there is no direct evidence for high bulk speeds on hundred-kpc scales in powerful objects, but there is also no evidence for the strong deceleration that would be required to account for the differences between pc and kpc scales. A plausible explanation is that the jet is structured and that most of the emission seen on kpc scales comes from a slow-moving component while most of the energy is carried by a relativistic outflow. There is some direct evidence for this picture in the shape of edge-brightened structures of a few resolved powerful jets (Swain et al., 1998; Hardcastle et al., 2016) but more observational work is needed.

In FRI radio galaxies the situation is clearer. These objects often show jets that are one-sided on small scales but two-sided on large scales, implying bulk deceleration if the sidedness is attributed to Doppler boosting. Because the jets are resolved both transversely and longitudinally, detailed models of the jet velocity field of individual objects can be constructed, using the polarization of the jets to break degeneracies involving the unknown angle of the jet axis to the line of sight. The results (e.g., Laing and Bridle, 2002, 2014) show that jets initially have $\beta \sim 0.8$ on the kpc scale and decelerate smoothly (but often more rapidly at the edges) to a constant, sub-relativistic speed. The bulk deceleration must involve entrainment of material initially at rest with respect to the jet (Bicknell, 1994), but it is not clear what this material is: stellar winds may provide some of the required mass (Bowman et al., 1996; Wykes et al., 2015) but if this is insufficient, as it probably is in the most powerful sources, then entrainment of the external medium in some form may be required. It is important to note that the *lobe dynamics* of FRIs should not in themselves be affected by this entrainment — the momentum and energy flux of the jet are essentially unchanged by it.

4.2. Environments

For the purposes of dynamical modelling, profiles of the pressure and density in the external medium are required. These can be derived from deprojection (normally spherical deprojection) of the observed X-ray surface brightness profile if we assume that the X-ray-emitting gas dominates density and pressure — an assumption that is more valid on larger scales than smaller ones — and from X-ray spectroscopy to estimate the temperature (profile) of the hot gas. Bulk inference of radio galaxy environments from X-ray data is now relatively routine (see e.g., Worrall and Birkinshaw (2000); Hardcastle and Worrall (2000b); Croston et al. (2008c); Ineson et al. (2015)) though systematic uncertainties may arise through the assumption of spherical symmetry. It is far more difficult to estimate the environmental density and pressure profiles based on optical information alone.

4.3. Lobe energy density and particle content

Traditionally estimates of the lobe energy density have involved the minimum-energy condition (Burbidge, 1956) (or, equivalently, equipartition of energy between electrons and magnetic field). Interpreted as lower limits, these are valid, but they do not give many constraints on source dynamics. In minimum-energy calculations in the literature widely differing assumptions are often made about the energetic contribution of

non-radiating protons, and care is also needed to distinguish between calculations made using a minimum and maximum *frequency* for the radiating particles (which implies field-dependent energy integration limits) and one using a minimum and maximum *energy* or Lorentz factor. Beck and Krause (2005) discuss some of these issues in detail.

A better approach, where possible, is to infer magnetic field strength and so energetics from observation. Observations of inverse-Compton emission from the lobes and hotspots of FRII RLAGN (Hardcastle et al., 2002, 2004; Kataoka and Stawarz, 2005; Croston et al., 2005; Ineson et al., 2017) measure the number of inverse-Compton-scattering electrons and so allow the characteristic magnetic field strength to be estimated based on the observed synchrotron emission. This gives typical field strengths of a factor $\sim$ 2–3 below the equipartition values and so energy densities in field and electrons a factor 2.5–5 higher than the equipartition value. On these assumptions radio lobes tend to be strongly overpressured at the radio lobe tip (with respect to the environment at that location) and moderately overpressured at the mid-point of the lobe. It is then possible to argue (Hardcastle et al., 2002; Croston et al., 2018) that protons cannot be strongly energetically dominant over electrons in these lobes, as, if they were, this good agreement over a number of objects between the inferred internal pressures and observed external pressures would be a coincidence. This argument does not rule out a contribution to the energy density from protons that is comparable to that of the electrons or the magnetic field; there is some evidence that FRIIs in rich environments may have a higher non-radiating particle content (e.g., Hardcastle and Croston, 2010). It has long been known from low-frequency polarization observations that the number density of internal *thermal* electrons in FRII lobes must be relatively low (Scheuer, 1974), consistent with the idea that their internal pressure is dominated by the radiating particle population.

The situation is more complicated for the FRI radio galaxies for two reasons. Firstly, there are few direct measurements of X-ray inverse-Compton from the lobes that would allow a magnetic field measurement, as the thermal emission tends to dominate over inverse-Compton (Hardcastle and Croston, 2010); secondly, a comparison between radio emission and external pressure often requires departures from equipartition much more substantial than those measured in the FRII population (Morganti et al., 1988; Killeen et al., 1988; Feretti et al., 1990; Taylor et al., 1990; Feretti et al., 1992; Böhringer et al., 1993; Worrall et al., 1995; Hardcastle et al., 1998; Worrall and Birkinshaw, 2000; Hard-

castle et al., 2005; Croston et al., 2003; Dunn et al., 2005; Croston et al., 2018). In some cases these highly sub-equipartition fields are ruled out by the lack of observed inverse-Compton emission in the X-ray. Observations of cavities (Section 3.3) and of low-frequency polarization from the lobes rule out a model in which the lobe is filled with thermal particles similar to those in the external medium. The most plausible hypothesis is that an additional population of high-energy particles dominates the lobe energetics in the FRIs, but not the FRIIs. Relating this to the other known difference between the two populations, we can hypothesise that the material that is entrained as the FRI jets decelerate is then heated to provide the missing pressure (e.g., Croston and Hardcastle, 2014; Croston et al., 2018). This has the effect that FRI radio galaxies, where the lobe dynamics are dominated by an invisible, non-radiating particle population, are much more difficult to model than the higher-power but less numerous FRIIs. A prediction of this model is that internal depolarization, due to entrained thermal electrons, might be visible in lobes of low-power sources, and broad-band polarimetry is starting to probe this regime (e.g. Anderson et al., 2018)

Finally, it is worth noting that there are as yet few direct measurements of lobe kinematics. For the smallest class of double radio sources known, the CSOs, the lobe expansion speeds in the plane of the sky can be measured directly using VLBI (e.g., Owsianik and Conway, 1998; Polatidis and Conway, 2003; Gugliucci et al., 2005), giving sub-relativistic expansion speeds of order a few tenths of *c*. A few objects drive observable shocks into the external medium which can give an instantaneous estimate of the lobe advance speed if the properties of the unshocked medium are known (Croston et al., 2007, 2009, 2011; Snios et al., 2018); however, numerical modelling of the shocked shells suggests that it is not trivial to interpret these measurements. Next-generation X-ray satellites such as *Athena* (Nandra et al., 2013) will provide measurements of shock properties for large samples of radio galaxies. For larger sources, a traditional method to estimate lobe advance speeds statistically is to consider lobe length asymmetries in complete (low-frequency selected) samples (e.g., Longair and Riley, 1979; Scheuer, 1995) since light travel time effects from the nearer to the further lobe will give an apparent difference in lobe length between the two which depends on the lobe advance speed. However, this method is biased if it is assumed that the lobe length difference arises purely from light travel time effects, since environmental effects may also play a role in lobe asymmetry (i.e. the longer lobe may not always be the nearer). If the lobe containing the (brighter) jet, rather than the

longer lobe, is taken to be the nearer lobe in order to reduce this bias, as was done by Scheuer (1995) (relying on the assumption that kpc-scale jets are beamed as discussed in Section 4.1), the method gives lobe advance speeds of order a few per cent of the speed of light. These would still be highly supersonic, $\mathcal{M} = 10$, with respect to the sound speeds even in a rich cluster medium. By contrast, the pressure ratio estimates of Ineson et al. (2017) (which however exclude the ram pressure of the jet) suggest a median $\mathcal{M} \sim 2$. It is not as yet clear what causes the discrepancy.

4.4. Lobe ages

Estimating the ages of RLAGN is difficult. The one exception is where a direct estimate of the current source expansion speed exists; then a simple 'kinematic age' can be calculated on the (clearly incorrect but not badly wrong) assumption of constant expansion speed. This has been done using observed proper motions in CSOs, as described in the previous Section, yielding ages of the order of 10^3 years for these smallest of double-lobed objects. For larger objects a 'dynamical age' can be estimated based on the projected source size and estimated expansion speeds as described above — this would lead to estimates of dynamical age of between 10 and 100 Myr for a source with a lobe 100 kpc in length. However, as noted above, these speed estimates are very uncertain. A better approach to dynamical age estimation, where possible, is to fit some source model (see the next Section) to the observed radio properties of the source and optimize for dynamical age.

A very popular alternative approach is to estimate ages by 'spectral ageing' (e.g., Myers and Spangler, 1985), in which the energy-dependent loss rate of synchrotron-emitting electrons is used to estimate the age of the source (and/or, since it gives ages for all positions inside the lobe, the speed of the internal transport of the radiating plasma). This method tends to give ages of the order of 10^7 years for 100-kpc-scale lobes (Alexander and Leahy, 1987; Harwood et al., 2013) and there is therefore a discrepancy of up to an order of magnitude (in the sense that the spectral age is lower) between estimates of the spectral and dynamical ages. Although the spectral age is model-dependent, with the greatest difference being between models that assume effective pitch angle scattering of the radiating electrons (Jaffe and Perola, 1973) and those that do not (Kardashev, 1962; Pacholczyk, 1970), the derived ages are generally similar whichever model is used. This problem has been apparent for many years (Eilek, 1996) and at the time of writing the solution seems likely to

be a combination of several factors. Firstly, we now know (see above, Section 4.3) that the equipartition field strengths used in most spectral ageing studies overestimate the field strength by a factor of a few, and consequently these studies underestimate the spectral age, except in situations where inverse-Compton losses to the CMB dominate over synchrotron losses. Spectral ageing studies actually measure the break frequency ν, and this is related to the age t by

$$t = \left(\frac{CB}{(B^2 + B_p^2)^2 \nu} \right)^{\frac{1}{2}} \qquad (4)$$

where B is the magnetic field strength, B_p is the equivalent magnetic field to the energy density in photons u_p (in SI units, $B_p = \sqrt{2\mu_0 u_p}$; this term describes losses due to inverse-Compton scattering of background photons) and C is a constant. For $B \gg B_p$, $t \propto B^{-3/2}$ and so decreasing B can increase the estimate of t. Secondly, it remains possible that there is some *in situ* particle acceleration in the lobes, which would tend to reduce the observed spectral ages: indeed such distributed (leptonic) particle acceleration must take place at some level in models in which RLAGN are responsible for the ultra-high-energy cosmic ray population (Section 9.4). Thirdly, the mixing of old and young electron populations within the lobes can in principle allow a source to continue to show an apparent age gradient while reducing the apparent maximum age, as shown recently by Turner et al. (2018). It seems plausible that a combination of these, particularly the first and third, can bring spectral and dynamical ages into agreement (Mahatma et al., 2020).

It is finally worth noting that in the cavity power method of estimating jet powers, which we discuss further in the subsequent section, lobe ages are estimated from either the sound crossing time, the buoyant rise time, or the 'refilling timescale' of the cavity (Bîrzan et al., 2004): of these the sound crossing time of the source is generally the shortest. But for a typical powerful source, we expect the lobe expansion to have been supersonic for a significant fraction of the source's lifetime, and thus these age estimates are likely to be significant overestimates with respect to a true dynamical age.

4.5. Jet power

Given the uncertainties on both lobe energetic content (Section 4.3) and age (Section 4.4) it will come as no surprise that estimates of the lifetime-averaged jet kinetic power, which we denote Q, are also highly uncertain. Basic calculations from the lobe energetics and

lifetimes given above for large sources suggest that jet powers should lie in the range $10^{36} – 10^{40}$ W, but these do not take into account the work done on the external medium. Other than the case of a small number of FRIs with well-modelled jet dynamics (e.g., Laing and Bridle, 2002) the situation is best for the powerful FRII-type sources where the lobe energetics are well constrained and dynamical models are well understood. It is then possible to try to relate observable quantities like radio luminosity to the jet power by way of a model (Willott et al., 1999), making some assumptions about the energy transfer to the source environment. In practice, this is simplistic, since we know that the radio luminosity for a source of constant jet power must vary not just with time but also with the environment of the radio source (Hardcastle and Krause, 2013) and with redshift, since inverse-Compton losses are redshift-dependent. More sophisticated approaches to jet power inference try to take these effects into account (Hardcastle et al., 2019b).

An alternative approach is to construct jet power estimates from X-ray observations of cavities excavated by the lobes in the external medium, estimating the $p\Delta V$ work done to inflate the cavity using estimates of pressure derived from fitting to the X-ray spectrum. This has the advantage that a quantity directly related to the work done on the external medium can be calculated. However, it only works when cavities are observed, which rules its use out in the case of the most powerful 'classical double' AGN, where typically the lobes are brighter in inverse-Compton than their surroundings (Hardcastle and Croston, 2010); these sources also generally drive shocks into the external medium which are not accounted for in the $p\Delta V$ calculation. The method is biased towards small sources in rich cluster environments (Bîrzan et al., 2012) and relies on expensive X-ray observations that are not available for large samples of sources. As a method for calculating jet power, it also relies on poorly known source ages, as discussed above. For all of these reasons, though the jet power estimates from this methods do seem to show some correlation with radio luminosity (Cavagnolo et al., 2010), the scatter and biases mean that any inference of a jet power from the calibration of such a relation must be done with extreme caution. Indeed, Godfrey and Shabala (2016) suggest that there is no physically meaningful correlation between radio luminosity and calculated jet power for these objects at all. Whether this is the case or not, more sophisticated power inference methods are likely to be needed in future.

Observations of restarting radio galaxies (Section 3.4) imply that it is possible for the jet power to drop to very low levels (perhaps, but not necessarily, to zero) and then to recover on a timescale shorter than the overall source lifetime. We have very little information on the power spectrum of such variations in a typical source, and estimates based on the large-scale structure or the impact on the large-scale environment can only really provide a lifetime-averaged rather than an instantaneous value.

5. Dynamics: modelling and simulation

The basic dynamical picture of RLAGN has remained unchanged since the work of Scheuer, Blandford and Rees in the 1970s (Scheuer, 1974; Blandford and Rees, 1974). Oppositely directed light jets, sometimes called beams, are emitted from the central engine and impact on the external medium. Because the jets are light compared to the external medium, conservation of momentum dictates that the flow speed up the jet must be much higher than the advance speed of the contact surface, so the conditions are right (assuming that cooling is slow) for material to be redirected away from the head of the source and flow sideways and backwards to form lobes. Once lobes are present, their expansion is governed by their internal pressure as well as by the ram pressure of the jet material. If/when the expansion of the lobes is supersonic, they will drive a shock into the ambient medium, so we can then consider three zones of interest; the lobes themselves, the shell of swept-up, shocked gas around them, and the undisturbed external medium which has not so far been affected by the radio source. Scheuer (1974) introduced an important variation on this model: once the lobes are no longer strongly overpressured with respect to the external environment, they will cease to drive shocks in the transverse direction, and may eventually be squeezed outwards away from the central engine by the pressure of the external medium.

Modelling of radio galaxy lobes is simple in principle but complex in detail, particularly if we wish to use even modestly realistic environments. Early modelling, such as that of Scheuer (1974), laid out the basic principles of lobe dynamics in a uniform atmosphere. The important work of Kaiser and Alexander (1997) used a power-law atmosphere and, considering the collimation of the jet, derived equations for self-similar growth of radio sources that have been widely used (they were followed in some of these assumptions by, e.g., Kaiser et al. 1997, Blundell et al. 1999, Nath 2010, Mocz et al. 2011 and Godfrey et al. 2017) and allowed the prediction of source evolutionary tracks in a power/linear-size diagram like that of Fig. 2. But in fact radio galaxy atmo-

spheres are not scale-free power laws, but have a scale that relates to the mass of the halo (Arnaud et al., 2010; Sun et al., 2011), which invalidates the assumptions of self-similar lobe evolution. Moreover, the assumptions of the model of Kaiser and Alexander (1997) also restrict it to the case where the source remains strongly overpressured at all times, which is a self-consistent requirement (Begelman and Cioffi, 1989) but not obviously observationally the case. Hardcastle and Krause (2013) investigated a self-collimating jet model comparable to that of Kaiser and Alexander (1997) in numerical simulations and showed that in reasonably realistic β-model environments the self-similarity assumptions do not hold; sources show time-variable axial ratios in the sense that the ratio of lobe width over lobe length gets lower with time, and at late times the lobes come into transverse pressure balance with the external medium are pushed away from the central part of the host environment by buoyancy forces, as originally proposed by Scheuer (1974). On the other hand, analytical models such as those of Luo and Sadler (2010) which assume expansion in pressure balance do not seem likely to be realistic for young sources which must start out (and observationally are) overpressured on any assumption. For these reasons more recent analytical modelling tries to capture the insights from numerical models and deal with the evolution of the sources from the overpressured to the pressure-balanced phases. Examples of this more recent approach are Turner and Shabala (2015) and Hardcastle (2018b); these models predict, for example, evolution of the radio luminosity with time (or, equivalently, source size) that is qualitatively consistent with the results of numerical modelling. None of these models currently deals well with the possibility of strongly time-varying Q (Section 4.5) or of changes in the jet direction over time, e.g. due to precession induced by a close binary black hole pair (Krause et al., 2019).

A vast body of work exists on numerical modelling of the large-scale structure of radio sources and on their impact on the external medium; some of this will be discussed elsewhere in this volume. The value of numerical modelling has been recognised since the very earliest simulations (Norman et al., 1982; Williams and Gull, 1985) but there are many difficulties in carrying out detailed simulations of RLAGN, including the very large spatial dynamic range (in principle from the jet generation scale to the Mpc scales of the largest lobes), the fact that relativistic bulk motions and non-negligible magnetic fields are both expected to be present, the fact that radio sources are clearly not axisymmetric so that three-dimensional modelling is needed, the difficulty of ac-

curately modelling particle acceleration, transport and radiative losses and, at least in the early days of modelling, the very poorly known physical conditions in the lobes and environment (see previous Section).

Some approaches to simulations, which emphasise different parts of this parameter space, include:

1. Trying to reproduce large-scale lobe dynamics, often in the context of parameter studies varying jet and environmental properties (e.g., Norman et al., 1982; Cioffi and Blondin, 1992; Massaglia et al., 1996; Carvalho and O'Dea, 2002; Krause, 2003; O'Neill et al., 2005; Hardcastle and Krause, 2013). These models often omit relativistic effects and magnetic fields and neglect particle acceleration or transport, and may be simplified by the assumption of axisymmetry. They reproduce the inflation of lobes by light (but not heavy) jets and can generate internal jet termination shocks which are assumed to be related to the hotspots observed in FRIIs. As noted above, departures from self-similarity are observed in realistic environments.

2. Trying to reproduce detailed features of jets or lobes in total intensity or polarization (e.g., Bodo et al., 1998; Rossi et al., 2008; Perucho et al., 2010; Mignone et al., 2010; Gaibler et al., 2009; Huarte-Espinosa et al., 2011; Hardcastle and Krause, 2014). In this case relativistic effects are often important and magnetic fields may well be modelled, but large volumes and realistic environments are less important.

3. Modelling of particle acceleration, transport and loss (e.g., Jones et al., 1999; Tregillis et al., 2001, 2004; Mendygral et al., 2012; Vaidya et al., 2018). These models can qualitatively reproduce many of the complex features seen in the synchrotron emission of real sources, and also the effects of radiative losses on radio spectra.

4. Modelling of the impact of RLAGN on their environments. The impact of powerful sources on the hot gas has been particularly well studied (e.g., Basson and Alexander, 2003; Zanni et al., 2003; Omma and Binney, 2004; O'Neill et al., 2005; Gaibler et al., 2009; Hardcastle and Krause, 2013; Bourne and Sijacki, 2017) but more recently interaction with cold gas, which may be important in small-scale sources or at high redshift, has also been modelled (Sutherland and Bicknell, 2007; Gaibler et al., 2011, 2012; Mukherjee et al., 2018).

6. Central engines

6.1. Unified models and accretion modes

Observations of the optical spectra of radio galaxy hosts (Hine and Longair, 1979; Laing et al., 1994) show a wide range of possible optical behaviour. While some objects show strong high-excitation broad and narrow lines similar to those in Seyfert galaxies, others exhibit weak or no line emission. This observational dichotomy has been given a number of names but here we begin by following Laing et al. (1994) in separating RLAGN observationally into 'low-excitation radio galaxies' (LERGs) and 'high-excitation radio galaxies' (HERGs). The latter class includes both 'narrow-line radio galaxies' (NLRGs) and 'broad-line radio galaxies' (BLRGs) which have optical spectra resembling those of classical Seyfert 2 and Seyfert 1 galaxies respectively, as well as optically selected quasars, which have spectra similar to those of the BLRGs but by definition show dominant optical continuum emission as well.

Orientation-based unification models for radio-quiet AGN[1] (Antonucci, 1993) very successfully explain the difference between e.g., type 1 and type 2 Seyfert galaxies in terms of an anisotropic obscuring structure (the 'torus': Krolik and Begelman 1986). This structure, plausibly associated with the cold outer parts of the accretion flow itself, obscures the nuclear continuum and broad emission lines in objects where the line of sight passes through it (type 2), but allows them to be seen directly from other lines of sight (type 1). The most direct evidence for this picture comes from spectropolarimetry, which reveals the broad emission lines in scattered light in type 2 objects, showing them to be present but not directly visible to us (Antonucci and Miller, 1985). The simplest view of the torus as a smooth structure is known to be incorrect, e.g., from observations of sources where the obscuring column changes on short timescales (Risaliti et al., 2002), which leads to the idea that different types of AGN are selected from a distribution of both orientation and torus covering factor (Elitzur, 2012). However, orientation clearly has an important remaining role to play in our view of these objects.

In the case of radio-loud objects there are two additional complications. The first is the presence of the jet, which provides a source of broad-band anisotropic radiation on all spatial scales. The second is the existence

of LERGs, which have no counterpart in the Seyfert 1/2 orientation-based scheme, though they show some similarity to the radio-quiet LINER class.

RLAGN do have one advantage, which is that they can be selected on the basis of a roughly orientation-independent quantity, the low-frequency luminosity (expected to be dominated by the lobes and hence unbeamed). This means that a low-frequency flux-limited sample such as 3CRR, is (theoretically) unbiased with respect to orientation if redshifts can be found for all members. Barthel (1989) developed the first successful orientation-based unified model for RLAGN by noting that quasars in the 3CRR sample in the redshift range $0.5 < z < 1.0$ had systematically smaller projected linear sizes and brighter kpc-scale jets and cores. He showed that an orientation of quasars within $45°$ of our line of sight was sufficient to explain the fraction of observed quasars in the parent sample and their physical sizes. Hardcastle et al. (1998) showed that this model could be extended to the lower-redshift NLRGs and BLRGs in the 3CRR sample, so long as LERGs were excluded.

At this point, the role of LERGs in unified models was unclear: for example, it was possible that the missing narrow emission lines were simply obscured or that the emitting material was absent, while other features of standard AGN were still present. Work on the mid-IR and X-ray properties of the LERGs, however, ruled this possibility out (Chiaberge et al., 2002; Whysong and Antonucci, 2004; Hardcastle et al., 2006, 2009) by showing that there was no evidence for either heavily obscured X-ray emission or re-radiation of obscured emission in the mid-IR, both of which are seen in NLRG. Thus it appears that LERGs, while still possessing active jets, have no sign of a radiatively efficient accretion disk, torus, corona, or accretion-driven emission lines, while HERG behave like radio-quiet AGN with the addition of a jet. The nuclear optical and X-ray emission seen from some LERGs (Hardcastle and Worrall, 2000b) is consistent with coming from the jet only. The situation is confused by the existence of remnant sources (Section 3.4), where the jet has recently switched off — distinguishable from active LERGs by the absence of any nuclear emission associated with the jet — and by a very few peculiar objects that lack one or more of the standard AGN radiative components (Ramos Almeida et al., 2011), but these do not change the basic picture.

What drives the difference between LERGs and HERGs? Many authors have proposed (e.g., Ghisellini and Celotti, 2001; Merloni and Heinz, 2008) that the radiative efficiency of the accretion flow is governed by

---

[1] Here we use the term 'radio-quiet AGN' purely in contrast to 'RLAGN' to indicate sources without strong radio emission or extended radio lobes. Few if any AGN are entirely radio-silent, and our use of this term does not imply a belief in a true physical dichotomy between the two classes; see later discussion.

the Eddington-scaled accretion rate: only discs capable of generating more than a few per cent of the Eddington luminosity,

$$L_{\text{Edd}} = \frac{4\pi G M_{\text{BH}} c m_p}{\sigma_{\text{T}}} \quad (5)$$

can produce the optical luminosity which is directly observed in quasars and BLRG and which drives the broad and narrow emission lines, the X-ray corona and the mid-IR radiation from the torus. This model is supported by observations in which the HERG/LERG classification, black hole mass and bolometric radiative luminosity of large samples of sources have been measured (Best and Heckman, 2012; Mingo et al., 2014) and is consistent with expectations from theoretical disk models (Rees et al., 1982; Narayan and Yi, 1995). In this picture, the two classes are best referred to as radiatively inefficient (RI: the *bona fide* unobscured LERGs) and radiatively efficient (RE: HERGs, including NLRG, BLRG and radio-loud quasars). In RI objects, the estimated jet power may greatly exceed upper limits on the nuclear radiative luminosity.

Claims that the RI/RE dichotomy has a one-to-one mapping to the FRI/FRII dichotomy (that is, all RI objects are intrinsically FRIs and vice versa, and all RE objects are intrinsically FRIIs and vice versa) are widespread in the literature but, in their simplest form, have been falsified by observation since 1979 (Hine and Longair, 1979). It is certainly the case that in the 3CRR sample almost all FRIs are RI (with debatable exceptions such as 3C 84), and the majority of FRIIs are RE, but there are sufficient LERG/RI FRIIs even in that sample to make the situation more complex. The suggestion that all of these objects (which have nuclear X-ray radiation and VLBI-detected jets in most cases) are simply taking a short break from being radiatively efficient (Tadhunter, 2016) is inconsistent with observations that show other physical differences between LERG and HERG FRIIs at constant radio power (Ineson et al., 2015). It is also inconsistent with our best current explanation of the FRI/FRII difference. As discussed in Section 3.1, this difference is thought to come from the interplay between the power (momentum flux) of the jet and the extent to which it is forced to decelerate by entrainment on kpc scales (Bicknell, 1994). Though it is clear that the most powerful jets will be FRII-like and the most powerful accretion flows will be RE, there is no reason why a source which produces a jet with kinetic power Q marginally sufficient to generate an FRII-type source with terminal hotspots in a particular environment should necessarily also have an Eddington-scaled accretion rate high enough to make a RE accretion flow,

or vice versa. (We return to the question of the relationship between jet power and accretion power in the subsequent Section.)

Where does this leave unified models for RLAGN? The basic picture remains similar to that of e.g., Urry and Padovani (1995) but with some important differences in detail; in principle accretion rate, black hole mass, jet power, obscuration covering fraction as in Elitzur (2012) and angle to the line of sight are all independent parameters of a system. The only thing that is certain is that an object selected as 'radio-loud' presumably has some non-negligible jet kinetic power Q. For such a source, the accretion rate and black hole mass determine whether the source is RI or RE, and these can vary widely for a given Q as we discuss in the next Section. The nuclear emission from RI sources is jet-dominated at all angles to the line of sight. For both RI and RE sources, there will be some angle to the line of sight where the beamed small-scale jet dominates over the optical continuum from starlight, giving a blazar-type optical classification, but this will depend on jet power Q and host galaxy properties as well as orientation angle. Crucially, RI misaligned RLAGN (and not, as often claimed in the literature, FRI radio galaxies) should be the parent population of 'true' BL Lac objects with intrinsically weak lines – this is observationally confirmed by the existence of FRII-type structures in the extended emission from blazars: e.g., Rector and Stocke 2001). However, the situation is confused by objects classified as BL Lacs where intrinsically bright lines are normally hidden by strong optical continuum (Vermeulen et al., 1995). RE RLAGN must be the parent population of these objects and also of flat-spectrum radio quasars. For RE sources, an intermediate angle to the line of sight and an appropriate level of obscuration allows a direct view of the accretion disk/corona/broad-line region and classifies sources as BLRG or lobe-dominated quasars; these regions do not exist in RI sources, which are seen as LERG from all angles where the jet continuum does not dominate. Jet power, not accretion state, and host environment determine the large-scale radio morphology of a source. The unified model for RLAGN discussed here is summarized in Table 1.

6.2. Jet power and AGN power

As yet it is poorly understood, observationally, how jet power and AGN power are related. In RE AGN, we expect the radiative luminosity to be proportional to the accretion rate:

$$L = \eta \dot{M} c^2 \quad (6)$$

Table 1: The unified model for radio-loud sources

	Jet at large angles to line of sight	Intermediate angles	Jet closely aligned to line of sight
Radiatively inefficient (RI)	Low-excitation radio galaxy, LERG (FRI or FRII)	Low-excitation radio galaxy, LERG (FRI or FRII)	BL Lac object
Radiatively efficient (RE)	Narrow-line radio galaxy, NLRG (some FRI, mostly FRII)	Broad-line radio galaxy, BLRG, or lobe-dominated or steep-spectrum quasar (some FRI, mostly FRII)	Core-dominated, flat-spectrum or OVV quasar

where η is the traditional efficiency factor. Here there is no explicit dependence on black hole mass, but since accretion at super-Eddington rates (i.e. rates that generate $L \gg L_{\text{Edd}}$: eq. 5) must be short-lived, while accretion at rates much less than the Eddington rate will give rise to a RI system, there should be a quite narrow band of accretion rates $\dot{M}$ and so luminosities L that can be expected for a given M_{BH}, scaling linearly with M_{BH}, as observed (e.g., Steinhardt and Elvis, 2010).

On the other hand, jet power must be a result of a jet-generation process and the dependences on the parameters of the system are more complex. In the Penrose/Blandford-Znajek process (Penrose, 1969; Blandford and Znajek, 1977) accreting material transports magnetic field down to the event horizon where it can be twisted by the rotation of space-time close to the black hole; the work done in generating the jet comes directly from the rotation of the black hole. The power that can be extracted by this process is (Tchekhovskoy et al., 2011)

$$P_{\text{BZ}} \approx \frac{\kappa}{\mu_0 c} \Omega_{\text{H}}^2 \Phi_{\text{H}}^2 \qquad (7)$$

Here κ is a dimensionless constant that depends on the field geometry, and we drop a correction term that is important only for very large spins. Ω_{BH} is the angular frequency of the black hole horizon, given by

$$\Omega_{\text{H}} = \frac{ac}{2r_{\text{H}}} \qquad (8)$$

where in turn

$$r_{\text{H}} = \frac{GM}{c^2} \left(1 + \sqrt{1 - a^2} \right) \qquad (9)$$

and a is the dimensionless black hole spin parameter

$$a = \frac{Jc}{GM^2} \qquad (10)$$

Φ_{H} is the magnetic flux threading one hemisphere of the black hole, so loosely

$$\Phi_{\text{H}} = \frac{1}{2} \int \vec{B} . \text{d}\vec{S} \qquad (11)$$

The key dependences can be summarized as

$$P_{\text{BZ}} \propto U_B a^2 A \qquad (12)$$

where U_B is (in some sense) the *ordered* magnetic field energy density at the horizon and A is the horizon area, $A \propto r_{\text{H}}^2$. It's important to note that the field has to be ordered on large scales to give a non-zero value of Φ_{H}; simply estimating the plasma β of the accreting material is not sufficient. A dependence on black hole mass (as M_{BH}^2) comes from the area or radius term, so we could even more crudely write

$$P_{\text{BZ}} \propto (BaM_{\text{BH}})^2 \qquad (13)$$

From an observer's point of view, therefore, there are three controlling parameters of the jet power, $Q \approx P_{\text{BZ}}$. Black hole mass can in principle be estimated from AGN properties (this is done routinely for quasars), or estimated from the galaxy mass (or other properties for nearby objects). Black hole spin is not currently accessible except in the case of rapidly spinning, radiatively efficient black holes, and is certainly not easy to estimate for any known radio-loud AGN. And the strength

of the ordered component of field at the event horizon is completely unknown a priori — indeed, properties of radio AGN are the best current way we have of estimating this quantity (Zamaninasab et al., 2014). Notice that there is no *direct* dependence in eq. 13 on the accretion rate $\dot{M}$, but of course the transport of magnetic field down to the event horizon depends on mass accretion. The key point is that the different dependences on physical conditions at the horizon of radiative power (eq. 6) and jet power (eq. 13), notably the effects of spin and the non-linear dependence on black-hole mass in the latter, mean that we should expect a very wide scatter in the relationship between the two quantities both in RI[2] and RE systems.

Rawlings and Saunders (1991) found a relationship between the jet power Q and the narrow-line luminosity L_{NLR}, which is a proxy of the radiative AGN power in radiatively efficient AGN (see above), for a small sample of powerful (3CRR) radio galaxies. Many authors follow Rawlings and Saunders in inferring that there is a one-to-one relationship between accretion power and jet power. This inference is, however, untenable in the light of what we now know about RLAGN. Three criticisms of Rawlings and Saunders's work in the light of the current picture can be made:

1. Rawlings and Saunders used fairly inaccurate measurements of Q. Calculations of Q from observables is difficult, because both ages and lobe energetics of radio galaxies are hard to measure (Section 4.5). However, the main method they used, while it makes use of equipartition field strengths and spectral ages derived from those strengths and is therefore not correct in detail, should give a quantity that is proportional to Q. For the sake of argument, we can accept that this correlation really exists for the objects that Rawlings and Saunders studied.

2. Rawlings and Saunders were not aware of the LERG/HERG dichotomy. In LERGs, since there is no significant nuclear emission from the accretion flow, nuclear emission lines must be photoionized

either by processes irrelevant to the AGN or by the ionizing component of the radiation from the jet itself. Since we know that these objects contain jet-related optical and X-ray nuclear sources even when viewed at large angles to the line of sight (Hardcastle and Worrall, 2000a) they should have emission-line luminosity proportional to the luminosity of the nuclear jet, with substantial scatter imposed by geometrical factors and the availability of cold material in the vicinity of the nucleus. The correlation should be quite different from that exhibited by the HERGs, which is driven by radiative AGN power. Evidence for this can be seen in the radio-luminosity/emission-line-luminosity plots of e.g. Zirbel and Baum (1995); Hardcastle et al. (2009). The LERGs should be excluded from consideration in the work of Rawlings and Saunders. However, this does not invalidate the correlation that they observed for high-excitation objects.

3. Crucially, Rawlings and Saunders had a restricted sample composed of 3CRR objects. When much larger samples of radiatively efficient RLAGN with AGN power indicators are considered (e.g., Punsly and Zhang, 2011; Mingo et al., 2014; Gürkan et al., 2015) we find sources that have much lower radio luminosities for a given accretion power than would be expected from the correlations seen in the 3CRR objects. Thus the central result of Rawlings and Saunders seems to be due to some selection bias inherent in the selection of the most powerful radio-loud objects.

The observations instead motivate the following straw-man model for the relationship between Q and bolometric AGN radiative power L_{rad}:

1. Radiatively efficient AGN with a given L_{rad} can have jet powers Q that range continuously from zero up to a maximum $Q \approx L_{rad}$. (Note that in BZ models the jet power can exceed the accretion power for very high black hole spin parameters, but this would presumably not be the normal expectation.)

2. Selection of the most radio-luminous sources selects for large, mature sources with the highest Q, for which $Q \approx L_{rad}$: these are also the sources where a L_{radio}–Q correlation is expected. Therefore, for the most radio-luminous objects, we expect to see a correlation between Q, or radio luminosity, and L_{rad}, or its proxies, as observed by Rawlings and Saunders (1991) and many others.

3. However, as we relax the radio selection criteria we expect to see more sources that have lower jet

---

[2] The widely cited work of Merloni and Heinz (2007) argues for a correlation between the radiative output and Q in RI systems, but this is based on the use of the 2–10 keV X-ray nuclear emission as a proxy for AGN radiative output. In the picture presented here, the 2–10 keV emission from these systems comes from the jet itself — see e.g. Hardcastle et al. (2009) and references therein — and so does not provide any information about the AGN radiative power. The strong correlation that they observe is essentially showing that a reasonably constant fraction of the jet power emerges as X-rays in these systems, which by selection are relatively unaffected by beaming.

powers (radio luminosities) for a given L_{rad}, as observed (Gürkan et al., 2015)

4. In this picture, which is consistent with that of e.g. Kimball et al. (2011), there is no radio-loud/radio-quiet dichotomy. The so-called radio-quiet quasars simply have $Q \ll L_{\mathrm{rad}}$ (though $Q = 0$ is not excluded). Below a certain jet power, radio emission from star formation in the host galaxy, or from other processes, may dominate the integrated emission (Gürkan et al., 2019) though high-resolution radio observations may still detect a radio core.

We conclude that observations of optical AGN properties, even setting aside the important LERG population, are not useful for interpreting the distribution of jet power.

6.3. Fuelling the black hole

From a galaxy formation perspective we can imagine two different classes of mass to fuel black hole growth (setting aside black hole-black hole merger): gas channelled to the central regions of the galaxy by 'secular processes' within the host galaxy itself, including the very important channel (in massive galaxies) of cooling from the hot phase; and gas which is brought in to the host galaxy by a merger with a gas-rich system. The fuelling of black hole growth and hence AGN activity connects the nature of the AGN, as discussed earlier in this Section, with the 'feedback' role of (RL)AGN in galaxy formation models to be discussed in Section 8.

The present authors proposed some time ago (Hardcastle et al., 2007b) that there was a one-to-one relationship between the two fuel sources for RLAGN (roughly speaking 'hot gas' from inside the galaxy and 'cold gas' from outside) and the accretion mode (RI/RE), building on work that suggested that the fuelling of the jets could be accomplished by a simple Bondi flow (Allen et al., 2006). This model has now been superseded in its simplest form for two reasons. Firstly, if we can interpret the RI/RE difference as simply a transition in Eddington-scaled accretion rate as discussed above, then there is no reason why hot gas accretion should always contrive to stay below this boundary in accretion rate or why cold gas accretion should always be above it. Secondly, the current best understanding of accretion from the hot phase is that it is mediated by the cooling instability (e.g., Pizzolato and Soker, 2005; Gaspari et al., 2012, 2013), which causes clumps of cold material to 'rain' into the centre of the galaxy; thus the original argument that the material in a Bondi flow would be too hot to form a radiatively efficient accretion disk is no longer relevant or valid. It remains the case that some

(mostly RE) RLAGN appear to require a mass accretion rate far in excess of what can be provided by cooling, and it is plausible to invoke merger-triggered cold gas infall as a mechanism to fuel these objects. But our current view of the relationship between the fuel source and the accretion mode in RLAGN (set out in more detail by Hardcastle 2018a) is that there is an association between the two rather than a one-to-one correlation. Fuelling by (cooling-mediated) hot gas accretion will tend to take place in massive systems with massive central black holes and to generate rather low accretion rates, favouring RI accretion. Fuelling through gas-rich mergers will take place in lower-mass environments and will be capable of giving rise to high accretion rates, favouring RE accretion. However, in this picture, it is not safe to infer the fuel source of any particular object from its accretion mode. These connections are of importance for galaxy feedback, and are discussed further in this context in Section 8.

We finally note that the *availability* of fuel in a particular host galaxy should not be conflated with the actual *accretion* of that fuel. It is well known that the cold gas deposited by mergers may not trigger AGN activity until long after the merger event has begun. Similarly, objects that are currently RI appear to be able to accumulate quite large masses of molecular gas in the centre of the host galaxy but are clearly not accreting it at a high rate. If this gas represents a fuel reservoir for the AGN, it is not at all clear how the inflow and outflow from the reservoir are controlled by cooling. We return to this point in in Section 8.

7. Host galaxies and environments

The properties of the host galaxies in which radio-loud AGN live provide further information with which to test our understanding of unified models and the physical origin of the FR break (Section 3), but, perhaps more importantly, they allow the investigation of crucial questions about how AGN jets are triggered, and the energetic impact and feedback role of jets within the context of galaxy evolution. Efforts to characterise radio-galaxy hosts date back to the early studies of double radio sources, and the association of Cygnus A with a galaxy merger (Section 2.2). Below we discuss current understanding of the host galaxy properties and wider environments of radio galaxies.

7.1. Host galaxies

A long-standing question for radio-galaxy physics, and for galaxy evolution more widely, is why some

galaxies possess AGN jets and others don't: what triggers a galaxy to become radio-loud? The earliest clue to the galaxy conditions needed to trigger strong radio-loud AGN activity came from its association with massive elliptical galaxies (e.g., Matthews et al., 1964). Over the past few decades a detailed understanding of the host-galaxy properties of AGN in the local Universe has emerged, with investigations of large galaxy samples from the SDSS playing a particularly crucial role (e.g., Heckman and Best, 2014, and references therein). Below we discuss key relationships between radio AGN activity and host-galaxy properties: (1) links with host-galaxy stellar and black hole masses, (2) links with galaxy morphology and disturbance, and (3) links with star-formation properties. We also highlight any differences between observed relationships for FRI and FRII radio galaxies, and for LERG and HERG RLAGN populations. We emphasize that the majority of studies are based on low-redshift radio galaxy populations, and so some conclusions may not apply to high-redshift radio galaxy populations whose host galaxy properties remain poorly constrained.

7.1.1. Stellar and black-hole masses

A strong relationship between radio-loud AGN fraction and stellar mass was first pointed out by Auriemma et al. (1977), and was demonstrated for large samples by Best et al. (2005), who found that more than 30 per cent of galaxies with stellar mass $M_* > 5 \times 10^{11}$ M$_\odot$ possess a radio-loud AGN with $L_{1.4\text{GHz}} > 10^{23}$ W Hz^{-1}. Recently, Sabater et al. (2019) have shown with more sensitive radio data that the most massive galaxies ($> 10^{11}$ M$_\odot$) are always 'switched on' with radio AGN activity at a luminosity $L_{150\text{MHz}} > 10^{21}$ W Hz^{-1} (see also Brown et al. 2011), and also that radio AGN fraction has a stronger dependence on stellar mass than on black hole mass. Best et al. (2005) found no significant difference in the stellar mass dependence of radio activity for optically active AGN (i.e. HERGs) and optically inactive AGN (LERGs). However, it is known that as a population, HERGs are hosted by less massive galaxies than LERGs (e.g., Tasse et al., 2008; Smolčić et al., 2009; Best and Heckman, 2012). Morphology (FR class) has also been linked to host galaxy mass (e.g., Lin et al., 2010); however, Best and Heckman (2012) argue that these results are likely to be driven by the overlap between optical excitation and FR class (as discussed in Section 6.1), with evidence that strong emission-line FRIIs (i.e. HERGs) are most distinct from FRIs (predominantly LERGs). It is worth noting, however, that a link between host-galaxy mass and radio morphology — independent of accretion mode — would be expected

for samples matched in radio luminosity if the environmental jet disruption model for the FR break (Section 3.1) is correct (Mingo et al., 2019).

7.1.2. Mergers and interactions

Studies over many decades have looked for signatures of disturbance in radio-galaxy hosts that could be linked to the triggering of activity (e.g., Heckman et al., 1986). There is considerable evidence for disturbance in the host galaxies of powerful radio galaxies at high redshifts (e.g., Best et al., 1997). Ramos Almeida et al. (2012) found that evidence for disturbed host-galaxy morphologies was almost universal in a sample of powerful high-excitation radio galaxies, while present at a lower level in passive galaxies in the same redshift range. Recently Pierce et al. (2019) demonstrated that the prevalence of such features in HERGs is linked to radio luminosity, with a similar but less radio luminous sample showing a lower prevalence of disturbance. Pierce et al. (2019) also note a higher prevalence of late-type galaxy hosts at lower radio powers, and suggest that secular triggering mechanisms related to disk instabilities or bars may be relevant for this HERG population. However, there is also some evidence that interaction with neighbouring galaxies is relevant for the triggering of LERGs: both Sabater et al. (2015) and Pace and Salim (2014) present evidence that LERG activity is influenced by interaction with neighbours, independently of large-scale environment. A recent large-sample study by Gordon et al. (2019) found a higher prevalence of major mergers in LERG hosts compared to a control population, but the overall prevalence was only 10 per cent. However, Ellison et al. (2015) found that an enhanced prevalence of LERG activity in galaxy pairs was driven by a combination of halo mass and stellar population properties, suggesting that interactions may not be directly responsible for enhanced probability of radio AGN activity in LERGs.

7.1.3. Galaxy morphology

It has been long established that radio-loud AGN prefer early to late-type galaxy hosts (Matthews et al., 1964), but this does not mean that spirals are incapable of hosting radio jets: there are now a number of examples of spiral-hosted radio AGN with structures on $>$ kpc scales (e.g., Ledlow et al., 2001; Croston et al., 2008c; Hota et al., 2011; Mao et al., 2015; Mulcahy et al., 2016). Additionally, larger samples of spirals possessing smaller scale AGN-associated radio emission have been identified by Kaviraj et al. (2015), who also established that the spiral hosts typically had high stellar masses comparable to elliptical galaxy radio AGN

hosts. The observed strong relationship between morphology and radio AGN activity may be driven partly by stellar and black hole mass differences, but is likely ultimately to be controlled by differences in galaxy evolutionary state, accretion rate and the presence of a hot gas atmosphere (e.g., Krause et al., 2019).

7.1.4. Colours and stellar populations

Finally, there are firm connections between radio properties and galaxy colours, stellar populations and star-formation rates. In the current picture of galaxy evolution the properties of normal galaxies fall on a 'main sequence' of star formation in which the mean star-formation rate is proportional to the galaxy mass, with a redshift-dependent normalization (Elbaz et al., 2011). At some point star formation ceases and galaxies become 'red and dead', moving to a region below the main sequence in terms of star-formation rate. In the context of this picture, the vast majority of RLAGN in the local Universe are hosted by high-mass galaxies lying below the main sequence in terms of their star-formation rates (Gürkan et al., 2018). In general, radio-loud AGN are found to have lower star-formation rates than radio-quiet AGN (e.g., Gürkan et al., 2015). There are, however, differences in the star formation properties of LERG and HERG RLAGN. In addition to having lower stellar mass, HERG hosts are systematically bluer, and have higher star formation rates than those of LERGs (e.g., Baldi and Capetti, 2008; Smolčić et al., 2009; Best and Heckman, 2012; Janssen et al., 2012; Hardcastle et al., 2013). Evidence has also been found for enhanced blue light in the central regions of radio-loud AGN relative to control samples (Mahabal et al., 1999; Mannering et al., 2011), suggesting enhanced star formation that could be due to simultaneous triggering of AGN and star formation activity via an inflow of gas, or due to jet-induced star formation.

7.1.5. Summary

In summary, it is well established that all galaxies in the local Universe are not equally capable of hosting a radio-loud AGN. Radio AGN activity is strongly linked to stellar mass — this is also thought to be the driver of observed connections with galaxy colour/morphology, and black-hole mass. There are (at least) two possible origins for this connection, both related to the hot, hydrostatic halo typically associated with more massive galaxies at low redshifts. Krause et al. (2019) demonstrate that a substantial change in the halo density occurs at a stellar mass of $\sim 10^{11}$ M$_\odot$, and argue that jets of any power could be produced across the stellar mass range,
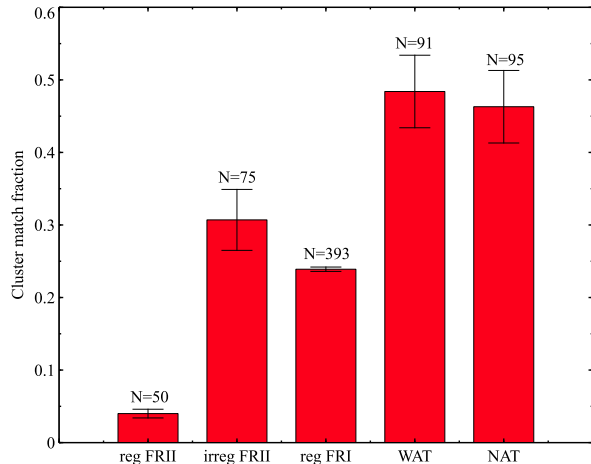
Figure 3: The relationship between radio morphology and large-scale environment for the $z < 0.4$ subset of the Mingo et al. (2019) LOFAR RLAGN sample: the SDSS (Wen et al., 2012) cluster match fraction and its uncertainty is determined via the method of Croston et al. (2019) for five morphological classes (Mingo et al., 2019), but with FRIIs further divided into morphologically regular and irregular subsets following the criteria of Croston et al. (2017).

but are only confined and radio-luminous in the higher-density haloes present at higher stellar mass. In reality it is likely that (at low redshifts) accretion rate is also linked to stellar mass — if the predominantly LERG radio jets in low-redshift samples are fuelled by material cooling out of the hot halo, the inferred higher density of the hot gas halo is required to achieve sufficiently high accretion rates.

7.2. Large-scale environments

The large-scale (galaxy group or cluster-scale) environments of radio galaxies are of interest for a number of reasons: for jets that grow to scales of tens of kpc or more they are a driving influence on subsequent jet evolution and morphology (as discussed in Section 5), and are the location where most of the jet energy is deposited, and for at least some radio-galaxy populations they are thought to be important for triggering and fuelling of the jets via a feedback cycle that has been particularly well studied in galaxy clusters — we discuss this feedback cycle in Section 8. Environmental studies of radio jets date back more than 40 years, with optical studies indicating links between radio galaxies and Abell clusters and connections between environment and radio morphology (e.g., Longair and Seldner, 1979; Prestage and Peacock, 1988).

7.2.1. Environments and radio properties

The relationship between radio-galaxy properties and large-scale environment is now well determined in the local Universe. Recent studies of radio galaxies spanning a wide luminosity range in narrow redshift slices have removed the potentially confounding effect of strong flux limits in early catalogues, enabling correlations and trends with radio properties to be more carefully investigated (e.g., Best, 2004; Ineson et al., 2015). While there are a number of famous and well-studied examples of nearby cluster-centre radio galaxies (e.g., Perseus A, M87), the bulk of the local radio galaxy population live in galaxy groups (e.g., Best, 2004; Croston et al., 2008a; Ineson et al., 2015; Ching et al., 2017; Croston et al., 2019).

Radio morphology is strongly linked to large-scale environment, as shown in Fig. 3, which shows the fraction of radio galaxies at $z < 0.4$ associated with SDSS galaxy clusters ($M_{500} > 10^{14} M_\odot$) for different morphological classes (from the LOFAR sample of Mingo et al. 2019). The average cluster match fractions are significantly different for FRI and FRII radio galaxies (e.g., Croston et al., 2019), as found in many previous studies, but it is particularly striking that the morphologically regular ('classical double') FRIIs are almost never found in rich environments, unlike all other classes.

A well-known relationship exists between bent-tailed radio galaxies and galaxy clusters: both the wide-angle tail (WATs) and narrow-angle tail radio galaxies (NATs) are found preferentially in richer environments than the general radio galaxy population (e.g., O'Dea and Owen, 1985; Mingo et al., 2019; Garon et al., 2019). The explanation for this is thought to be the movement of the host galaxy through the intracluster medium, which leads to curving and in some case extreme bending of the jets and tails in the direction opposite to the direction of travel. It has therefore been suggested that bent radio galaxies can be used as signposts to rich environments at high-redshift (e.g., Johnston-Hollitt et al., 2015; Paterno-Mahler et al., 2017). The present authors have suggested (Croston et al., 2017) that the strong preference of morphologically regular FRIIs for poor environments could also provide a powerful tool for finding and characterizing group-scale gas haloes at the epoch of cluster formation.

7.2.2. Environments and accretion mode

Another important conclusion from recent studies is that radio-galaxy large-scale environment is linked to accretion mode (e.g., Tasse et al., 2008; Lin et al., 2010). X-ray studies, which can provide more stringent constraints on cluster richness than galaxy number counts or two-point correlation functions, have found that low-excitation radio galaxies span the full range of environmental richness from poor groups to rich clusters, while high-excitation radio galaxies preferentially avoid rich environments (e.g., Ineson et al., 2013, 2015). It is not completely trivial to disentangle LERG/HERG environmental differences from FRI/II differences, because of the strong association between FRIs and LERGs in well-studied samples, but it has been known for some time that FRII LERGs prefer rich environments more consistent with the FRI LERG population (Hardcastle, 2004), and several studies find strong indications that accretion mode is linked to environment separately from morphology (Gendre et al., 2013; Ineson et al., 2015). For LERGs, a relationship has also been found, in both optical and X-ray environmental studies, between radio luminosity and environmental richness (Ineson et al., 2015; Ching et al., 2017), which appears not to be driven by a common link to black hole mass, and so may indicate a tight link between ICM properties and jet power. These environment–accretion mode connections provide support for AGN feedback models (see the following Section) and lend further support to arguments that accretion mode is linked to the evolutionary state of the host galaxy (Section 6.1).

7.3. Cosmic evolution of RLAGN, host galaxies and environments

In the context of a galaxy evolution model where the relationship between stellar mass, accretion rate, and the evolution of a hot gas atmosphere change significantly over cosmic time, we would expect to observe considerable evolution of the properties of radio-loud AGN. Evidence for such evolution is extensive. It has been known for many decades that the space density of RLAGN was higher at early times than in the local Universe (e.g., Schmidt, 1968). It has been shown that at lower radio luminosities, the space density begins to decline at redshifts higher than $z \sim 1$, but for higher luminosity RLAGN space density remains high out to $z \sim 3$ (Rigby et al., 2011). These changes are likely to be linked to strong differences in the evolution of low and high excitation RLAGN populations: the space density of high-excitation radio galaxies increases between $z < 0.5$ and $z = 1 - 2$, while that of low-excitation radio galaxies declines (Best et al., 2014; Williams et al., 2018). The implications for these results in the context of feedback from RLAGN are discussed in Section 8.

We would also expect to see evolution in the host galaxy properties for jets of a given power, but even setting aside the challenges of making accurate jet power inferences across a wide redshift range (see Section 4.5)

it is not straightforward to test such predictions due to the challenges of probing comparable ranges of radio luminosity and rest-frame host galaxy properties at different redshifts. The increase in space density of radio-loud AGN at $z \sim 2 - 3$ suggests that RLAGN activity must be more prevalent in lower mass host galaxies at high redshifts, and evidence indeed supports this conclusion. Williams and Röttgering (2015) found that the host galaxies of RLAGN at $1 < z < 2$ extend two orders of magnitude lower in stellar mass than hosts of local RLAGN (Best and Heckman, 2012) — this population of radio galaxies in low stellar mass hosts are predominantly HERGs (Williams and Röttgering, 2015; Williams et al., 2018). Other studies have reached somewhat different conclusions (e.g., Delvecchio et al., 2017), and deep radio surveys over wider areas (such as will shortly become available with LOFAR) should enable these questions to be investigated more fully with samples spanning a wide range in radio luminosity at high redshifts.

The conclusions relating to large-scale environments discussed in the previous Section have also been derived primarily for RLAGN populations in the local Universe (typically $z < 0.5$). At $z > 1$ environmental studies have only been possible to date for the rare objects at the high-luminosity tail of the population (e.g., Hardcastle and Worrall, 2000b; Belsole et al., 2007), leading to difficulties in making comparisons with local populations or examining relationships with radio properties. Luminous, high-redshift radio galaxies appear to be strongly associated with cluster and (at $z > 2$) protocluster environments, and have proved a useful tracer of the richest overdensities at $z > 2$ (e.g., Venemans et al., 2007; Miley and De Breuck, 2008; Wylezalek et al., 2013; Hatch et al., 2014). With new and upcoming surveys, it will be possible to obtain a more complete picture of high-redshift radio galaxies across the full radio luminosity range. Simple hydrodynamical considerations suggest that radio galaxies of similar luminosity and size (and hence internal pressure) at low and high redshift must be embedded in gas at similar pressures. For this reason the morphology and size distributions of high-redshift radio galaxy populations as a function of luminosity will also provide insights into how the environments of radio galaxies evolve with redshift.

8. The feedback role(s) of RLAGN

Much recent research on radio-galaxy populations has been motivated — at least in part — by the now widespread acceptance that RLAGN are an important galaxy feedback mechanism, playing a key role in the evolution of galaxies and large-scale structure (e.g., Cattaneo et al., 2009). Wider discussions of AGN feedback in galaxy formation models can be found in the recent reviews of Somerville and Davé (2015); Naab and Ostriker (2017), and of the observational evidence for AGN feedback in the reviews of Fabian (2012) and McNamara and Nulsen (2007, 2012). In this section we summarize current understanding of the potential galaxy feedback role(s) of RLAGN as indicated by cosmological simulations and galaxy evolution models, before discussing observational evidence of jet impact and the feedback roles of different radio-galaxy subpopulations. Fig. 4 draws together the discussions of RLAGN populations, accretion and jet power earlier in the Chapter with the authors' perspective on the potential feedback roles of AGN jets, which we explain further in the sections that follow.

8.1. The need for AGN jet-driven feedback in galaxy evolution

Galaxy feedback processes that regulate the formation of stars and growth in stellar mass are a key element of modern galaxy formation models (e.g., Somerville and Davé, 2015; Naab and Ostriker, 2017). A wide range of processes associated with star formation and black-hole growth affect the thermodynamical, chemical and star formation histories of galaxies, and much observational and theoretical/computational effort is currently being devoted to disentangling and quantifying these processes. The general argument that feedback processes are important is not controversial, but there is considerable debate about the extent to which some form of AGN feedback is needed to explain particular mismatches between models and observations, about the microphysics of feedback mechanisms and energy transport within the ISM and ICM, and about the relative importance of different AGN feedback mechanisms (which include the effects of winds, jets, cosmic rays, and radiation). Feedback from radio-galaxy jets is in some ways one of the best understood aspects of this problem, and we focus specifically on the potential role of mechanical feedback from AGN jets in the discussion that follows. A wide range of observational constraints on jet mechanical feedback in the local Universe have been assembled over the past two decades, particularly from *Chandra* and *XMM-Newton* observations of galaxy clusters and groups, and more recently from *Hitomi* and ALMA — these will be discussed in the next section. However, many questions still remain, including the details of how, when and where a feedback loop operates and the mechanisms by which the jet energy is coupled to surrounding gas in different contexts,
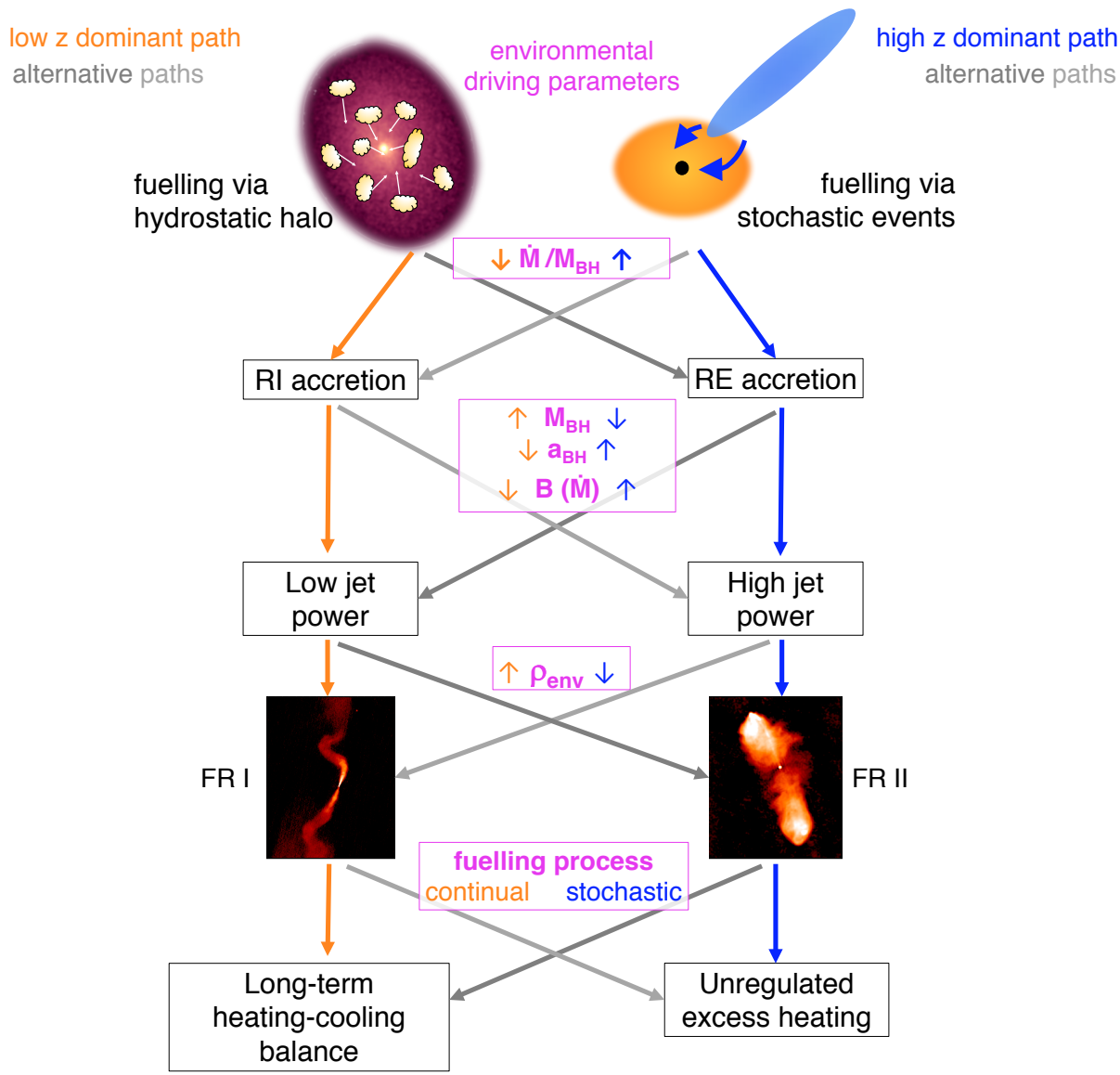
Figure 4: A diagrammatic summary of the relationship between fuelling, accretion, jet production and feedback, as described in Sections 6.1 and 8. In principle systems can follow any of the arrows connecting accretion and jet behaviour, but the choices of pathway are controlled by a series of environmental parameters (magenta boxes), which are interconnected and closely linked to the galaxy's evolutionary history.

as well as broader questions about the role of jets in different environments and at different epochs.

What problems can jet kinetic feedback solve? AGN feedback considered more broadly has been invoked in models of galaxy evolution primarily to address two major mismatches with observations: (i) the need to suppress star formation in the most massive galaxies in order to reproduce the high-mass end of the local galaxy luminosity function (e.g., Benson et al., 2003) and prevent cooling flows in galaxy clusters (e.g., Peterson et al., 2003; Sakelliou et al., 2002), and (ii) the need to explain the origin of the strong colour bimodality of galaxies (e.g., Strateva et al., 2001; Baldry et al., 2004), which requires rapid quenching of star formation, moving star-forming galaxies to the red sequence of quiescent galaxies. AGN feedback is also implicated in the origins of the well-known galaxy black-hole – bulge mass correlation, as suggested by Silk and Rees (1998), although such a relation can arise through mergers in the absence of feedback self-regulation (Peng, 2007). Finally, the evolution of the gas mass fraction of dark matter haloes, the properties of the circumgalactic medium, and the thermodynamic properties of gas in galaxy groups and clusters, are all highly sensitive to the injection of energy from AGN over a wide range in redshift (e.g., McCarthy et al., 2011; Le Brun et al., 2014; Davies et al., 2019; Voit et al., 2018; Kauffmann et al., 2019).

Modern hydrodynamical cosmological simulations take a range of approaches to modelling black hole growth and consequent AGN feedback, ranging from a single mode of feedback controlled by the mass accretion rate, coupling to the ISM with fixed efficiency (e.g., Schaye et al., 2015; McCarthy et al., 2017), to different modes associated with high and low accretion rates that may or may not explicitly be linked to specific outflow types or coupling mechanisms (e.g., Vogelsberger et al., 2014; Weinberger et al., 2018; Davé et al., 2019). The majority of implementations are in practice agnostic about the relative contributions of AGN jets, winds and radiative feedback, but provide insights into the importance of different accretion rate regimes in influencing particular aspects of galaxy growth (e.g., Rosas-Guevara et al., 2016). In general it is found that most black hole growth for moderately massive black holes must take place when AGN are accreting at a high fraction of the Eddington rate, so that radiatively efficient AGN activity is associated with the evolution of the $M_{BH}-M_{bulge}$ relation. Low Eddington-scaled accretion rates occur at later times, with the associated radiatively inefficient AGN activity linked to the suppression of star formation in massive galaxies. There is less consensus as to which accretion regime is relevant for the quenching of star formation by AGN (e.g., Bower et al., 2017; Terrazas et al., 2019).

The association of radiatively inefficient accretion with jet generation (see also the X-ray binary context elsewhere in this volume), together with the strong observational evidence for the impact of jets in massive galaxies at low redshift, initially led to a widely discussed paradigm of separate 'radio' and 'quasar' modes of AGN feedback, with the former responsible for solving the mismatch at the massive end of the galaxy luminosity function, and the latter associated with black-hole growth (e.g., Croton et al., 2006). There remains a focus in the literature on jet kinetic feedback as a 'maintenance' process that regulates star formation at late stages of evolution (e.g., Fabian, 2012) — we discuss this scenario further in the next two subsections. However, as we emphasise in Section 6.1 and in Fig. 4, powerful AGN jets also occur at high Eddington-scaled accretion rates, with increasing prevalence towards the peak of cosmic star formation, and so in Section 8.4 we also consider the potential relevance of feedback from RLAGN for other aspects of galaxy formation including at earlier stages in galaxy evolution.

8.2. Observational evidence for jet kinetic feedback

The observational evidence for the energetic impact of RLAGN jets in the local Universe is extensive and we only summarize it briefly here — see McNamara and Nulsen (2007, 2012) for more comprehensive discussion. Direct estimates of jet energy input come from X-ray surface brightness deficits in galaxy clusters and groups ('cavities'), from detections of shock fronts associated with expanding radio lobes on galaxy scales and in clusters, and from ripples believed to be transporting and spreading out the injected energy through the ICM gas in cluster cores. Indirect energy budget estimates based on improved knowledge of the physical conditions within radio-galaxy lobes provide corroborating information, as do increasingly sophisticated hydrodynamical simulations of radio-lobe propagation that reproduce observations.

Cavities excavated by expanding radio lobes were first identified in *ROSAT* images (Böhringer et al., 1993; Hardcastle et al., 1998) and subsequently found in many clusters and studied in depth using *Chandra* (e.g., Dunn and Fabian, 2004; Dunn et al., 2005; Bîrzan et al., 2004; Bîrzan et al., 2008). They provide a direct measure of the $p\mathrm{d}V$ work carried out on the surrounding medium as radio lobes expand (Section 4.5), and such observations have demonstrated firmly that sufficient energy is being transferred from expanding radio galaxy lobes to

offset the current rate of gas cooling in the centres of cool core clusters in the nearby Universe. Cluster cavities have been detected out to $z \sim 1$ (Hlavacek-Larrondo et al., 2015), but there remain observational limitations and selection effects that affect our ability to draw robust population-wide conclusions (e.g., Bîrzan et al., 2012). There is also substantial observational evidence for energy transfer from jets to their environments via shocks, which have been detected in a range of environments (e.g., Kraft et al., 2003; Croston et al., 2007; Forman et al., 2007; Croston et al., 2009; Randall et al., 2015), on scales ranging from the central ISM to hundreds of kpc.

While shock heating is likely to be important in some situations, the identification of ripple features in the intracluster medium of the Perseus cluster (Fabian et al., 2003, 2006) demonstrated that there is a means of distributing jet energy injection azimuthally to influence the entire cluster core region in which heating is needed to balance cooling. Similar ripples have now been identified in several other clusters and groups (Forman et al., 2005; Sanders and Fabian, 2008; Blanton et al., 2011). Recently the (sadly short-lived) *Hitomi* mission was able to make the first precise measurements of gas motions in the core of the Perseus cluster (Hitomi Collaboration et al., 2016), providing constraints on the energy stored in turbulent motions and the nature of energy transport. There has been some debate about the apparent 'quiescent' nature of the gas in the cluster core region revealed by *Hitomi*, but several studies have shown that this is not inconsistent with the gentle mode of AGN feedback heating that appears to be in operation in cool-core regions (e.g. Lau et al., 2017; Fabian et al., 2017).

Further important observational clues to the nature of jet feedback come from a wealth of observations of atomic and molecular filaments and outflows of gas in the central regions of galaxies hosting RLAGN. Evidence for outflowing atomic gas has been found in both powerful RLAGN (e.g., Tadhunter, 1991) and 'radio-quiet' systems with small-scale jets (e.g., Morganti et al., 1998; Rupke and Veilleux, 2011) — see Morganti and Oosterloo (2018) for a recent overview of outflow properties inferred from HI absorption studies. There is growing evidence, particular from recent ALMA studies, of massive outflows of molecular material entrained or uplifted by jets or rising radio lobes (e.g., Alatalo et al., 2011; Dasyra et al., 2015; McNamara et al., 2014; Russell et al., 2014, 2016, 2017; Tremblay et al., 2018). A number of these examples are cool-core clusters, the environments in which AGN feedback is required to act most strongly to suppress cooling and star formation. These systems have long been known to contain spec-

tacular filamentary nebulae (e.g., Crawford et al., 1999), of both atomic and molecular gas (e.g., Edge, 2001; Hatch et al., 2005; O'Dea et al., 2008). The physics of these filaments is complex, and their origins are still under debate, but substantial evidence points to cold, low entropy gas being lifted from the cluster centre to distances of tens of kpc, most likely in the wake of rising radio bubbles (e.g., Fabian, 2012). The kinematics and locations of cold gas in cooling hot gas haloes provide crucial clues to how jet feedback from AGN can self-regulate so as to maintain a long-term balance between heating and cooling as required by observations (e.g., McDonald et al., 2018) and by galaxy evolution models (see previous Section).

8.3. Self-regulation and heating-cooling balance

In parallel with observational advances in studying heating and cooling in hot hydrostatic haloes, there has been much research around the mechanisms of achieving a self-regulating AGN feedback loop. As mentioned in Section 6.3, it has been proposed that thermally unstable gas cooling is triggered under conditions related to the ratio of cooling to free-fall time (e.g., Sharma et al., 2012; McCourt et al., 2012; Gaspari et al., 2012; Voit et al., 2015), leading to the condensation of clumps of cold material that 'rain' onto the central AGN, losing angular momentum via collisions so as to accrete onto the central black hole (e.g., Pizzolato and Soker, 2005; Gaspari et al., 2012, 2013). This 'chaotic cold accretion' (CCA) powers the RLAGN, leading to outward flow of energy and consequent heating, and so enabling self-regulation of the cooling process. Observations of gas conditions in galaxy, group and cluster halos (e.g., McNamara et al., 2016; Hogan et al., 2017; Pulido et al., 2018) suggest that the uplift and movement of thermally unstable gas driven by the AGN outflow may play a crucial role in stimulating the self-regulating feedback cycle. A more in-depth discussion of current debates around the physics of heating, cooling and the AGN feedback loop in hot atmospheres can be found in the recent review of Werner et al. (2019).

As well as detailed individual and small sample studies of jet feedback, there have been a number of attempts to assess the population-wide balance between cooling and heating in hot atmospheres (on galaxy, group and cluster scales). Such estimates rely on a well-determined radio luminosity function (and ideally also well constrained evolution of the luminosity function), and on robust methods to translate from radio luminosity to jet kinetic power. The radio luminosity function is now well determined in the local Universe (Mauch and Sadler, 2007). There remain substantial caveats in

converting to jet power (see Section 4.5), but it is possible to draw some reliable general conclusions about the heating and cooling balance at low redshifts. Best et al. (2006) compared the rate of heating via mechanical jet energy input, based on an estimate of the local radio luminosity function obtained from cross-correlation of SDSS with NVSS and FIRST and conversion to jet power via X-ray cavity relations, to cooling rates in elliptical galaxies determined from the relationship between X-ray and optical luminosity, finding remarkably good agreement. Smolčić et al. (2017) recently used the deep COSMOS field radio data to investigate the cosmic evolution of the RLAGN 'kinetic luminosity function' finding good agreement with the results of Best et al. (2006) at low redshift, with the kinetic luminosity density increasing out to $z \sim 1.5$ and then declining gradually towards $z \sim 5$. Observational constraints on cooling rates do not exist beyond $z \sim 1.5$, but they find reasonable agreement with the cooling rates required in the semi-analytical model of Croton et al. (2016). The present authors recently constructed (Hardcastle et al., 2019b) a sample of $\sim 23,000$ RLAGN from the LoTSS DR1 catalogue and used a new analytic model for radio-lobe dynamical evolution, accounting for the effects of environmental variation, radiative losses and redshift, to obtain more realistic conversions from radio luminosity to jet power and thus make similar estimates of the kinetic luminosity function and overall heating rate at $z < 0.7$. As with previous work, it is concluded that the rate of heating from RLAGN jets in the local Universe is well matched to the cooling luminosities of galaxy groups and clusters.

At the level of individual objects it remains unclear how tightly cooling and heating processes are coupled across the full range of RLAGN environments at low redshift. The observational evidence in support of the CCA mechanism relates mainly to brightest cluster galaxies, while, as noted in Section 6.1, a number of nearby radio galaxies possess apparently stable disks of molecular gas (e.g. Lim et al., 2000; Prandoni et al., 2010) whose origin and relationship to AGN fuelling is unclear. Nevertheless, while the observational picture remains complex and timescales relating to heating and cooling balance poorly constrained, there is now substantial evidence for a self-regulated feedback scenario in massive systems at low redshift, linked to the presence of hot hydrostatic haloes. We suggest that the pathway indicated by orange arrows in Fig. 4 represents the most common RLAGN population at low redshifts: RI accretion ultimately originates from cooling out of a hot-gas halo, with long-term balance between heating and cooling mediated by low-power, FRI morphol-ogy jets. However, as indicated by the grey arrows, the RLAGN population is complex, and under some conditions RE sources (HERGs) and/or FRIIs will also participate in self-regulated feedback. Conversely, not all RI and/or FRI morphology sources will be in environments where heating and cooling are in balance.

8.4. Jet kinetic feedback at high redshifts

It is difficult to extrapolate the self-regulated RLAGN feedback scenario described in the previous Section to higher redshifts. One reason is our limited knowledge of the high-redshift radio luminosity function, and another is the increasingly large systematic uncertainty and potential biases in conversions from radio luminosity to jet power beyond the local Universe, due to the increasing importance of radiative losses and increased uncertainty in environmental properties (see Section 4). A further important factor is redshift evolution in the distribution of accretion mode for RLAGN. Section 6.1 discussed our current understanding of accretion mode in RLAGN: the local population is dominated by radiatively inefficient (RI) systems, but a substantial population of radiatively efficient (RE) RLAGN exist, and are more prevalent at higher redshifts, as discussed in the previous Section. This evolution in the RLAGN population may have interesting implications for jet feedback at $z > 1$.

As argued above (Sections 6.1, 6.3), accretion mode in RLAGN is controlled by the ratio of accretion rate to black-hole mass, and not by the source of accreting material: in principle the chaotic cold accretion mechanism discussed in the previous section can achieve accretion rates high enough to power RE RLAGN, particularly in systems with lower mass black holes. However, powerful RE (high-excitation) RLAGN are observed to be located systematically in lower mass galaxies and poorer large-scale environments than RI RLAGN of similar inferred jet powers (Section 7). From the perspective of self-regulating feedback, this population appears anomalous: their accretion rates (in absolute terms) from CCA, or other processes related to the hot-gas halo, must be lower than for their RI counterparts in richer haloes and more massive host galaxies, but their jets are transporting similar amounts of energy into their surroundings. The simplest explanation — consistent with the high prevalence of galaxy merger signatures in the hosts of the most powerful high-excitation RLAGN (e.g., Ramos Almeida et al., 2012) — is that powerful RE systems achieve the high accretion rates necessary to power their jets via an additional mechanism of cold gas inflow driven by galaxy mergers and interactions. The energetic output of powerful RE systems is then

decoupled from a self-regulating feedback loop, so that we might expect larger imbalances between heating and cooling in these systems compared to those (predominantly, but probably not exclusively, RI) systems that are accreting only from their hot-gas halo. We note that the conclusion that powerful HERGs inhabit poor environments derives from observations at $z < 1$ (Section 7), but simple hydrodynamical arguments indicate that radio galaxies of similar jet power and size will inhabit similarly rich large-scale gas haloes at any redshift (e.g., Croston et al., 2017). We suggest that a substantial proportion of the $z > 1$ HERG population are likely to be 'over-heating' their environments: this population could be responsible for the known excess entropy present in hot gas haloes at low mass (e.g., Pratt et al., 2009; Short et al., 2010; Fabian, 2012). We indicate this feedback mode as the possible endpoint of the dominant high redshift pathway, indicated by blue arrows, in Fig. 4, but again emphasise that under appropriate conditions sources may instead follow the grey pathways in which accretion, jet and feedback properties deviate from the majority behaviour. Such populations could form significant sub-populations for particular combinations of redshift and galaxy/halo mass.

Another high-redshift jet population of particular interest are the galaxy-scale jet structures found in 'radio-quiet' quasars (Jarvis et al., 2019), Seyferts (Gallimore et al., 2006; Morganti et al., 1999; Mingo et al., 2011), and in ordinary galaxies at low redshift (e.g., Croston et al., 2007, 2008c), as discussed in Section 3. The prevalence of these radio outflows on scales of a few to several tens of kpc is not yet well determined either in the local Universe or during the epoch of peak quasar activity, although high-z examples of jets interacting with the IGM are known to exist (Nesvadba et al., 2017). Kinetic feedback from small jets on galaxy scales could therefore comprise an overlooked feedback mechanism during the epoch of high accretion rates and black hole growth, and exciting opportunities to investigate this question will be provided by upcoming sensitive, high resolution radio facilities. Better constraints on the energetic impact of the variety of jet sub-populations expected to be present at the peak of quasar activity and black-hole growth will make it possible to quantify the relative contributions of winds and jets at this epoch, and will inform substantial improvements to feedback treatments in cosmological simulations.

More generally, by obtaining well-determined luminosity functions at $z \sim 2$ and beyond, down to luminosities corresponding to the dominant populations in well-studied local samples (e.g., Best and Heckman, 2012), surveys such as those with LOFAR and MeerKAT,

should lead to the first robust estimates of the energy available from radio jet feedback at the peak of star formation and quasar activity, and enable the host-galaxy and large-scale environmental properties of these new populations of lower luminosity high-z RLAGN to be determined. Complementary constraints on the evolution of baryons in the presence of jet and wind feedback from AGN will come from future, more sensitive X-ray facilities, such as *Athena* (Nandra et al., 2013), that will directly measure group-scale hot-gas atmospheres at $z > 2$, and trace the evolution of group and cluster gas entropy profiles. We therefore look forward to an improved understanding of the relevance of jet kinetic feedback beyond the local Universe over the next decade.

9. Astrophysical uses of radio galaxies

In this Section we briefly discuss the relevance and use of RLAGN for other areas of astrophysics, namely measurements of cosmic magnetic fields, the non-thermal content of galaxy clusters, cosmology, and cosmic rays.

9.1. Cosmic magnetism

The origins and evolution of magnetic fields in the Universe are a substantial uncertainty in structure formation models, and an important science driver for the Square Kilometre Array. Faraday rotation techniques (see Section 2) have been used to measure magnetic field strengths and structure in a range of astrophysical environments.

Magnetic field strengths in groups and clusters of galaxies can be measured both via embedded radio galaxies, and radio galaxies located beyond the group/cluster but along a line of sight that passes through the group/cluster gas. Faraday rotation studies of cluster-centre radio galaxies date back to the 1970s, with radio galaxies at the centre of rich, 'cooling flow' clusters found to have high rotation measures (Carilli and Taylor, 2002). Studies of background radio galaxies have also been used to measure cluster magnetic field strengths (e.g., Clarke et al., 1992). More recently this approach has enabled mapping of cluster magnetic field distributions (Bonafede et al., 2010) and investigation of relationships between cluster thermodynamic conditions and magnetic fields (Govoni et al., 2010). Cluster and group magnetic field distributions provide important constraints on ICM transport processes and on models for the origin and evolution of their magnetic fields.

A related topic of interest is the potential role of AGN in injecting magnetic fields (e.g. Xu et al., 2011), and/or altering the magnetic field structures within galaxy groups and clusters. Recent high-resolution rotation measure studies of resolved radio galaxies in galaxy groups with well-measured gas density distributions have revealed complex magnetic field structure, with ordered field components associated with compression of the gas as the radio lobes expand (Guidetti et al., 2011, 2012). Detailed studies with current and future radio instruments should enable further advances in understanding the influence of radio galaxies on magnetic field properties of groups and clusters.

Radio galaxies also have the potential to be used to provide 'rotation measure grids' — sufficiently many strongly polarized radio sources across the sky will enable magnetic fields to be determined on a range of scales and cosmic environments (e.g., Beck and Gaensler, 2004; Johnston-Hollitt et al., 2004; Krause et al., 2009). With SKA pathfinders and eventually the SKA itself it should be possible to build grids of background sources that will enable the magnetic field of the Milky Way to be mapped on arcmin scales, as well as enabling detailed investigations of magnetic fields in nearby galaxies via the effect of propagation of emission from background radio galaxies through their ISMs. A recent LOFAR study has demonstrated the potential of this technique for studying filaments of large-scale structure (O'Sullivan et al., 2019). However, even with sensitive polarimetry over broad frequency ranges there remain challenges in disentangling multiple contributions to the observed rotation measure, including material intrinsic to the background sources being used. Nevertheless, over the next decade, radio galaxies are likely to be a powerful tool for understanding magnetic fields in a range of environments.

9.2. Non-thermal particle populations in clusters

Galaxy clusters contain an important non-thermal particle population, which contributes to pressure support within the cluster, and results in diffuse extended radio sources, known as radio haloes and relics. Halos are Mpc-scale structures, thought to be caused by turbulent reacceleration of particles pervading the ICM. Relics are narrow features, sometimes found in pairs (e.g., van Weeren et al., 2011), thought to trace shock waves in the ICM. For a detailed review of these diffuse cluster radio sources, see Feretti et al. (2012).

Particle acceleration models for diffuse radio sources in clusters suggest that a seed population of relativistic particles is required to produce the observed extended radio structures (e.g., Brunetti and Jones, 2014).

RLAGN are an obvious source for such a particle population, and low-frequency radio observations are beginning to provide more concrete evidence in favour of this picture. Several examples of radio 'phoenices', relic structures whose morphology and/or spectral structure indicate a revived/re-accelerated region of plasma associated with an AGN, have recently emerged (e.g., Bonafede et al., 2014; van Weeren et al., 2017, 2019), as well as examples of very extended and complex radio-galaxy tail structures in clusters (Hardcastle et al., 2019a; Clarke et al., 2019).

Hence, it appears that there are strong links between remnant radio lobes and non-thermal particle populations in galaxy clusters. Low-frequency studies, and particularly broad-band spectral investigations, should enable substantial progress in determining the long-term effects of RLAGN on the properties of the intracluster plasma. Additionally, the mixing of radio-lobe plasma into the ICM is expected to be important for the evolution of cluster magnetic fields (e.g., Xu et al., 2010). Better constraints on these processes will enable improved modelling of energy transport processes within the ICM and feedback effects on the evolution of cluster baryon content.

9.3. Radio galaxies in cosmology

Historically RLAGN (including quasars) were used as signposts of high-redshift objects; as discussed above, early identifications of RLAGN with quasar hosts opened up the study of the high-redshift universe. Throughout the 80s and 90s, the practice of selecting candidate high-redshift galaxies starting from radio surveys led to samples of hundreds of objects with $z > 2$ being compiled (McCarthy, 1993; Miley and De Breuck, 2008). More recently, of course, high-z objects can be more conveniently selected from large-area, deep optical sky surveys and radio selection is no longer a primary tool. Nevertheless, interest in finding high-redshift, powerful objects persists: if even a single bright source could be found at a redshift $z > 6$, in the presumed Epoch of Reionization, then redshifted 21-cm absorption against its synchrotron continuum, the so-called 21-cm forest, would provide a unique probe of the state of matter at that point in the early universe (Carilli et al., 2002). Currently the redshift record holders are just below $z = 6$ (Bañados et al., 2018; Saxena et al., 2018) and it is not clear whether powerful radio galaxies can even exist at much higher redshifts, given the effects of the CMB on inverse-Compton losses in the lobes. Future radio surveys will enable much deeper searches for high-z objects.

RLAGN have various other applications as tracers of large-scale structure when cross-matched with the CMB or with optical surveys (see, e.g., Raccanelli et al. 2012), constraining models of dark energy and/or modified gravity. However, these techniques require large-area, homogeneous survey data that do not yet exist for their full effectiveness. One cosmological application that has already been explored is the use of radio galaxies as standardizable rulers (Daly, 1994; Daly and Guerra, 2002). This approach, which has a long history (e.g., Hoyle, 1959; Kapahi, 1987) is somewhat similar to the use of supernovae as standardizable candles, but has the disadvantage that it relies on a particular model of radio source evolution when the environments of radio sources, particularly at high z, are not well understood.

9.4. Radio galaxies and the origin of cosmic rays

It has long been clear (Hillas, 1984) that the large volumes and strong magnetic fields in radio galaxies mean that their large-scale components (lobes and hotspots) are possible sites of the acceleration of the highest-energy cosmic rays, with energies above $\sim 10^{19}$ eV (hereafter ultra-high-energy cosmic rays, UHECR). Observationally the presence of high-energy leptons (albeit at much lower energies) implies that efficient hadronic particle acceleration is possible, and inverse-Compton measurements allow us to estimate the field strengths in the acceleration regions. Additional constraints are that the sources of UHECR must be nearby, since UHECR suffer from strong attenuation due to photopion production on the cosmic microwave background and/or photodisintegration of nuclei on scales of the Greisen-Zat'sepin-Kuzmin cutoff (GZK: Greisen 1966) of ~ 100 Mpc, and that they must be capable of accelerating not just protons but also heavy nuclei, since a heavy nuclear component seems to be necessary to explain the composition observations (Taylor, 2014). The first constraint disfavours FRII hotspots as the dominant sources of UHECR, since their space density is very low and there are few within the GZK cutoff; the dominant population is low-power sources and many such systems with the capability to confine UHECR exist within 100 Mpc (Hardcastle, 2010). The second constraint requires nuclei to be found inside radio galaxy lobes, but entrainment of stellar winds can permit that (Wykes et al., 2015).

The acceleration *mechanisms* for UHECR in these sources are less clear, and we defer detailed discussion to another review in this collection. Possibilities include first- or second-order Fermi acceleration in the lobes (Hardcastle et al., 2009; Matthews et al., 2018),

acceleration in the jets (Honda, 2009; Meli and Biermann, 2013) or some combination of the two. As yet there is no model that relates the distribution of the size/luminosity/jet power of RLAGN to the observed cosmic ray flux, sky distribution, spectrum and energy-dependent composition measured at Earth, but many of the ingredients for constructing such a model now exist. The discovery of a high-energy neutrino plausibly associated with a flare in the jet of the blazar TXS 0506+056 (IceCube Collaboration et al., 2018) should give new impetus to the development of such models.

10. Future prospects

A great deal has been learnt about radio galaxies and other RLAGN in the hundred years since the first observation of non-thermal radiation from a jet (Curtis, 1918). We start the next century of RLAGN studies with the clear idea that these objects, almost invisible in traditional optical studies, have a profound effect on their host environments and on the evolution of galaxies in the Universe. We have also developed a good working understanding of the basic dynamics of, and physical conditions in, the large-scale structures that are the main focus of this review.

Many challenges remain. Observationally, progress in the radio is expected to be rapid as a result of the next generation of radio instruments, particularly in the realm of radio surveys: wide and deep radio surveys with LOFAR, ASKAP, MeerKAT and the forthcoming SKA are starting to allow radio astronomers to catch up with optical astronomy in terms of sheer numbers of sources. Surveys now being carried out have the capability to detect all objects where radio AGN activity dominates over star formation out to very high redshifts. High-fidelity, high-resolution imaging is still a little way behind, but long-baseline LOFAR and the mid-frequency SKA both have the capability to provide this. Time-domain radio work and broad-band polarimetry are likely to be other fruitful areas in the coming years. In the optical, wide-area radio surveys rely on the next generation of wide-area optical surveys for optical identification — this includes the existing PanSTARRS and Legacy surveys in the Northern hemisphere and the forthcoming LSST surveys in the South. Complementary spectroscopic surveys, or good photometric redshifts, are also needed to make progress. In the X-ray, the other key area for RLAGN studies because of its capability to probe environments, magnetic fields and particle acceleration as well as to allow the study of (radiatively efficient) AGN activity, we can expect interesting results on host environments

in the nearby universe, from the recently launched *e-ROSITA*, while in around a decade's time *Athena* should provide the capability to carry out very detailed studies of the feedback mechanisms and the dynamics of the hot gas, as well as the evolution of RLAGN environments. A key complement to *Athena* would be a high-resolution, high-sensitivity X-ray telescope — the US mission concepts *Lynx* and/or *AXIS* could provide this capability. Again, time-domain studies in the X-ray have great potential for studies of the particle acceleration mechanism in jets and hotspots, and are so far only possible in a handful of bright nearby objects. In high-energy gamma rays, the Cerenkov Telescope Array (CTA) will allow the resolution of a number of nearby objects, as discussed in Section 2.5, and should give inverse-Compton constraints on magnetic fields for a number of FRI sources that are currently inaccessible to inverse-Compton studies, as well as potentially constraining particle content through the detection of accelerated high-energy protons.

In terms of modelling, we expect to see the gradual convergence of cosmological models (where RLAGN feedback is 'sub-grid physics') and detailed modelling of RLAGN physics. In principle cosmological models can provide estimates of many of the key quantities (local environment, time-dependent mass accretion rates, black hole mass and (vector) spin...) to allow the self-consistent simulation of an entire mock RLAGN population while also reproducing standard constraints such as the galaxy luminosity function. This sort of large-volume modelling work will be key to the interpretation of the very large datasets to be provided by the next-generation radio and optical surveys.

Acknowledgements

References

Abdo, A. A., et al., 2010. Fermi Gamma-Ray Imaging of a Radio Galaxy. Science 328, 725–. doi:10.1126/science.1184656, arXiv:1006.3986.

Ackermann, M., et al., 2015. The Third Catalog of Active Galactic Nuclei Detected by the Fermi Large Area Telescope. Astrophys. J. 810, 14. doi:10.1088/0004-637X/810/1/14, arXiv:1501.06054.

Ackermann, M., et al., 2016. Fermi Large Area Telescope Detection of Extended Gamma-Ray Emission from the Radio Galaxy Fornax A. Astrophys. J. 826, 1. doi:10.3847/0004-637X/826/1/1, arXiv:1606.04905.

Alatalo, K., et al., 2011. Discovery of an Active Galactic Nucleus Driven Molecular Outflow in the Local Early-type Galaxy NGC 1266. The Astrophysical Journal 735, 88. doi:10.1088/0004-637X/735/2/88, arXiv:1104.2326.

Alexander, P., & Leahy, J. P., 1987. Ageing and speeds in a representative sample of 21 classical double radio sources. Mon. Not. R. Astron. Soc. 224, 1.

Allen, S. W., et al., 2006. The relation between accretion rate and jet power in X-ray luminous elliptical galaxies. Mon. Not. R. Astron. Soc. 372, 21.

An, T., & Baan, W. A., 2012. The Dynamic Evolution of Young Extragalactic Radio Sources. Astrophys. J. 760, 77. doi:10.1088/0004-637X/760/1/77, arXiv:1211.1760.

Anderson, C. S., et al., 2018. Broadband Radio Polarimetry of Fornax A. I. Depolarized Patches Generated by Advected Thermal Material from NGC 1316. Astrophys. J. 855, 41. doi:10.3847/1538-4357/aaaec0, arXiv:1802.04812.

Antonucci, R., 1993. Unified models for active galactic nuclei and quasars. Ann. Rev. Astron. Astrophys. 31, 473.

Antonucci, R. R. J., & Miller, J. S., 1985. Spectropolarimetry and the nature of NGC 1068. Astrophys. J. 297, 621–632. doi:10.1086/163559.

Arnaud, M., et al., 2010. The universal galaxy cluster pressure profile from a representative sample of nearby systems (REXCESS) and the Y_{SZ} - M_{500} relation. Astron. Astrophys. 517, A92. doi:10.1051/0004-6361/200913416, arXiv:0910.1234.

Arshakian, T. G., & Longair, M. S., 2004. On the jet speeds of classical double radio sources. Mon. Not. R. Astron. Soc. 251, 727.

Auriemma, C., et al., 1977. A Determination of the Local Radio Luminosity Function of Elliptical Galaxies. Astron. Astrophys. 57, 41.

Bañados, E., et al., 2018. A Powerful Radio-loud Quasar at the End of Cosmic Reionization. Astrophys. J. 861, L14. doi:10.3847/2041-8213/aac511, arXiv:1807.02531.

Baade, W., 1956. Polarization in the Jet of Messier 87. Astrophys. J. 123, 550–551. doi:10.1086/146194.

Baade, W., & Minkowski, R., 1954a. Identification of the Radio Sources in Cassiopeia, Cygnus A, and Puppis A. Astrophys. J. 119, 206. doi:10.1086/145812.

Baade, W., & Minkowski, R., 1954b. On the Identification of Radio Sources. Astrophys. J. 119, 215. doi:10.1086/145813.

Baldi, R. D., & Capetti, A., 2008. Recent star formation in nearby 3CR radio-galaxies from UV HST observations. Astron. Astrophys. 489, 989.

Baldi, R. D., Capetti, A., & Giovannini, G., 2015. Pilot study of the radio-emitting AGN population: the emerging new class of FR 0 radio-galaxies. Astron. Astrophys. 576, A38. doi:10.1051/0004-6361/201425426, arXiv:1502.00427.

Baldi, R. D., Capetti, A., & Giovannini, G., 2019. High-resolution VLA observations of FR0 radio galaxies: the properties and nature of compact radio sources. Monthly Notices of the Royal Astronomical Society 482, 2294–2304. doi:10.1093/mnras/sty2703, arXiv:1810.01894.

Baldi, R. D., Capetti, A., & Massaro, F., 2018a. FR0CAT: a FIRST catalog of FR 0 radio galaxies. Astronomy and Astrophysics 609, A1. doi:10.1051/0004-6361/201731333, arXiv:1709.00015.

Baldi, R. D., et al., 2018b. LeMMINGs - I. The eMERLIN legacy survey of nearby galaxies. 1.5-GHz parsec-scale radio structures and cores. Mon. Not. R. Astron. Soc. 476, 3478–3522. doi:10.1093/mnras/sty342, arXiv:1802.02162.

Baldry, I. K., et al., 2004. Quantifying the Bimodal Color-Magnitude Distribution of Galaxies. Astrophys. J. 600, 681–694. doi:10.1086/380092, arXiv:astro-ph/0309710.

Baldwin, J. E., 1982. Evolutionary tracks of extended radio sources, in: Heeschen, D. S., & Wade, C. M. (Eds.), Extragalactic Radio Sources, pp. 21–24.

Barthel, P., et al., 2012. Extreme Host Galaxy Growth in Powerful Early-epoch Radio Galaxies. Astrophys. J. 757, L26. doi:10.1088/2041-8205/757/2/L26, arXiv:1209.0324.

Barthel, P. D., 1989. Is every quasar beamed? Astrophys. J. 336, 606.

Basson, J. F., & Alexander, P., 2003. The long-term effect of radio sources on the intracluster medium. Mon. Not. R. Astron. Soc. 339, 353.

Beck, R., & Gaensler, B. M., 2004. Observations of magnetic fields in the Milky Way and in nearby galaxies with a Square Kilometre Array. New Astron. Reviews 48, 1289–1304. doi:10.1016/j.newar.2004.09.013, arXiv:astro-ph/0409368.

Beck, R., & Krause, M., 2005. Revised equipartition and minimum energy formula for magnetic field strength estimates from radio synchrotron observations. AN 326, 414.

Begelman, M. C., & Cioffi, D. F., 1989. Overpressured cocoons in extragalactic radio sources. Astrophys. J. 345, L21.

Belsole, E., et al., 2007. High-redshift Fanaroff-Riley type II radio sources: large-scale X-ray environment. Mon. Not. R. Astron. Soc. 381, 1109–1126. doi:10.1111/j.1365-2966.2007.12298.x, arXiv:0709.3635.

Bennett, A. S., 1962. . Mem. R. Astron. Soc. 68, 163.

Benson, A. J., et al., 2003. What Shapes the Luminosity Function of Galaxies? Astrophys. J. 599, 38–49. doi:10.1086/379160, arXiv:astro-ph/0302450.

Best, P. N., 2004. The environmental dependence of radio-loud AGN activity and star formation in the 2dFGRS. Mon. Not. R. Astron. Soc. 351, 70–82. doi:10.1111/j.1365-2966.2004.07752.x, arXiv:astro-ph/0402523.

Best, P. N., 2009. Radio source populations: Results from SDSS. Astronomische Nachrichten 330, 184–189. doi:10.1002/asna.200811152.

Best, P. N., & Heckman, T. M., 2012. On the fundamental dichotomy in the local radio-AGN population: accretion, evolution and host galaxy properties. Mon. Not. R. Astron. Soc. 421, 1569–1582. doi:10.1111/j.1365-2966.2012.20414.x, arXiv:1201.2397.

Best, P. N., et al., 2006. AGN-controlled cooling in elliptical galaxies. Mon. Not. R. Astron. Soc. 368, L67.

Best, P. N., et al., 2005. The host galaxies of radio-loud active galactic nuclei: mass dependences, gas cooling and active galactic nuclei feedback. Mon. Not. R. Astron. Soc. 362, 25.

Best, P. N., et al., 2014. The cosmic evolution of radio-AGN feedback to z = 1. Mon. Not. R. Astron. Soc. 445, 955–969. doi:10.1093/mnras/stu1776, arXiv:1409.0263.

Best, P. N., Longair, M. S., & Röttgering, H. J. A., 1997. A jet-cloud interaction in 3C34 at redshift z = 0.69. Mon. Not. R. Astron. Soc. 286, 785.

Bicknell, G. V., 1994. On the relationship between BL Lac objects and Fanaroff-Riley I galaxies. Astrophys. J. 422, 542.

Bicknell, G. V., 1995. Relativistic Jets and the Fanaroff-Riley Classification of Radio Galaxies. Astrophys. J. Suppl. 101, 29. doi:10.1086/192232, arXiv:astro-ph/9406064.

Bîrzan, L., et al., 2008. Radiative Efficiency and Content of Extragalactic Radio Sources: Toward a Universal Scaling Relation between Jet Power and Radio Power. Astrophys. J. 686, 859–880.

doi:10.1086/591416, arXiv:0806.1929.

Bîrzan, L., et al., 2004. A Systematic Study of Radio-induced X-Ray Cavities in Clusters, Groups, and Galaxies. Astrophys. J. 607, 800–809. doi:10.1086/383519, arXiv:arXiv:astro-ph/0402348.

Bîrzan, L., et al., 2012. The duty cycle of radio-mode feedback in complete samples of clusters. Mon. Not. R. Astron. Soc. 427, 3468–3488. doi:10.1111/j.1365-2966.2012.22083.x, arXiv:1210.7100.

Black, A. R. S., et al., 1992. A study of FRII radio galaxies with z < 0.15: I. High resolution maps of 8 sources at 3.6 cm. Mon. Not. R. Astron. Soc. 256, 186.

Blandford, R. D., & Rees, M. J., 1974. A 'twin-exhaust' model for double radio sources. Mon. Not. R. Astron. Soc. 169, 395.

Blandford, R. D., & Znajek, R. L., 1977. Electromagnetic extraction of energy from Kerr black holes. Mon. Not. R. Astron. Soc. 179, 433–456. doi:10.1093/mnras/179.3.433.

Blanton, E. L., et al., 2011. A Very Deep Chandra Observation of A2052: Bubbles, Shocks, and Sloshing. Astrophys. J. 737, 99. doi:10.1088/0004-637X/737/2/99, arXiv:1105.4572.

Blundell, K. M., Rawlings, S., & Willott, C. J., 1999. The Nature and Evolution of Classical Double Radio Sources from Complete Samples. Astron. J. 117, 677–706. doi:10.1086/300721, arXiv:astro-ph/9810197.

Bodo, G., et al., 1998. Three-dimensional simulations of jets. Astron. Astrophys. 333, 1117–1129.

Böhringer, H., et al., 1993. A ROSAT HRI study of the interaction of the X-ray emitting gas and radio lobes of NGC 1275. Mon. Not. R. Astron. Soc. 264, L25.

Bolton, J. G., Gardner, F. F., & Mackey, M. B., 1964. The Parkes catalogue of radio sources, declination zone -20deg to −60deg. Australian Journal of Physics 17, 340. doi:10.1071/PH640340.

Bonafede, A., et al., 2010. The Coma cluster magnetic field from Faraday rotation measures. Astron. Astrophys. 513, A30. doi:10.1051/0004-6361/200913696, arXiv:1002.0594.

Bonafede, A., et al., 2014. Evidence for Particle Re-acceleration in the Radio Relic in the Galaxy Cluster PLCKG287.0+32.9. Astrophys. J. 785, 1. doi:10.1088/0004-637X/785/1/1, arXiv:1402.1492.

Bourne, M. A., & Sijacki, D., 2017. AGN jet feedback on a moving mesh: cocoon inflation, gas flows and turbulence. Monthly Notices of the Royal Astronomical Society 472, 4707–4735. doi:10.1093/mnras/stx2269, arXiv:1705.07900.

Bower, R. G., et al., 2017. The dark nemesis of galaxy formation: why hot haloes trigger black hole growth and bring star formation to an end. Mon. Not. R. Astron. Soc. 465, 32–44. doi:10.1093/mnras/stw2735, arXiv:1607.07445.

Bowman, M., Leahy, J. P., & Komissarov, S. S., 1996. The deceleration of relativistic jets by entrainment. Mon. Not. R. Astron. Soc. 279, 899.

Bridle, A. H., et al., 1989. The Unusual Radio Galaxy 3C 288. Astron. J. 97, 674. doi:10.1086/115013.

Bridle, A. H., et al., 1994. Deep VLA imaging of twelve extended 3CR quasars. Astron. J. 108, 766.

Bridle, A. H., & Perley, R. A., 1984. Extragalactic radio jets. Ann. Rev. Astron. Astrophys. 22, 319.

Brienza, M., et al., 2017. Search and modelling of remnant radio galaxies in the LOFAR Lockman Hole field. ArXiv e-prints arXiv:1708.01904.

Brienza, M., et al., 2018. Duty cycle of the radio galaxy B2 0258+35. Astron. Astrophys. 618, A45. doi:10.1051/0004-6361/201832846, arXiv:1807.07280.

Brown, M. J. I., et al., 2011. The Ubiquitous Radio Continuum Emission from the Most Massive Early-type Galaxies. Astrophys. J. 731, L41. doi:10.1088/2041-8205/731/2/L41,

arXiv:1103.2828.

Brunetti, G., & Jones, T. W., 2014. Cosmic Rays in Galaxy Clusters and Their Nonthermal Emission. International Journal of Modern Physics D 23, 1430007–98. doi:10.1142/S0218271814300079, arXiv:1401.7519.

Burbidge, G., 1956. On synchrotron radiation from Messier 87. Astrophys. J. 124, 416.

Burch, S. F., 1977. The variation of spectral index across the radio galaxy 3C452. Mon. Not. R. Astron. Soc. 180, 623.

Burn, B. J., 1966. On the depolarization of discrete radio sources by Faraday dispersion. Mon. Not. R. Astron. Soc. 133, 67.

Burns, J. O., 1990. The Radio Properties of cD Galaxies in Abell Clusters. I. an X-ray Selected Sample. Astron. J. 99, 14. doi:10.1086/115307.

Callingham, J. R., et al., 2017. Extragalactic Peaked-spectrum Radio Sources at Low Frequencies. Astrophys. J. 836, 174. doi:10.3847/1538-4357/836/2/174, arXiv:1701.02771.

Capetti, A., Massaro, F., & Baldi, R. D., 2017. FRIICAT: A FIRST catalog of FR II radio galaxies. Astron. Astrophys. 601, A81. doi:10.1051/0004-6361/201630247, arXiv:1703.03427.

Cara, M., et al., 2013. Polarimetry and the High-energy Emission Mechanisms in Quasar Jets: The Case of PKS 1136-135. Astrophys. J. 773, 186. doi:10.1088/0004-637X/773/2/186, arXiv:1305.2535.

Carilli, C. L., Gnedin, N. Y., & Owen, F., 2002. H I 21 Centimeter Absorption beyond the Epoch of Reionization. Astrophys. J. 577, 22–30. doi:10.1086/342179, arXiv:astro-ph/0205169.

Carilli, C. L., et al., 1991. Multifrequency radio observations of Cygnus A: spectral aging in powerful radio galaxies. Astrophys. J. 383, 554.

Carilli, C. L., & Taylor, G. B., 2002. Cluster Magnetic Fields. Ann. Rev. Astron. Astrophys. 40, 319–348. doi:10.1146/annurev.astro.40.060401.093852, arXiv:astro-ph/0110655.

Carvalho, J. C., & O'Dea, C. P., 2002. Evolution of Global Properties of Powerful Radio Sources. II. Hydrodynamical Simulations in a Declining Density Atmosphere and Source Energetics. Astrophys. J. Suppl. 141, 371–414. doi:10.1086/340646.

Cattaneo, A., et al., 2009. The role of black holes in galaxy formation and evolution. Nature 460, 213–219. doi:10.1038/nature08135, arXiv:0907.1608.

Cavagnolo, K. W., et al., 2010. A Relationship Between AGN Jet Power and Radio Power. Astrophys. J. 720, 1066–1072. doi:10.1088/0004-637X/720/2/1066, arXiv:1006.5699.

Celotti, A., Ghisellini, G., & Chiaberge, M., 2001. Large scale jets in AGN: multiwavelength mapping. Mon. Not. R. Astron. Soc. 321, L1.

Chiaberge, M., et al., 2002. The Nuclei of Radio Galaxies in the Ultraviolet: The Signature of Different Emission Processes. Astrophys. J. 571, 247.

Ching, J. H. Y., et al., 2017. Galaxy And Mass Assembly (GAMA): the environments of high- and low-excitation radio galaxies. Mon. Not. R. Astron. Soc. 469, 4584–4599. doi:10.1093/mnras/stx1173, arXiv:1705.04502.

Cioffi, D. F., & Blondin, J. M., 1992. The evolution of cocoons surrounding light, extragalactic jets. Astrophys. J. 392, 458–464. doi:10.1086/171445.

Cioffi, D. F., & Jones, T. W., 1980. Internal Faraday rotation effects in transparent synchrotron sources. Astron. J. 85, 368.

Clarke, A. O., et al., 2019. Signatures from a merging galaxy cluster and its AGN population: LOFAR observations of Abell 1682. Astron. Astrophys. 627, A176. doi:10.1051/0004-6361/201935584, arXiv:1906.07792.

Clarke, D. A., et al., 1992. Origin of the structures and polarization in the classical double 3C219. Astrophys. J. 385, 173.

Clarke, D. A., & Burns, J. O., 1991. Numerical Simulations of a

Restarting Jet. Astrophys. J. 369, 308. doi:10.1086/169762.

Crawford, C. S., et al., 1999. The ROSAT Brightest Cluster Sample - III. Optical spectra of the central cluster galaxies. Monthly Notices of the Royal Astronomical Society 306, 857–896. doi:10.1046/j.1365-8711.1999.02583.x, arXiv:astro-ph/9903057.

Croston, J. H., & Hardcastle, M. J., 2014. The particle content of low-power radio galaxies in groups and clusters. Mon. Not. R. Astron. Soc. 438, 3310–3321. doi:10.1093/mnras/stt2436, arXiv:1312.5183.

Croston, J. H., Hardcastle, M. J., & Birkinshaw, M., 2005. Evidence for radio-source heating of groups. Mon. Not. R. Astron. Soc. 357, 279.

Croston, J. H., et al., 2003. *XMM-Newton* observations of the hot-gas atmospheres of 3C 66B and 3C 449. Mon. Not. R. Astron. Soc. 346, 1041.

Croston, J. H., et al., 2008a. An XMM-Newton study of the environments, particle content and impact of low-power radio galaxies. Mon. Not. R. Astron. Soc. 386, 1709.

Croston, J. H., et al., 2008b. Chandra Evidence for AGN Feedback in the Spiral Galaxy NGC 6764. Astrophys. J. 688, 190–197. doi:10.1086/592268, arXiv:0807.4136.

Croston, J. H., et al., 2008c. Chandra Evidence for AGN Feedback in the Spiral Galaxy NGC 6764. Astrophys. J. 688, 190.

Croston, J. H., et al., 2019. The environments of radio-loud AGN from the LOFAR Two-Metre Sky Survey (LoTSS). Astron. Astrophys. 622, A10. doi:10.1051/0004-6361/201834019, arXiv:1811.07949.

Croston, J. H., et al., 2011. A Large-scale Shock Surrounding a Powerful Radio Galaxy? Astrophys. J. 734, L28. doi:10.1088/2041-8205/734/2/L28, arXiv:1011.6405.

Croston, J. H., Ineson, J., & Hardcastle, M. J., 2018. Particle content, radio-galaxy morphology, and jet power: all radio-loud AGN are not equal. Mon. Not. R. Astron. Soc. 476, 1614–1623. doi:10.1093/mnras/sty274, arXiv:1801.10172.

Croston, J. H., et al., 2017. A new method for finding and characterizing galaxy groups via low-frequency radio surveys. Monthly Notices of the Royal Astronomical Society 470, 1943–1949. doi:10.1093/mnras/stx1347, arXiv:1705.09510.

Croston, J. H., Kraft, R. P., & Hardcastle, M. J., 2007. Shock heating in the nearby radio galaxy NGC 3801. Astrophys. J. 660, 191.

Croston, J. H., et al., 2009. High-energy particle acceleration at the radio-lobe shock of Centaurus A. Mon. Not. R. Astron. Soc. 395, 1999–2012. doi:10.1111/j.1365-2966.2009.14715.x, arXiv:0901.1346.

Croton, D., et al., 2006. . Mon. Not. R. Astron. Soc. 365, 111.

Croton, D. J., et al., 2016. Semi-Analytic Galaxy Evolution (SAGE): Model Calibration and Basic Results. Astrophys. J. Suppl. 222, 22. doi:10.3847/0067-0049/222/2/22, arXiv:1601.04709.

Curtis, H. D., 1918. Descriptions of 762 Nebulae and Clusters Photographed with the Crossley Reflector. Publications of Lick Observatory 13, 9–42.

Daly, R. A., 1994. Cosmology with powerful extended radio sources. Astrophys. J. 426, 38–50. doi:10.1086/174037.

Daly, R. A., & Guerra, E. J., 2002. Quintessence, Cosmology, and Fanaroff-Riley Type IIb Radio Galaxies. Astron. J. 124, 1831–1838. doi:10.1086/342741, arXiv:astro-ph/0209503.

Dasyra, K. M., et al., 2015. A Radio Jet Drives a Molecular and Atomic Gas Outflow in Multiple Regions within One Square Kiloparsec of the Nucleus of the nearby Galaxy IC5063. The Astrophysical Journal 815, 34. doi:10.1088/0004-637X/815/1/34, arXiv:1503.05484.

Davé, R., et al., 2019. SIMBA: Cosmological simulations with black hole growth and feedback. Mon. Not. R. Astron. Soc. 486, 2827–2849. doi:10.1093/mnras/stz937, arXiv:1901.10203.

Davies, J. J., et al., 2019. The gas fractions of dark matter haloes host-

ing simulated L* galaxies are governed by the feedback history of their black holes. Mon. Not. R. Astron. Soc. 485, 3783–3793. doi:10.1093/mnras/stz635, arXiv:1810.07696.

de Gasperin, F., et al., 2012. M 87 at metre wavelengths: the LOFAR picture. Astron. Astrophys. 547, A56. doi:10.1051/0004-6361/201220209, arXiv:1210.1346.

Delvecchio, I., et al., 2017. The VLA-COSMOS 3 GHz Large Project: AGN and host-galaxy properties out to z ≲ 6. Astron. Astrophys. 602, A3. doi:10.1051/0004-6361/201629367, arXiv:1703.09720.

Dreher, J. W., Carilli, C. L., & Perley, R. A., 1987. The Faraday rotation of Cygnus A: magnetic fields in cluster gas. Astrophys. J. 316, 611.

Dunn, R. J. H., & Fabian, A. C., 2004. Particle energies and filling fractions of radio bubbles in cluster cores. Mon. Not. R. Astron. Soc. 355, 862.

Dunn, R. J. H., Fabian, A. C., & Taylor, G. B., 2005. Radio bubbles in clusters of galaxies. Mon. Not. R. Astron. Soc. 364, 1343.

Edge, A. C., 2001. The detection of molecular gas in the central galaxies of cooling flow clusters. Mon. Not. R. Astron. Soc. 328, 762–782. doi:10.1046/j.1365-8711.2001.04802.x, arXiv:astro-ph/0106225.

Eilek, J. A., 1996. How radio sources stay young: spectral aging revisited, in: Hardee P.E., Bridle A.H., Zensus J.A. (Ed.), Energy Transport in Radio Galaxies and Quasars, ASP Conference Series vol. 100, San Francisco. p. 281.

Elbaz, D., et al., 2011. GOODS-Herschel: an infrared main sequence for star-forming galaxies. Astron. Astrophys. 533, A119. doi:10.1051/0004-6361/201117239, arXiv:1105.2537.

Elitzur, M., 2012. On the Unification of Active Galactic Nuclei. Astrophys. J. 747, L33. doi:10.1088/2041-8205/747/2/L33, arXiv:1202.1776.

Ellison, S. L., Patton, D. R., & Hickox, R. C., 2015. Galaxy pairs in the Sloan Digital Sky Survey - XII. The fuelling mechanism of low-excitation radio-loud AGN. Mon. Not. R. Astron. Soc. 451, L35–L39. doi:10.1093/mnrasl/slv061, arXiv:1504.06255.

Fabian, A. C., 2012. Observational Evidence of Active Galactic Nuclei Feedback. Ann. Rev. Astron. Astrophys. 50, 455–489. doi:10.1146/annurev-astro-081811-125521, arXiv:1204.4114.

Fabian, A. C., Celotti, A., & Johnstone, R. M., 2003. Chandra revals X-rays along the radio axis in the quasar 3C9 at z=2.012. Mon. Not. R. Astron. Soc. 338, L7.

Fabian, A. C., et al., 2006. A very deep Chandra observation of the Perseus cluster: shocks, ripples and conduction. Mon. Not. R. Astron. Soc. 366, 417–428. doi:10.1111/j.1365-2966.2005.09896.x, arXiv:astro-ph/0510476.

Fabian, A. C., et al., 2017. Do sound waves transport the AGN energy in the Perseus cluster? Mon. Not. R. Astron. Soc. 464, L1–L5. doi:10.1093/mnrasl/slw170, arXiv:1608.07088.

Fanaroff, B. L., & Riley, J. M., 1974. The morphology of extragalactic radio sources of high and low luminosity. Mon. Not. R. Astron. Soc. 167, 31P.

Feain, I. J., et al., 2011. The Radio Continuum Structure of Centaurus A at 1.4 GHz. Astrophys. J. 740, 17. doi:10.1088/0004-637X/740/1/17, arXiv:1104.0077.

Feretti, L., & Giovannini, G., 1996. Diffuse Cluster Radio Sources (Review), in: Ekers, R. D., Fanti, C., & Padrielli, L. (Eds.), Extragalactic Radio Sources, p. 333.

Feretti, L., et al., 2012. Clusters of galaxies: observational properties of the diffuse radio emission. A&AR 20, 54. doi:10.1007/s00159-012-0054-z, arXiv:1205.1919.

Feretti, L., Perola, G. C., & Fanti, R., 1992. Tailed radio sources as probes of the intergalactic medium pressure. Astron. Astrophys. 265, 9.

Feretti, L., et al., 1990. Confinement of radio galaxies in rich clusters.

Astron. Astrophys. 233, 325.

Fernini, I., et al., 1993. Very large array imaging of 5 FRII 3CR radio galaxies. Astron. J. 105, 1690.

Fernini, I., Burns, J. O., & Perley, R. A., 1997. VLA imaging of Fanaroff-Riley II 3CR radio galaxies. II. Eight new images and comparisons with 3CR quasars. Astron. J. 114, 2292.

Forman, W., et al., 2007. Filaments, Bubbles, and Weak Shocks in the Gaseous Atmosphere of M87. Astrophys. J. 665, 1057–1066. doi:10.1086/519480, arXiv:astro-ph/0604583.

Forman, W., et al., 2005. Reflections of Active Galactic Nucleus Outbursts in the Gaseous Atmosphere of M87. Astrophys. J. 635, 894–906. doi:10.1086/429746.

Gabuzda, D. C., Murray, É., & Cronin, P., 2004. Helical magnetic fields associated with the relativistic jets of four BL Lac objects. Mon. Not. R. Astron. Soc. 351, L89–L93. doi:10.1111/j.1365-2966.2004.08037.x, arXiv:astro-ph/0405394.

Gaibler, V., Khochfar, S., & Krause, M., 2011. Asymmetries in extragalactic double radio sources: clues from 3D simulations of jet-disc interaction. Mon. Not. R. Astron. Soc. 411, 155–161. doi:10.1111/j.1365-2966.2010.17674.x, arXiv:1008.2757.

Gaibler, V., et al., 2012. Jet-induced star formation in gas-rich galaxies. Mon. Not. R. Astron. Soc. 425, 438–449. doi:10.1111/j.1365-2966.2012.21479.x, arXiv:1111.4478.

Gaibler, V., Krause, M., & Camenzind, M., 2009. Very light magnetized jets on large scales - I. Evolution and magnetic fields. Mon. Not. R. Astron. Soc. 400, 1785–1802. doi:10.1111/j.1365-2966.2009.15625.x, arXiv:0908.4055.

Gallimore, J. F., et al., 2006. A Survey of Kiloparsec-Scale Radio Outflows in Radio-Quiet Active Galactic Nuclei. Astron. J. 132, 546–569. doi:10.1086/504593, arXiv:astro-ph/0604219.

Garon, A. F., et al., 2019. Radio Galaxy Zoo: The Distortion of Radio Galaxies by Galaxy Clusters. Astron. J. 157, 126. doi:10.3847/1538-3881/aaff62, arXiv:1901.05480.

Garrington, S., et al., 1988. A systematic asymmetry in the polarization properties of double radio sources with one jet. Nature 331, 147.

Gaspari, M., Brighenti, F., & Temi, P., 2012. Mechanical AGN feedback: controlling the thermodynamical evolution of elliptical galaxies. Mon. Not. R. Astron. Soc. 424, 190–209. doi:10.1111/j.1365-2966.2012.21183.x, arXiv:1202.6054.

Gaspari, M., Ruszkowski, M., & Oh, S. P., 2013. Chaotic cold accretion on to black holes. Mon. Not. R. Astron. Soc. 432, 3401–3422. doi:10.1093/mnras/stt692, arXiv:1301.3130.

Gendre, M. A., et al., 2013. The relation between morphology, accretion modes and environmental factors in local radio AGN. Mon. Not. R. Astron. Soc. 430, 3086–3101. doi:10.1093/mnras/stt116, arXiv:1301.1526.

Ghisellini, G., & Celotti, A., 2001. The dividing line between FR I and FR II radio-galaxies. Astron. Astrophys. 379, L1.

Gilbert, G., et al., 2004. High-resolution observations of a complete sample of 27 FRII radio galaxies and quasars with 0.3 < z < 0.6. Mon. Not. R. Astron. Soc. 351, 845.

Giroletti, M., et al., 2004. A Sample of Low-Redshift BL Lacertae Objects. I. The Radio Data. Astrophys. J. 613, 752–769. doi:10.1086/423231, arXiv:astro-ph/0406255.

Godfrey, L. E. H., Morganti, R., & Brienza, M., 2017. On the population of remnant Fanaroff-Riley type II radio galaxies and implications for radio source dynamics. Mon. Not. R. Astron. Soc. 471, 891–907. doi:10.1093/mnras/stx1538, arXiv:1706.05909.

Godfrey, L. E. H., & Shabala, S. S., 2016. Mutual distance dependence drives the observed jet-power-radio-luminosity scaling relations in radio galaxies. Mon. Not. R. Astron. Soc. 456, 1172–1184. doi:10.1093/mnras/stv2712, arXiv:1511.06007.

Gordon, Y. A., et al., 2019. The Effect of Minor and Major Mergers on the Evolution of Low-excitation Radio Galaxies. Astrophys. J. 878,

88. doi:`10.3847/1538-4357/ab203f`, `arXiv:1905.00018`.

Govoni, F., et al., 2010. Rotation measures of radio sources in hot galaxy clusters. Astron. Astrophys. 522, A105. doi:`10.1051/0004-6361/200913665`, `arXiv:1007.5207`.

Greisen, K., 1966. End to the cosmic-ray spectrum? PRL 16, 748.

Gugliucci, N. E., et al., 2005. Dating COINS: Kinematic Ages for Compact Symmetric Objects. The Astrophysical Journal 622, 136–148. doi:`10.1086/427934`, `arXiv:astro-ph/0412199`.

Guidetti, D., et al., 2011. Ordered magnetic fields around radio galaxies: evidence for interaction with the environment. Mon. Not. R. Astron. Soc. 413, 2525–2544. doi:`10.1111/j.1365-2966.2011.18321.x`, `arXiv:1101.1807`.

Guidetti, D., et al., 2012. The magnetized medium around the radio galaxy B2 0755+37: an interaction with the intragroup gas. Mon. Not. R. Astron. Soc. 423, 1335–1350. doi:`10.1111/j.1365-2966.2012.20961.x`, `arXiv:1203.4582`.

Gürkan, G., et al., 2019. LoTSS/HETDEX: Optical quasars. I. Low-frequency radio properties of optically selected quasars. Astron. Astrophys. 622, A11. doi:`10.1051/0004-6361/201833892`, `arXiv:1811.07933`.

Gürkan, G., et al., 2015. Herschel-ATLAS: the connection between star formation and AGN activity in radio-loud and radio-quiet active galaxies. Mon. Not. R. Astron. Soc. 452, 3776–3794. doi:`10.1093/mnras/stv1502`, `arXiv:1507.01552`.

Gürkan, G., et al., 2018. LOFAR/H-ATLAS: the low-frequency radio luminosity-star formation rate relation. Mon. Not. R. Astron. Soc. 475, 3010–3028. doi:`10.1093/mnras/sty016`, `arXiv:1801.02629`.

H. E. S. S. Collaboration et al., 2018. The γ-ray spectrum of the core of Centaurus A as observed with H.E.S.S. and Fermi-LAT. Astron. Astrophys. 619, A71. doi:`10.1051/0004-6361/201832640`, `arXiv:1807.07375`.

Hada, K., et al., 2015. A strong radio brightening at the jet base of M87 in the period of the elevated TeV gamma-ray state in 2012. arXiv e-prints `arXiv:1502.05177`.

Hamer, S. L., et al., 2014. Cold gas dynamics in Hydra-A: evidence for a rotating disc. Mon. Not. R. Astron. Soc. 437, 862–878. doi:`10.1093/mnras/stt1949`, `arXiv:1310.4501`.

Hardcastle, M., 2018a. Interpreting radiative efficiency in radio-loud AGNs. Nature Astronomy 2, 273–274. doi:`10.1038/s41550-018-0424-1`, `arXiv:1804.04043`.

Hardcastle, M. J., 2004. Bgg revisited: The environments of low-excitation radio galaxies and unified models. Astron. Astrophys. 414, 927.

Hardcastle, M. J., 2006. Testing the beamed inverse-Compton model for jet X-ray emission: velocity structure and deceleration? Mon. Not. R. Astron. Soc. 366, 1465.

Hardcastle, M. J., 2010. Which radio galaxies can make the highest energy cosmic rays? Mon. Not. R. Astron. Soc. 405, 2810–2816. doi:`10.1111/j.1365-2966.2010.16668.x`, `arXiv:1003.2500`.

Hardcastle, M. J., 2018b. A simulation-based analytic model of radio galaxies. Mon. Not. R. Astron. Soc. 475, 2768–2786. doi:`10.1093/mnras/stx3358`, `arXiv:1801.00667`.

Hardcastle, M. J., et al., 1997. High resolution observations at 3.6 cm of seventeen FRII radio galaxies with 0.15 < z < 0.3. Mon. Not. R. Astron. Soc. 288, 859.

Hardcastle, M. J., et al., 1998. FR II radio galaxies with z < 0.3 – I. Properties of jets, cores and hot spots. Mon. Not. R. Astron. Soc. 296, 445.

Hardcastle, M. J., et al., 1999. FRII radio galaxies with z < 0.3 - II. Beaming and unification. Mon. Not. R. Astron. Soc. 304, 135.

Hardcastle, M. J., et al., 2002. Magnetic field strengths in the hotspots and lobes of three powerful FRII radio sources. Astrophys. J. 581, 948.

Hardcastle, M. J., Birkinshaw, M., & Worrall, D. M., 2001. A *Chandra* detection of the radio hotspot of 3C 123. Mon. Not. R. Astron. Soc. 323, L17.

Hardcastle, M. J., et al., 2013. Herschel-ATLAS/GAMA: a difference between star formation rates in strong-line and weak-line radio galaxies. Mon. Not. R. Astron. Soc. 429, 2407–2424. doi:`10.1093/mnras/sts510`, `arXiv:1211.6440`.

Hardcastle, M. J., & Croston, J. H., 2010. Searching for the inverse-Compton emission from bright cluster-centre radio galaxies. Mon. Not. R. Astron. Soc. 404, 2018–2027. doi:`10.1111/j.1365-2966.2010.16420.x`, `arXiv:1001.4742`.

Hardcastle, M. J., & Croston, J. H., 2011. Modelling TeV γ-ray emission from the kiloparsec-scale jets of Centaurus A and M87. Mon. Not. R. Astron. Soc. 415, 133–142. doi:`10.1111/j.1365-2966.2011.18678.x`, `arXiv:1103.1744`.

Hardcastle, M. J., Croston, J. H., & Kraft, R. P., 2007a. A Chandra study of particle acceleration in the multiple hotspots of nearby radio galaxies. Astrophys. J. 669, 893.

Hardcastle, M. J., et al., 2019a. NGC 326: X-shaped no more. Mon. Not. R. Astron. Soc. 488, 3416–3422. doi:`10.1093/mnras/stz1910`, `arXiv:1907.03274`.

Hardcastle, M. J., Evans, D. A., & Croston, J. H., 2006. The X-ray nuclei of intermediate-redshift radio sources. Mon. Not. R. Astron. Soc. 370, 1893.

Hardcastle, M. J., Evans, D. A., & Croston, J. H., 2007b. Hot and cold gas accretion and feedback in radio-loud active galaxies. Mon. Not. R. Astron. Soc. 376, 1849.

Hardcastle, M. J., Evans, D. A., & Croston, J. H., 2009. The active nuclei of z < 1.0 3CRR radio sources. Mon. Not. R. Astron. Soc. 396, 1929.

Hardcastle, M. J., et al., 2004. The origins of X-ray emission from the hotspots of FRII radio sources. Astrophys. J. 612, 729.

Hardcastle, M. J., & Krause, M. G. H., 2013. Numerical modelling of the lobes of radio galaxies in cluster environments. Mon. Not. R. Astron. Soc. 430, 174–196. doi:`10.1093/mnras/sts564`, `arXiv:1301.2531`.

Hardcastle, M. J., & Krause, M. G. H., 2014. Numerical modelling of the lobes of radio galaxies in cluster environments II: Magnetic field configuration and observability. Mon. Not. R. Astron. Soc. 443, 1482–1499. doi:`10.1093/mnras/stu1229`, `arXiv:1406.5300`.

Hardcastle, M. J., et al., 2016. Deep Chandra observations of Pictor A. Mon. Not. R. Astron. Soc. 455, 3526–3545. doi:`10.1093/mnras/stv2553`, `arXiv:1510.08392`.

Hardcastle, M. J., & Looney, L. W., 2008. The properties of powerful radio sources at 90 GHz. Mon. Not. R. Astron. Soc. 388, 176.

Hardcastle, M. J., et al., 2012. The nature of the jet-driven outflow in the radio galaxy 3C 305. Mon. Not. R. Astron. Soc. 424, 1774–1789. doi:`10.1111/j.1365-2966.2012.21247.x`, `arXiv:1205.0962`.

Hardcastle, M. J., et al., 2019b. Radio-loud AGN in the first LoTSS data release. The lifetimes and environmental impact of jet-driven sources. Astron. Astrophys. 622, A12. doi:`10.1051/0004-6361/201833893`, `arXiv:1811.07943`.

Hardcastle, M. J., & Worrall, D. M., 2000a. Radio, optical and X-ray nuclei in nearby 3CRR radio galaxies. Mon. Not. R. Astron. Soc. 314, 359.

Hardcastle, M. J., & Worrall, D. M., 2000b. The environments of FRII radio galaxies. Mon. Not. R. Astron. Soc. 319, 562.

Hardcastle, M. J., et al., 2005. A *Chandra* observation of the X-ray environment and jet of 3C 296. Mon. Not. R. Astron. Soc. 358, 843.

Harris, D. E., & Stern, C. P., 1987. X-ray emission associated with the jet in 3C273. Astrophys. J. 313, 136.

Harwood, J. J., et al., 2013. Spectral ageing in the lobes of FR-II

radio galaxies: new methods of analysis for broad-band radio data. Mon. Not. R. Astron. Soc. 435, 3353–3375. doi:10.1093/mnras/stt1526, arXiv:1308.4137.

Hatch, N. A., et al., 2005. Detections of molecular hydrogen in the outer filaments of NGC1275. Mon. Not. R. Astron. Soc. 358, 765–773. doi:10.1111/j.1365-2966.2005.08787.x, arXiv:astro-ph/0411446.

Hatch, N. A., et al., 2014. Why z > 1 radio-loud galaxies are commonly located in protoclusters. Mon. Not. R. Astron. Soc. 445, 280–289. doi:10.1093/mnras/stu1725, arXiv:1409.1218.

Heckman, T. M., & Best, P. N., 2014. The Coevolution of Galaxies and Supermassive Black Holes: Insights from Surveys of the Contemporary Universe. Ann. Rev. Astron. Astrophys. 52, 589–660. doi:10.1146/annurev-astro-081913-035722, arXiv:1403.4620.

Heckman, T. M., et al., 1986. Galaxy collisions and mergers: the genesis of very powerful radio sources? Astrophys. J. 311, 526.

Hillas, A. M., 1984. . Ann. Rev. Astron. Astrophys. 22, 425.

Hine, R. G., & Longair, M. S., 1979. Optical spectra of 3CR radio galaxies. Mon. Not. R. Astron. Soc. 188, 111.

Hitomi Collaboration et al., 2016. The quiescent intracluster medium in the core of the Perseus cluster. Nature 535, 117–121. doi:10.1038/nature18627, arXiv:1607.04487.

Hlavacek-Larrondo, J., et al., 2015. X-Ray Cavities in a Sample of 83 SPT-selected Clusters of Galaxies: Tracing the Evolution of AGN Feedback in Clusters of Galaxies out to z=1.2. Astrophys. J. 805, 35. doi:10.1088/0004-637X/805/1/35, arXiv:1410.0025.

Ho, L. C., 1999. The Spectral Energy Distributions of Low-Luminosity Active Galactic Nuclei. Astrophys. J. 516, 672.

Hogan, M. T., et al., 2017. The Onset of Thermally Unstable Cooling from the Hot Atmospheres of Giant Galaxies in Clusters: Constraints on Feedback Models. The Astrophysical Journal 851, 66. doi:10.3847/1538-4357/aa9af3, arXiv:1704.00011.

Honda, M., 2009. Ultra-high Energy Cosmic-ray Acceleration in the Jet of Centaurus A. Astrophys. J. 706, 1517.

Hota, A., & Saikia, D. J., 2006. Radio bubbles in the composite AGN-starburst galaxy NGC6764. Mon. Not. R. Astron. Soc. 371, 945–956. doi:10.1111/j.1365-2966.2006.10738.x, arXiv:astro-ph/0607477.

Hota, A., et al., 2011. Discovery of a spiral-host episodic radio galaxy. Mon. Not. R. Astron. Soc. 417, L36–L40. doi:10.1111/j.1745-3933.2011.01115.x, arXiv:1107.4742.

Hoyle, F., 1959. The relation of radio astronomy to cosmology, in: Bracewell, R. N. (Ed.), URSI Symp. 1: Paris Symposium on Radio Astronomy, p. 529.

Huarte-Espinosa, M., Krause, M., & Alexander, P., 2011. Interaction of Fanaroff-Riley class II radio jets with a randomly magnetized intracluster medium. Mon. Not. R. Astron. Soc. 418, 1621–1639. doi:10.1111/j.1365-2966.2011.19545.x, arXiv:1108.0430.

IceCube Collaboration et al., 2018. Multimessenger observations of a flaring blazar coincident with high-energy neutrino IceCube-170922A. Science 361, eaat1378. doi:10.1126/science.aat1378, arXiv:1807.08816.

Ineson, J., et al., 2013. Radio-loud Active Galactic Nucleus: Is There a Link between Luminosity and Cluster Environment? Astrophys. J. 770, 136. doi:10.1088/0004-637X/770/2/136, arXiv:1305.1050.

Ineson, J., et al., 2015. The link between accretion mode and environment in radio-loud active galaxies. Mon. Not. R. Astron. Soc. 453, 2682–2706. doi:10.1093/mnras/stv1807, arXiv:1508.01033.

Ineson, J., et al., 2017. A representative survey of the dynamics and energetics of FR II radio galaxies. Mon. Not. R. Astron. Soc. 467, 1586–1607. doi:10.1093/mnras/stx189, arXiv:1701.05612.

Jaffe, W. J., & Perola, G. C., 1973. Dynamical Models of Tailed Radio Sources in Clusters of Galaxies. Astron. Astrophys. 26, 423.

Jamrozy, M., et al., 2007. Intermittent jet activity in the radio galaxy 4C29.30? Mon. Not. R. Astron. Soc. 378, 581–593. doi:10.1111/j.1365-2966.2007.11782.x, arXiv:astro-ph/0703723.

Janssen, R. M. J., et al., 2012. The triggering probability of radio-loud AGN. A comparison of high and low excitation radio galaxies in hosts of different colors. Astron. Astrophys. 541, A62. doi:10.1051/0004-6361/201219052, arXiv:1206.0578.

Jarvis, M., et al., 2016. The MeerKAT International GHz Tiered Extragalactic Exploration (MIGHTEE) Survey, in: Proceedings of MeerKAT Science: On the Pathway to the SKA. 25-27 May, 2016 Stellenbosch, South Africa (MeerKAT2016). Online at https://pos.sissa.it/cgi-bin/reader/conf.cgi?confid=277, p. 6. arXiv:1709.01901.

Jarvis, M. E., et al., 2019. Prevalence of radio jets associated with galactic outflows and feedback from quasars. Mon. Not. R. Astron. Soc. 485, 2710–2730. doi:10.1093/mnras/stz556, arXiv:1902.07727.

Jetha, N. N., et al., 2008. The nature of the ghost cavity in the NGC 741 group. Mon. Not. R. Astron. Soc. 384, 1344–1354. doi:10.1111/j.1365-2966.2007.12829.x, arXiv:0712.1150.

Johnston-Hollitt, M., Dehghan, S., & Pratley, L., 2015. Using Tailed Radio Galaxies to Probe the Environment and Magnetic Field of Galaxy Clusters in the SKA Era, in: Advancing Astrophysics with the Square Kilometre Array (AASKA14), p. 101. arXiv:1501.00761.

Johnston-Hollitt, M., Hollitt, C. P., & Ekers, R. D., 2004. Statistical Analysis of Extra-galactic Rotation Measures, in: Uyaniker, B., Reich, W., & Wielebinski, R. (Eds.), The Magnetized Interstellar Medium, pp. 13–18. arXiv:astro-ph/0410659.

Jones, S., et al., 2011. Radio and X-ray variability in the Seyfert galaxy NGC 4051. Mon. Not. R. Astron. Soc. 412, 2641–2652. doi:10.1111/j.1365-2966.2010.18105.x, arXiv:1011.6633.

Jones, T. W., Ryu, D., & Engel, A., 1999. Simulating Electron Transport and Synchrotron Emission in Radio Galaxies: Shock Acceleration and Synchrotron Aging in Axisymmetric Flows. The Astrophysical Journal 512, 105–124. doi:10.1086/306772, arXiv:astro-ph/9809081.

Kaiser, C. R., & Alexander, P., 1997. A self-similar model for extragalactic radio sources. Mon. Not. R. Astron. Soc. 286, 215.

Kaiser, C. R., Dennett-Thorpe, J., & Alexander, P., 1997. Evolutionary tracks of FRII sources through the P-D diagram. Mon. Not. R. Astron. Soc. 292, 723.

Kapahi, V. K., 1987. The angular size-redshift relation as a cosmological tool, in: Hewitt, A., Burbidge, G., & Fang, L. Z. (Eds.), Observational Cosmology, pp. 251–265.

Kardashev, N. S., 1962. Nonstationarity of Spectra of Young Sources of Nonthermal Radio Emission. Soviet Astronomy 6, 317.

Kataoka, J., & Stawarz, Ł., 2005. X-ray emission properties of large scale jets, hotspots and lobes in active galactic nuclei. Astrophys. J. 622, 797.

Kauffmann, G., et al., 2019. The morphology and kinematics of the gaseous circumgalactic medium of Milky Way mass galaxies - II. Comparison of IllustrisTNG and Illustris simulation results. Mon. Not. R. Astron. Soc. 486, 4686–4700. doi:10.1093/mnras/stz1029, arXiv:1904.07274.

Kaviraj, S., et al., 2015. Radio AGN in spiral galaxies. Mon. Not. R. Astron. Soc. 454, 1595–1604. doi:10.1093/mnras/stv1957, arXiv:1412.5602.

Killeen, N. E. B., Bicknell, G. V., & Ekers, R. D., 1988. The thermally confined radio source in NGC 1399. Astrophys. J. 325, 180.

Kimball, A. E., et al., 2011. The Two-component Radio Luminosity Function of Quasi-stellar Objects: Star Formation and Active

Galactic Nucleus. The Astrophysical Journal 739, L29. doi:`10.1088/2041-8205/739/1/L29`, `arXiv:1107.3551`.

Kraft, R. P., et al., 2003. X-ray emission from the hot ISM and SW radio lobe of the nearby radio galaxy Centaurus A. Astrophys. J. 592, 129.

Krause, M., 2003. Very light jets. I. Axisymmetric parameter study and analytic approximation. Astron. Astrophys. 398, 113–125. doi:`10.1051/0004-6361:20021649`, `arXiv:arXiv:astro-ph/0211448`.

Krause, M., et al., 2009. Measurements of the cosmological evolution of magnetic fields with the Square Kilometre Array. Mon. Not. R. Astron. Soc. 400, 646–656. doi:`10.1111/j.1365-2966.2009.15489.x`, `arXiv:0908.0830`.

Krause, M. G. H., et al., 2019. How frequent are close supermassive binary black holes in powerful jet sources? Mon. Not. R. Astron. Soc. 482, 240–261. doi:`10.1093/mnras/sty2558`, `arXiv:1809.04050`.

Krolik, J. H., & Begelman, M. C., 1986. An X-ray heated wind in NGC 1068. Astrophys. J. 308, L55–L58. doi:`10.1086/184743`.

Kukula, M. J., et al., 1998. The radio properties of radio-quiet quasars. Monthly Notices of the Royal Astronomical Society 297, 366–382. doi:`10.1046/j.1365-8711.1998.01481.x`, `arXiv:astro-ph/9802148`.

Kuźmicz, A., et al., 2017. Optical and radio properties of extragalactic radio sources with recurrent jet activity. Mon. Not. R. Astron. Soc. 471, 3806–3826. doi:`10.1093/mnras/stx1830`, `arXiv:1709.01802`.

Laing, R. A., 1980. A model of the magnetic field structure in extended radio sources. Mon. Not. R. Astron. Soc. 193, 439.

Laing, R. A., 1988. The sidedness of jets and depolarization in powerful extragalactic radio sources. Nature 331, 149.

Laing, R. A., 1989. Radio observations of hot spots, in: Meisenheimer K., Röser H.-J. (Ed.), Hotspots in Extragalactic Radio Sources, Springer-Verlag, Heidelberg. p. 27.

Laing, R. A., & Bridle, A. H., 2002. Dynamical models for jet deceleration in the radio galaxy 3C 31. Mon. Not. R. Astron. Soc. 336, 1161–1180. doi:`10.1046/j.1365-8711.2002.05873.x`, `arXiv:astro-ph/0207427`.

Laing, R. A., & Bridle, A. H., 2014. Systematic properties of decelerating relativistic jets in low-luminosity radio galaxies. Mon. Not. R. Astron. Soc. 437, 3405–3441. doi:`10.1093/mnras/stt2138`, `arXiv:1311.1015`.

Laing, R. A., et al., 2008. Multifrequency VLA observations of the FR I radio galaxy 3C 31: morphology, spectrum and magnetic field. Mon. Not. R. Astron. Soc. 386, 657–672. doi:`10.1111/j.1365-2966.2008.13091.x`, `arXiv:0803.2597`.

Laing, R. A., et al., 1994. Spectrophotometry of a complete sample of 3CR radio sources: implications for unified models, in: Bicknell G.V., Dopita M.A., Quinn P.J. (Ed.), The First Stromlo Symposium: the Physics of Active Galaxies, ASP Conference Series vol. 54, San Francisco. p. 201.

Laing, R. A., Riley, J. M., & Longair, M. S., 1983. . Mon. Not. R. Astron. Soc. 204, 151.

Lau, E. T., et al., 2017. Physical Origins of Gas Motions in Galaxy Cluster Cores: Interpreting Hitomi Observations of the Perseus Cluster. Astrophys. J. 849, 54. doi:`10.3847/1538-4357/aa8c00`, `arXiv:1705.06280`.

Le Brun, A. M. C., et al., 2014. Towards a realistic population of simulated galaxy groups and clusters. Mon. Not. R. Astron. Soc. 441, 1270–1290. doi:`10.1093/mnras/stu608`, `arXiv:1312.5462`.

Leahy, J. P., et al., 1997. A study of FRII radio galaxies with $z < 0.15$ – II. High-resolution maps of eleven sources at 3.6 cm. Mon. Not. R. Astron. Soc. 291, 20.

Ledlow, M. J., & Owen, F. N., 1996. 20 CM VLA Survey of Abell Clusters of Galaxies. VI. Radio/Optical Luminosity Functions. As-

tron. J. 112, 9.

Ledlow, M. J., et al., 2001. A Large-Scale Jet and FR I Radio Source in a Spiral Galaxy: The Host Properties and External Environment. Astrophys. J. 552, 120–132. doi:`10.1086/320458`, `arXiv:astro-ph/0012328`.

Lim, J., et al., 2000. Molecular Gas in the Powerful Radio Galaxies 3C 31 and 3C 264: Major or Minor Mergers? Astrophys. J. 545, L93–L97. doi:`10.1086/317885`, `arXiv:astro-ph/0011520`.

Lin, Y.-T., et al., 2010. On the Populations of Radio Galaxies with Extended Morphology at z < 0.3. Astrophys. J. 723, 1119–1138. doi:`10.1088/0004-637X/723/2/1119`, `arXiv:1006.5452`.

Lister, M. L., et al., 2016. MOJAVE: XIII. Parsec-scale AGN Jet Kinematics Analysis Based on 19 years of VLBA Observations at 15 GHz. Astron. J. 152, 12. doi:`10.3847/0004-6256/152/1/12`, `arXiv:1603.03882`.

Longair, M. S., 2010. High Energy Astrophysics. Cambridge University Press, Cambridge.

Longair, M. S., & Riley, J. M., 1979. Statistical evidence on the dynamical evolution of radio sources. Mon. Not. R. Astron. Soc. 188, 625.

Longair, M. S., Ryle, M., & Scheuer, P. A. G., 1973. Models of extended radio sources. Mon. Not. R. Astron. Soc. 164, 243.

Longair, M. S., & Seldner, M., 1979. The clustering of galaxies about extragalactic radio sources. Mon. Not. R. Astron. Soc. 189, 433.

Longair, M. S., & Willmore, A. P., 1974. The X-ray spectrum of Cygnus-A. Mon. Not. R. Astron. Soc. 168, 479–490. doi:`10.1093/mnras/168.3.479`.

Luo, Q., & Sadler, E. M., 2010. The Evolution of Extragalactic Radio Sources. Astrophys. J. 713, 398–409. doi:`10.1088/0004-637X/713/1/398`, `arXiv:1003.0667`.

Lynden-Bell, D., 1969. Galactic nuclei as collapsed old quasars. Nature 223, 690.

Mahabal, A., Kembhavi, A., & McCarthy, P. J., 1999. Effective Radii and Color Gradients in Radio Galaxies. Astrophys. J. 516, L61–L64. doi:`10.1086/311995`, `arXiv:astro-ph/9903104`.

Mahatma, V. H., et al., 2020. Investigating the spectral age problem with powerful radio galaxies. Mon. Not. R. Astron. Soc. 491, 5015–5034. doi:`10.1093/mnras/stz3396`, `arXiv:1912.01028`.

Mahatma, V. H., et al., 2019. LoTSS DR1: Double-double radio galaxies in the HETDEX field. Astron. Astrophys. 622, A13. doi:`10.1051/0004-6361/201833973`, `arXiv:1811.08194`.

Mahatma, V. H., et al., 2018. Remnant radio-loud AGN in the Herschel-ATLAS field. Mon. Not. R. Astron. Soc. 475, 4557–4578. doi:`10.1093/mnras/sty025`, `arXiv:1801.01067`.

Mannering, E. J. A., Worrall, D. M., & Birkinshaw, M., 2011. The host galaxies of radio-loud active galactic nuclei: colour structure. Mon. Not. R. Astron. Soc. 416, 2869–2881. doi:`10.1111/j.1365-2966.2011.19235.x`, `arXiv:1106.5498`.

Mao, M. Y., et al., 2015. J1649+2635: a grand-design spiral with a large double-lobed radio source. Mon. Not. R. Astron. Soc. 446, 4176–4185. doi:`10.1093/mnras/stu2302`, `arXiv:1410.8520`.

Massaglia, S., Bodo, G., & Ferrari, A., 1996. Dynamical and radiative properties of astrophysical supersonic jets. I. Cocoon morphologies. Astron. Astrophys. 307, 997–1008. `arXiv:astro-ph/9506142`.

Matthews, J. H., et al., 2018. Fornax A, Centaurus A, and other radio galaxies as sources of ultrahigh energy cosmic rays. Mon. Not. R. Astron. Soc. 479, L76–L80. doi:`10.1093/mnrasl/sly099`, `arXiv:1805.01902`.

Matthews, T. A., Morgan, W. W., & Schmidt, M., 1964. A discussion of galaxies identified with radio sources. Astrophys. J. 140, 35.

Mauch, T., & Sadler, E., 2007. Radio sources in the 6dFGS: local luminosity functions at 1.4GHz for star-forming galaxies and radio-loud AGN. Mon. Not. R. Astron. Soc. 375, 931.

McCarthy, I. G., et al., 2017. The BAHAMAS project: calibrated hydrodynamical simulations for large-scale structure cosmology. Mon. Not. R. Astron. Soc. 465, 2936–2965. doi:10.1093/mnras/stw2792, arXiv:1603.02702.

McCarthy, I. G., et al., 2011. Gas expulsion by quasar-driven winds as a solution to the overcooling problem in galaxy groups and clusters. Mon. Not. R. Astron. Soc. 412, 1965–1984. doi:10.1111/j.1365-2966.2010.18033.x, arXiv:1008.4799.

McCarthy, P. J., 1993. High redshift radio galaxies. Ann. Rev. Astron. Astrophys. 31, 639.

McCarthy, P. J., et al., 1987. A correlation between the radio and optical morphologies of distant 3Cr radio galaxies. Astrophys. J. 321, L29–L33. doi:10.1086/185000.

McCourt, M., et al., 2012. Thermal instability in gravitationally stratified plasmas: implications for multiphase structure in clusters and galaxy haloes. Mon. Not. R. Astron. Soc. 419, 3319–3337. doi:10.1111/j.1365-2966.2011.19972.x, arXiv:1105.2563.

McDonald, M., et al., 2018. Revisiting the Cooling Flow Problem in Galaxies, Groups, and Clusters of Galaxies. Astrophys. J. 858, 45. doi:10.3847/1538-4357/aabace, arXiv:1803.04972.

McNamara, B. R., & Nulsen, P. E. J., 2007. Heating Hot Atmospheres with Active Galactic Nuclei. Annual Review of Astronomy and Astrophysics 45, 117–175. doi:10.1146/annurev.astro.45.051806.110625, arXiv:0709.2152.

McNamara, B. R., & Nulsen, P. E. J., 2012. Mechanical feedback from active galactic nuclei in galaxies, groups and clusters. New Journal of Physics 14, 055023. doi:10.1088/1367-2630/14/5/055023, arXiv:1204.0006.

McNamara, B. R., et al., 2014. A 10^{10} Solar Mass Flow of Molecular Gas in the A1835 Brightest Cluster Galaxy. The Astrophysical Journal 785, 44. doi:10.1088/0004-637X/785/1/44, arXiv:1309.0013.

McNamara, B. R., et al., 2016. A Mechanism for Stimulating AGN Feedback by Lifting Gas in Massive Galaxies. Astrophys. J. 830, 79. doi:10.3847/0004-637X/830/2/79, arXiv:1604.04629.

Meli, A., & Biermann, P. L., 2013. Active galactic nuclei jets and multiple oblique shock acceleration: starved spectra. Astron. Astrophys. 556, A88. doi:10.1051/0004-6361/201016299, arXiv:1207.4397.

Mendygral, P. J., Jones, T. W., & Dolag, K., 2012. MHD Simulations of Active Galactic Nucleus Jets in a Dynamic Galaxy Cluster Medium. Astrophys. J. 750, 166. doi:10.1088/0004-637X/750/2/166, arXiv:1203.2312.

Merloni, A., & Heinz, S., 2007. Measuring the kinetic power of active galactic nuclei in the radio mode. Mon. Not. R. Astron. Soc. 381, 589–601. doi:10.1111/j.1365-2966.2007.12253.x, arXiv:0707.3356.

Merloni, A., & Heinz, S., 2008. A synthesis model for AGN evolution: supermassive black holes growth and feedback modes. Mon. Not. R. Astron. Soc. 388, 1011–1030. doi:10.1111/j.1365-2966.2008.13472.x, arXiv:0805.2499.

Meyer, E. T., et al., 2015. Ruling out IC/CMB X-rays in PKS 0637-752 and the Implications for TeV Emission from Large-scale Quasar Jets. Astrophys. J. 805, 154. doi:10.1088/0004-637X/805/2/154, arXiv:1504.00577.

Mignone, A., et al., 2010. High-resolution 3D relativistic MHD simulations of jets. Mon. Not. R. Astron. Soc. 402, 7–12. doi:10.1111/j.1365-2966.2009.15642.x, arXiv:0908.4523.

Miley, G., & De Breuck, C., 2008. Distant radio galaxies and their environments. A&AR 15, 67–144. doi:10.1007/s00159-007-0008-z, arXiv:0802.2770.

Miley, G. K., & Perola, G. C., 1975. The Large Scale Radio Structure of NGC 1275. Astron. Astrophys. 45, 223.

Mingo, B., et al., 2019. Revisiting the Fanaroff-Riley dichotomy and radio-galaxy morphology with the LOFAR Two-Metre Sky Survey (LoTSS). Mon. Not. R. Astron. Soc. 488, 2701–2721. doi:10.1093/mnras/stz1901, arXiv:1907.03726.

Mingo, B., et al., 2014. An X-ray survey of the 2 Jy sample - I. Is there an accretion mode dichotomy in radio-loud AGN? Mon. Not. R. Astron. Soc. 440, 269–297. doi:10.1093/mnras/stu263, arXiv:1402.1770.

Mingo, B., et al., 2011. Markarian 6: Shocking the Environment of an Intermediate Seyfert. Astrophys. J. 731, 21. doi:10.1088/0004-637X/731/1/21, arXiv:1101.6000.

Mingo, B., et al., 2012. Shocks, Seyferts, and the Supernova Remnant Connection: A Chandra Observation of the Circinus Galaxy. Astrophys. J. 758, 95. doi:10.1088/0004-637X/758/2/95, arXiv:1209.0348.

Miraghaei, H., & Best, P. N., 2017. The nuclear properties and extended morphologies of powerful radio galaxies: the roles of host galaxy and environment. Mon. Not. R. Astron. Soc. 466, 4346–4363. doi:10.1093/mnras/stx007, arXiv:1701.00919.

Mocz, P., Fabian, A. C., & Blundell, K. M., 2011. Inverse-Compton ghosts and double-lobed radio sources in the X-ray sky. Mon. Not. R. Astron. Soc. 413, 1107–1120. doi:10.1111/j.1365-2966.2011.18198.x, arXiv:1008.2188.

Morganti, R., et al., 1988. Low luminosity radio galaxies: effects of gaseous environment. Astron. Astrophys. 189, 11.

Morganti, R., et al., 1999. Centaurus A: multiple outbursts or bursting bubble? Mon. Not. R. Astron. Soc. 307, 750.

Morganti, R., & Oosterloo, T., 2018. The interstellar and circumnuclear medium of active nuclei traced by H i 21 cm absorption. A&AR 26, 4. doi:10.1007/s00159-018-0109-x, arXiv:1807.01475.

Morganti, R., Oosterloo, T., & Tsvetanov, Z., 1998. A Radio Study of the Seyfert Galaxy IC 5063: Evidence for Fast Gas Outflow. Astron. J. 115, 915–927. doi:10.1086/300236, arXiv:astro-ph/9711285.

Mukherjee, D., et al., 2018. Relativistic jet feedback - III. Feedback on gas discs. Monthly Notices of the Royal Astronomical Society 479, 5544–5566. doi:10.1093/mnras/sty1776, arXiv:1803.08305.

Mulcahy, D. D., et al., 2016. Discovery of a low-luminosity spiral DRAGN. Astron. Astrophys. 595, L8. doi:10.1051/0004-6361/201629536, arXiv:1609.04820.

Mullin, L. M., & Hardcastle, M. J., 2009. Bayesian inference of jet speeds in radio galaxies. Mon. Not. R. Astron. Soc. 398, 1989.

Mullin, L. M., Hardcastle, M. J., & Riley, J. M., 2006. High-resolution observations of radio sources with $0.6 < z < 1.0$. Mon. Not. R. Astron. Soc. 372, 510.

Murgia, M., et al., 1999. Synchrotron spectra and ages of compact steep spectrum radio sources. Astron. Astrophys. 345, 769–777.

Murgia, M., et al., 2011. Dying radio galaxies in clusters. Astron. Astrophys. 526, A148. doi:10.1051/0004-6361/201015302, arXiv:1011.0567.

Myers, S. T., & Spangler, S. R., 1985. Synchrotron aging in the lobes of luminous radio galaxies. Astrophys. J. 291, 52.

Naab, T., & Ostriker, J. P., 2017. Theoretical Challenges in Galaxy Formation. Ann. Rev. Astron. Astrophys. 55, 59–109. doi:10.1146/annurev-astro-081913-040019, arXiv:1612.06891.

Nandi, S., & Saikia, D. J., 2012. Double-double radio galaxies from the FIRST survey. Bulletin of the Astronomical Society of India 40, 121–137. arXiv:1208.1941.

Nandra, K., et al., 2013. The Hot and Energetic Universe: A White Paper presenting the science theme motivating the Athena+ mission. arXiv e-prints , arXiv:1306.2307arXiv:1306.2307.

Narayan, R., & Yi, I., 1995. Advection-dominated Accretion: Underfed Black Holes and Neutron Stars. Astrophys. J. 452, 710. doi:10.1086/176343, arXiv:astro-ph/9411059.

Nath, B. B., 2010. Extended X-ray emission from radio galaxy co-

coons. Mon. Not. R. Astron. Soc. 407, 1998–2006. doi:10.1111/j.1365-2966.2010.17058.x, arXiv:1005.4189.

Nesvadba, N. P. H., et al., 2017. Gas kinematics in powerful radio galaxies at z 2: Energy supply from star formation, AGN, and radio jets⋆. Astron. Astrophys. 600, A121. doi:10.1051/0004-6361/201629357, arXiv:1610.01627.

Norman, M. L., et al., 1982. Structure and dynamics of supersonic jets. Astron. Astrophys. 113, 285–302.

Norris, R. P., et al., 2011. EMU: Evolutionary Map of the Universe. Publ. Astron. Soc. Australia 28, 215–248. doi:10.1071/AS11021, arXiv:1106.3219.

North, E. V., et al., 2019. WISDOM project - V. Resolving molecular gas in Keplerian rotation around the supermassive black hole in NGC 0383. Mon. Not. R. Astron. Soc. 490, 319–330. doi:10.1093/mnras/stz2598, arXiv:1909.05884.

Northover, K. J. E., 1973. The radio galaxy 3C 66. Mon. Not. R. Astron. Soc. 165, 369.

O'Dea, C. P., 1998. The Compact Steep-Spectrum and Gigahertz Peaked-Spectrum Radio Sources. Publ. Astron. Soc. Pacific 110, 493–532. doi:10.1086/316162.

O'Dea, C. P., & Baum, S. A., 1997. Constraints on Radio Source Evolution from the Compact Steep Spectrum and GHz Peaked Spectrum Radio Sources. Astron. J. 113, 148–161. doi:10.1086/118241.

O'Dea, C. P., et al., 2008. An Infrared Survey of Brightest Cluster Galaxies. II. Why are Some Brightest Cluster Galaxies Forming Stars? Astrophys. J. 681, 1035–1045. doi:10.1086/588212, arXiv:0803.1772.

O'Dea, C. P., et al., 2002. Hubble Space Telescope STIS Observations of the Kinematics of Emission-Line Nebulae in Three Compact Steep-Spectrum Radio Sources. Astron. J. 123, 2333.

O'Dea, C. P., & Owen, F. N., 1985. The global properties of a representative sample of 51 narrow-angle-tail radio sources in the directions of Abell clusters. Astron. J. 90, 954–972. doi:10.1086/113802.

Omma, H., & Binney, J., 2004. Structural stability of cooling flows. Mon. Not. R. Astron. Soc. 350, L13–L16. doi:10.1111/j.1365-2966.2004.07809.x, arXiv:arXiv:astro-ph/0312658.

O'Neill, S. M., et al., 2005. Three-dimensional Simulations of MHD Jet Propagation through Uniform and Stratified External Environments. Astrophys. J. 633, 717–732. doi:10.1086/491618, arXiv:arXiv:astro-ph/0507623.

Orienti, M., 2016. Radio properties of Compact Steep Spectrum and GHz-Peaked Spectrum radio sources. Astronomische Nachrichten 337, 9. doi:10.1002/asna.201512257, arXiv:1511.00436.

O'Sullivan, S. P., & Gabuzda, D. C., 2009. Magnetic field strength and spectral distribution of six parsec-scale active galactic nuclei jets. Mon. Not. R. Astron. Soc. 400, 26–42. doi:10.1111/j.1365-2966.2009.15428.x, arXiv:0907.5211.

O'Sullivan, S. P., et al., 2019. The intergalactic magnetic field probed by a giant radio galaxy. Astron. Astrophys. 622, A16. doi:10.1051/0004-6361/201833832, arXiv:1811.00932.

Owen, F. N., Eilek, J. A., & Kassim, N. E., 2000. M87 at 90 Centimeters: A Different Picture. Astrophys. J. 543, 611–619. doi:10.1086/317151, arXiv:astro-ph/0006150.

Owen, F. N., & Ledlow, M. J., 1997. A 20 Centimeter VLA Survey of Abell Clusters of Galaxies. VII. Detailed Radio Images. Astrophys. J. Suppl. 108, 41.

Owen, F. N., & Rudnick, L., 1976. Radio sources with wide-angle tails in Abell clusters of galaxies. Astrophys. J. 205, L1.

Owsianik, I., & Conway, J. E., 1998. First detection of hotspot advance in a Compact Symmetric Object. Evidence for a class of very young extragalactic radio sources. Astronomy and Astrophysics 337, 69–79. arXiv:astro-ph/9712062.

Pace, C., & Salim, S., 2014. Satellites of Radio AGN in SDSS: Insights into AGN Triggering and Feedback. Astrophys. J. 785, 66. doi:10.1088/0004-637X/785/1/66, arXiv:1403.0003.

Pacholczyk, A. G., 1970. Radio Astrophysics. Freeman, San Francisco.

Parma, P., et al., 2007. In search of dying radio sources in the local universe. Astron. Astrophys. 470, 875–888. doi:10.1051/0004-6361:20077592, arXiv:0705.3209.

Paterno-Mahler, R., et al., 2017. The High-redshift Clusters Occupied by Bent Radio AGN (COBRA) Survey: The Spitzer Catalog. Astrophys. J. 844, 78. doi:10.3847/1538-4357/aa7b89, arXiv:1611.00746.

Peng, C. Y., 2007. How Mergers May Affect the Mass Scaling Relation between Gravitationally Bound Systems. Astrophys. J. 671, 1098–1107. doi:10.1086/522774, arXiv:0704.1860.

Penrose, R., 1969. Gravitational Collapse: the Role of General Relativity. Nuovo Cimento Rivista Serie 1.

Perucho, M., et al., 2010. Stability of three-dimensional relativistic jets: implications for jet collimation. Astron. Astrophys. 519, A41. doi:10.1051/0004-6361/200913012, arXiv:1005.4332.

Peterson, J. R., et al., 2003. High-Resolution X-Ray Spectroscopic Constraints on Cooling-Flow Models for Clusters of Galaxies. The Astrophysical Journal 590, 207–224. doi:10.1086/374830, arXiv:astro-ph/0210662.

Pierce, J. C. S., et al., 2019. Do AGN triggering mechanisms vary with radio power? I. Optical morphologies of radio-intermediate HERGs. Mon. Not. R. Astron. Soc. , 1208doi:10.1093/mnras/stz1253, arXiv:1905.01315.

Pizzolato, F., & Soker, N., 2005. On the Nature of Feedback Heating in Cooling Flow Clusters. Astrophys. J. 632, 821–830. doi:10.1086/444344, arXiv:astro-ph/0407042.

Polatidis, A. G., & Conway, J. E., 2003. Proper Motions in Compact Symmetric Objects. Publications of the Astronomical Society of Australia 20, 69–74. doi:10.1071/AS02053, arXiv:astro-ph/0212122.

Prandoni, I., et al., 2010. Molecular disks in radio galaxies. The pathway to ALMA. Astron. Astrophys. 523, A38. doi:10.1051/0004-6361/201015456, arXiv:1009.0156.

Pratt, G. W., et al., 2009. Galaxy cluster X-ray luminosity scaling relations from a representative local sample (REXCESS). Astron. Astrophys. 498, 361–378. doi:10.1051/0004-6361/200810994, arXiv:0809.3784.

Prestage, R. M., & Peacock, J. A., 1988. The cluster environments of powerful radio galaxies. Mon. Not. R. Astron. Soc. 230, 131.

Pulido, F. A., et al., 2018. The Origin of Molecular Clouds in Central Galaxies. The Astrophysical Journal 853, 177. doi:10.3847/1538-4357/aaa54b, arXiv:1710.04664.

Punsly, B., & Zhang, S., 2011. The Jet Power and Emission-line Correlations of Radio-loud Optically Selected Quasars. Astrophys. J. 735, L3. doi:10.1088/2041-8205/735/1/L3, arXiv:1105.1543.

Raccanelli, A., et al., 2012. Cosmological measurements with forthcoming radio continuum surveys. Mon. Not. R. Astron. Soc. 424, 801–819. doi:10.1111/j.1365-2966.2012.20634.x, arXiv:1108.0930.

Ramos Almeida, C., et al., 2012. Are luminous radio-loud active galactic nuclei triggered by galaxy interactions? Mon. Not. R. Astron. Soc. 419, 687–705. doi:10.1111/j.1365-2966.2011.19731.x, arXiv:1109.0021.

Ramos Almeida, C., et al., 2011. Clear detection of dusty torus signatures in a weak-line radio galaxy: the case of PKS 0043-42. Mon. Not. R. Astron. Soc. 413, 2358–2364. doi:10.1111/j.1365-2966.2011.18309.x, arXiv:1101.1868.

Randall, S. W., et al., 2015. A Very Deep Chandra Observation of the Galaxy Group NGC 5813: AGN Shocks, Feedback, and Out-

burst History. The Astrophysical Journal 805, 112. doi:10.1088/0004-637X/805/2/112, arXiv:1503.08205.

Rawlings, S., et al., 1996. A study of 4C13.66 – the final identification and redshift for the revised sample. Mon. Not. R. Astron. Soc. 279, L13.

Rawlings, S., & Saunders, R., 1991. Evidence for a common central-engine mechanism in all radio sources. Nature 349, 138.

Rector, T. A., & Stocke, J. T., 2001. The Properties of the Radio-Selected 1 Jy Sample of BL Lacertae Objects. Astron. J. 122, 565–584. doi:10.1086/321179, arXiv:astro-ph/0105100.

Rees, M. J., et al., 1982. Ion-supported tori and the origin of radio jets. Nature 295, 17–21. doi:10.1038/295017a0.

Rieger, F., & Levinson, A., 2018. Radio Galaxies at VHE Energies. Galaxies 6, 116. doi:10.3390/galaxies6040116, arXiv:1810.05409.

Rigby, E. E., et al., 2011. Herschel-ATLAS: first data release of the Science Demonstration Phase source catalogues. Mon. Not. R. Astron. Soc. 415, 2336–2348. doi:10.1111/j.1365-2966.2011.18864.x, arXiv:1010.5787.

Risaliti, G., Elvis, M., & Nicastro, F., 2002. Ubiquitous Variability of X-Ray-absorbing Column Densities in Seyfert 2 Galaxies. Astrophys. J. 571, 234–246. doi:10.1086/324146, arXiv:astro-ph/0107510.

Robitaille, T., & Bressert, E., 2012. APLpy: Astronomical Plotting Library in Python. Astrophysics Source Code Library. arXiv:1208.017.

Rosas-Guevara, Y., et al., 2016. Supermassive black holes in the EAGLE Universe. Revealing the observables of their growth. Mon. Not. R. Astron. Soc. 462, 190–205. doi:10.1093/mnras/stw1679, arXiv:1604.00020.

Rose, T., et al., 2019. Constraining cold accretion on to supermassive black holes: molecular gas in the cores of eight brightest cluster galaxies revealed by joint CO and CN absorption. Mon. Not. R. Astron. Soc. 489, 349–365. doi:10.1093/mnras/stz2138, arXiv:1907.13526.

Rossi, P., et al., 2008. Formation of dynamical structures in relativistic jets: the FRI case. Astron. Astrophys. 488, 795–806. doi:10.1051/0004-6361:200809687, arXiv:0806.1648.

Ruffa, I., et al., 2019. The AGN fuelling/feedback cycle in nearby radio galaxies I. ALMA observations and early results. Mon. Not. R. Astron. Soc. 484, 4239–4259. doi:10.1093/mnras/stz255, arXiv:1901.07513.

Rupke, D. S. N., & Veilleux, S., 2011. Integral Field Spectroscopy of Massive, Kiloparsec-scale Outflows in the Infrared-luminous QSO Mrk 231. The Astrophysical Journal 729, L27. doi:10.1088/2041-8205/729/2/L27, arXiv:1102.4349.

Russell, H. R., et al., 2014. Massive Molecular Gas Flows in the A1664 Brightest Cluster Galaxy. The Astrophysical Journal 784, 78. doi:10.1088/0004-637X/784/1/78, arXiv:1309.0014.

Russell, H. R., et al., 2017. Close entrainment of massive molecular gas flows by radio bubbles in the central galaxy of Abell 1795. Monthly Notices of the Royal Astronomical Society 472, 4024–4037. doi:10.1093/mnras/stx2255, arXiv:1708.08935.

Russell, H. R., et al., 2016. ALMA observations of cold molecular gas filaments trailing rising radio bubbles in PKS 0745-191. Monthly Notices of the Royal Astronomical Society 458, 3134–3149. doi:10.1093/mnras/stw409, arXiv:1602.05962.

Rybicki, G. B., & Lightman, A. P., 1979. Radiative processes in astrophysics. Wiley, New York.

Ryle, M., 1952. A New Radio Interferometer and Its Application to the Observation of Weak Radio Stars. Proceedings of the Royal Society of London Series A 211, 351–375. doi:10.1098/rspa.1952.0047.

Sabater, J., et al., 2019. The LoTSS view of radio AGN in the local Universe. The most massive galaxies are always switched on. Astron. Astrophys. 622, A17. doi:10.1051/0004-6361/201833883, arXiv:1811.05528.

Sabater, J., Best, P. N., & Heckman, T. M., 2015. Triggering optical AGN: the need for cold gas, and the indirect roles of galaxy environment and interactions. Mon. Not. R. Astron. Soc. 447, 110–116. doi:10.1093/mnras/stu2429, arXiv:1411.5031.

Sadler, E. M., et al., 2014. The local radio-galaxy population at 20 GHz. Mon. Not. R. Astron. Soc. 438, 796–824. doi:10.1093/mnras/stt2239, arXiv:1304.0268.

Sakelliou, I., et al., 2002. High resolution soft X-ray spectroscopy of M 87 with the reflection grating spectrometers on XMM-Newton. Astronomy and Astrophysics 391, 903–909. doi:10.1051/0004-6361:20020900, arXiv:astro-ph/0206249.

Sanders, J. S., & Fabian, A. C., 2008. Sound waves in the intra-cluster medium of the Centaurus cluster. Mon. Not. R. Astron. Soc. 390, L93–L97. doi:10.1111/j.1745-3933.2008.00549.x, arXiv:0808.2384.

Saripalli, L., et al., 2012. ATLBS Extended Source Sample: The Evolution in Radio Source Morphology with Flux Density. Astrophys. J. Suppl. 199, 27. doi:10.1088/0067-0049/199/2/27, arXiv:1202.4516.

Saxena, A., et al., 2018. Discovery of a radio galaxy at z = 5.72. Mon. Not. R. Astron. Soc. 480, 2733–2742. doi:10.1093/mnras/sty1996, arXiv:1806.01191.

Schaye, J., et al., 2015. The EAGLE project: simulating the evolution and assembly of galaxies and their environments. Mon. Not. R. Astron. Soc. 446, 521–554. doi:10.1093/mnras/stu2058, arXiv:1407.7040.

Scheuer, P. A. G., 1974. Models of extragalactic radio sources with a continuous energy supply from a central object. Mon. Not. R. Astron. Soc. 166, 513.

Scheuer, P. A. G., 1995. Lobe asymmetry and the expansion speeds of radio sources. Mon. Not. R. Astron. Soc. 277, 331.

Schmidt, M., 1963. . Nature 197, 1040.

Schmidt, M., 1968. Space Distribution and Luminosity Functions of Quasi-Stellar Radio Sources. Astrophys. J. 151, 393. doi:10.1086/149446.

Schoenmakers, A. P., et al., 2000. Radio galaxies with a 'double-double morphology' - I. Analysis of the radio properties and evidence for interrupted activity in active galactic nuclei. Mon. Not. R. Astron. Soc. 315, 371–380. doi:10.1046/j.1365-8711.2000.03430.x, arXiv:arXiv:astro-ph/9912141.

Schwartz, D. A., et al., 2000. Chandra Discovery of a 100 kiloparsec X-Ray Jet in PKS 0637-752. Astrophys. J. 540, L69.

Seymour, N., et al., 2012. Rapid Coeval Black Hole and Host Galaxy Growth in MRC 1138-262: The Hungry Spider. Astrophys. J. 755, 146. doi:10.1088/0004-637X/755/2/146, arXiv:1206.5821.

Shabala, S. S., 2018. The role of environment in the observed Fundamental Plane of radio active galactic nuclei. Mon. Not. R. Astron. Soc. 478, 5074–5080. doi:10.1093/mnras/sty1328, arXiv:1805.06600.

Sharma, P., et al., 2012. Thermal instability and the feedback regulation of hot haloes in clusters, groups and galaxies. Mon. Not. R. Astron. Soc. 420, 3174–3194. doi:10.1111/j.1365-2966.2011.20246.x, arXiv:1106.4816.

Shimwell, T. W., et al., 2017. The LOFAR Two-metre Sky Survey. I. Survey description and preliminary data release. Astron. Astrophys. 598, A104. doi:10.1051/0004-6361/201629313, arXiv:1611.02700.

Short, C. J., et al., 2010. The evolution of galaxy cluster X-ray scaling relations. Mon. Not. R. Astron. Soc. 408, 2213–2233. doi:10.1111/j.1365-2966.2010.17267.x, arXiv:1002.4539.

Silk, J., & Rees, M. J., 1998. Quasars and galaxy formation. Astron. Astrophys. 331, L1–L4. arXiv:astro-ph/9801013.

Singal, A. K., & Rajpurohit, K., 2014. Fanaroff-Riley dichotomy of radio galaxies and the Malmquist bias. Mon. Not. R. Astron. Soc. 442, 1656–1660. doi:10.1093/mnras/stu986, arXiv:1405.3828.

Smolčić, V., et al., 2017. The VLA-COSMOS 3 GHz Large Project: Multiwavelength counterparts and the composition of the faint radio population. Astron. Astrophys. 602, A2. doi:10.1051/0004-6361/201630223, arXiv:1703.09719.

Smolčić, V., et al., 2009. The Dust-Unbiased Cosmic Star-Formation History from the 20 CM VLA-COSMOS Survey. Astrophys. J. 690, 610–618. doi:10.1088/0004-637X/690/1/610, arXiv:0808.0493.

Snios, B., et al., 2018. The Cocoon Shocks of Cygnus A: Pressures and Their Implications for the Jets and Lobes. Astrophys. J. 855, 71. doi:10.3847/1538-4357/aaaf1a, arXiv:1802.10106.

Sobolewska, M., et al., 2019. The Impact of the Environment on the Early Stages of Radio Source Evolution. Astrophys. J. 871, 71. doi:10.3847/1538-4357/aaee78, arXiv:1812.02147.

Somerville, R. S., & Davé, R., 2015. Physical Models of Galaxy Formation in a Cosmological Framework. Ann. Rev. Astron. Astrophys. 53, 51–113. doi:10.1146/annurev-astro-082812-140951, arXiv:1412.2712.

Stawarz, Ł., et al., 2004. On Multiwavelength Emission of Large-Scale Quasar Jets. Astrophys. J. 608, 95.

Steinhardt, C. L., & Elvis, M., 2010. The quasar mass-luminosity plane - I. A sub-Eddington limit for quasars. Mon. Not. R. Astron. Soc. 402, 2637–2648. doi:10.1111/j.1365-2966.2009.16084.x, arXiv:0911.1355.

Strateva, I., et al., 2001. Color Separation of Galaxy Types in the Sloan Digital Sky Survey Imaging Data. Astron. J. 122, 1861–1874. doi:10.1086/323301, arXiv:astro-ph/0107201.

Sun, M., et al., 2011. The Pressure Profiles of Hot Gas in Local Galaxy Groups. Astrophys. J. 727, L49. doi:10.1088/2041-8205/727/2/L49, arXiv:1012.0312.

Sutherland, R. S., & Bicknell, G. V., 2007. Interactions of a Light Hypersonic Jet with a Nonuniform Interstellar Medium. Astrophys. J. Suppl. 173, 37–69. doi:10.1086/520640, arXiv:0707.3668.

Swain, M. R., Bridle, A. H., & Baum, S. A., 1998. Internal Structure of the Jets in 3C 353. Astrophys. J. 507, L29–L33. doi:10.1086/311663.

Tadhunter, C., 2016. Radio AGN in the local universe: unification, triggering and evolution. A&AR 24, 10. doi:10.1007/s00159-016-0094-x, arXiv:1605.08773.

Tadhunter, C. N., 1991. High-velocity gas in powerful radio galaxies. Mon. Not. R. Astron. Soc. 251, 46P. doi:10.1093/mnras/251.1.46P.

Tasse, C., et al., 2008. Radio-loud AGN in the XMM-LSS field. II. A dichotomy on environment and accretion mode? Astron. Astrophys. 490, 893.

Tavecchio, F., et al., 2000. The X-Ray jet of PKS 0637-752: inverse Compton radiation from the cosmic microwave background? Astrophys. J. 544, L23.

Taylor, A. M., 2014. UHECR composition models. Astroparticle Physics 54, 48–53. doi:10.1016/j.astropartphys.2013.11.006, arXiv:1401.0199.

Taylor, G. B., & Perley, R. A., 1993. Magnetic Fields in the Hydra A Cluster. Astrophys. J. 416, 554. doi:10.1086/173257.

Taylor, G. B., et al., 1990. VLA observations of the radio galaxy Hydra A (3C218). Astrophys. J. 360, 41.

Tchekhovskoy, A., & Bromberg, O., 2016. Three-dimensional relativistic MHD simulations of active galactic nuclei jets: magnetic kink instability and Fanaroff-Riley dichotomy. Mon. Not. R. Astron. Soc. 461, L46–L50. doi:10.1093/mnrasl/slw064, arXiv:1512.04526.

Tchekhovskoy, A., Narayan, R., & McKinney, J. C., 2011. Efficient generation of jets from magnetically arrested accretion on a rapidly spinning black hole. Mon. Not. R. Astron. Soc. 418, L79–L83. doi:10.1111/j.1745-3933.2011.01147.x, arXiv:1108.0412.

Terrazas, B. A., et al., 2019. The relationship between black hole mass and galaxy properties: Examining the black hole feedback model in IllustrisTNG. arXiv e-prints , arXiv:1906.02747 arXiv:1906.02747.

Tregillis, I. L., Jones, T. W., & Ryu, D., 2001. Simulating Electron Transport and Synchrotron Emission in Radio Galaxies: Shock Acceleration and Synchrotron Aging in Three-dimensional Flows. Astrophys. J. 557, 475.

Tregillis, I. L., Jones, T. W., & Ryu, D., 2004. Synthetic Observations of Simulated Radio Galaxies. I. Radio and X-Ray Analysis. Astrophys. J. 601, 778–797. doi:10.1086/380756, arXiv:astro-ph/0310719.

Tremblay, G. R., et al., 2018. A Galaxy-scale Fountain of Cold Molecular Gas Pumped by a Black Hole. Astrophys. J. 865, 13. doi:10.3847/1538-4357/aad6dd, arXiv:1808.00473.

Turner, R. J., et al., 2018. RAiSE II: resolved spectral evolution in radio AGN. Mon. Not. R. Astron. Soc. 473, 4179–4196. doi:10.1093/mnras/stx2591, arXiv:1710.01078.

Turner, R. J., & Shabala, S. S., 2015. Energetics and Lifetimes of Local Radio Active Galactic Nuclei. Astrophys. J. 806, 59. doi:10.1088/0004-637X/806/1/59, arXiv:1504.05204.

Urry, C. M., & Padovani, P., 1995. Unified schemes for radio-loud active galactic nuclei. Publ. Astron. Soc. Pacific 107, 803.

Urry, C. M., Padovani, P., & Stickel, M., 1991. FRI galaxies as the parent population of BL Lac objects. III: radio constraints. Astrophys. J. 382, 501.

Vaidya, B., et al., 2018. A Particle Module for the PLUTO Code. II. Hybrid Framework for Modeling Nonthermal Emission from Relativistic Magnetized Flows. The Astrophysical Journal 865, 144. doi:10.3847/1538-4357/aadd17, arXiv:1808.08960.

van Breugel, W., Miley, G., & Heckman, T., 1984. Studies of kiloparsec-scale, steep-spectrum radio cores. I. VLA maps. Astron. J. 89, 5–22. doi:10.1086/113480.

van Weeren, R. J., et al., 2017. The case for electron re-acceleration at galaxy cluster shocks. Nature Astronomy 1, 0005. doi:10.1038/s41550-016-0005, arXiv:1701.01439.

van Weeren, R. J., et al., 2011. Using double radio relics to constrain galaxy cluster mergers: a model of double radio relics in CIZA J2242.8+5301. Mon. Not. R. Astron. Soc. 418, 230–243. doi:10.1111/j.1365-2966.2011.19478.x, arXiv:1108.1398.

van Weeren, R. J., et al., 2019. Diffuse Radio Emission from Galaxy Clusters. Sp. Science Reviews 215, 16. doi:10.1007/s11214-019-0584-z, arXiv:1901.04496.

Venemans, B. P., et al., 2007. Protoclusters associated with z > 2 radio galaxies . I. Characteristics of high redshift protoclusters. Astron. Astrophys. 461, 823–845. doi:10.1051/0004-6361:20053941, arXiv:astro-ph/0610567.

Vermeulen, R. C., et al., 1995. When Is BL Lac Not a BL Lac? Astrophys. J. 452, L5.

Vogelsberger, M., et al., 2014. Introducing the Illustris Project: simulating the coevolution of dark and visible matter in the Universe. Mon. Not. R. Astron. Soc. 444, 1518–1547. doi:10.1093/mnras/stu1536, arXiv:1405.2921.

Voit, G. M., et al., 2015. Regulation of star formation in giant galaxies by precipitation, feedback and conduction. Nature 519, 203–206. doi:10.1038/nature14167, arXiv:1409.1598.

Voit, G. M., et al., 2018. A General Precipitation-limited L_X-T-R Relation among Early-type Galaxies. The Astrophysical Journal 853, 78. doi:10.3847/1538-4357/aaa084, arXiv:1708.02189.

Wardle, J. F. C., & Aaron, S. E., 1997. How fast are the large-scale jets in quasars? Constraints on both Doppler beaming and intrinsic

asymmetries. Mon. Not. R. Astron. Soc. 286, 425.

Weinberger, R., et al., 2018. Supermassive black holes and their feedback effects in the IllustrisTNG simulation. Mon. Not. R. Astron. Soc. 479, 4056–4072. doi:10.1093/mnras/sty1733, arXiv:1710.04659.

Wen, Z. L., Han, J. L., & Liu, F. S., 2012. A Catalog of 132,684 Clusters of Galaxies Identified from Sloan Digital Sky Survey III. Astrophys. J. Suppl. 199, 34. doi:10.1088/0067-0049/199/2/34, arXiv:1202.6424.

Werner, N., et al., 2019. Hot Atmospheres, Cold Gas, AGN Feedback and the Evolution of Early Type Galaxies: A Topical Perspective. Space Science Reviews 215, 5. doi:10.1007/s11214-018-0571-9, arXiv:1811.05004.

Whysong, D., & Antonucci, R., 2004. A Hidden Nucleus in Cygnus A, but Not in M87. Astrophys. J. 602, 116.

Williams, A. G., & Gull, S. F., 1985. Multiple hotspots in extragalactic radio sources. Nature 313, 34.

Williams, D. R. A., et al., 2017. Radio jets in NGC 4151: where eMERLIN meets HST. Mon. Not. R. Astron. Soc. 472, 3842–3853. doi:10.1093/mnras/stx2205, arXiv:1708.07011.

Williams, W. L., et al., 2018. LOFAR-Boötes: properties of high- and low-excitation radio galaxies at 0.5 < z < 2.0. Mon. Not. R. Astron. Soc. 475, 3429–3452. doi:10.1093/mnras/sty026, arXiv:1711.10504.

Williams, W. L., & Röttgering, H. J. A., 2015. Radio-AGN feedback: when the little ones were monsters. Mon. Not. R. Astron. Soc. 450, 1538–1545. doi:10.1093/mnras/stv692, arXiv:1503.08927.

Willott, C. J., et al., 1999. The emission line-radio correlation for radio sources using the 7C Redshift Survey. Mon. Not. R. Astron. Soc. 309, 1017.

Wilson, A. S., Young, A. J., & Shopbell, P. L., 2001. Chandra X-ray observations of Pictor A: high energy cosmic rays in a radio galaxy. Astrophys. J. 547, 740.

Wing, J. D., & Blanton, E. L., 2011. Galaxy Cluster Environments of Radio Sources. Astron. J. 141, 88. doi:10.1088/0004-6256/141/3/88, arXiv:1008.1099.

Worrall, D. M., 2009. The X-ray jets of active galaxies. A&AR 17, 1–46. doi:10.1007/s00159-009-0016-7, arXiv:0812.3401.

Worrall, D. M., & Birkinshaw, M., 2000. X-ray-emitting Atmospheres of B2 Radio Galaxies. Astrophys. J. 530, 719.

Worrall, D. M., Birkinshaw, M., & Cameron, R. A., 1995. The X-ray environment of the dumbbell radio galaxy NGC 326. Astrophys. J. 449, 93.

Wykes, S., et al., 2015. Internal entrainment and the origin of jet-related broad-band emission in Centaurus A. Mon. Not. R. Astron. Soc. 447, 1001–1013. doi:10.1093/mnras/stu2440, arXiv:1409.5785.

Wylezalek, D., et al., 2013. Galaxy Clusters around Radio-loud Active Galactic Nuclei at 1.3 < z < 3.2 as Seen by Spitzer. Astrophys. J. 769, 79. doi:10.1088/0004-637X/769/1/79, arXiv:1304.0770.

Xu, H., et al., 2010. Evolution and Distribution of Magnetic Fields from Active Galactic Nuclei in Galaxy Clusters. I. The Effect of Injection Energy and Redshift. Astrophys. J. 725, 2152–2165. doi:10.1088/0004-637X/725/2/2152, arXiv:1011.0030.

Xu, H., et al., 2011. Evolution and Distribution of Magnetic Fields from Active Galactic Nuclei in Galaxy Clusters. II. The Effects of Cluster Size and Dynamical State. Astrophys. J. 739, 77. doi:10.1088/0004-637X/739/2/77, arXiv:1107.2599.

Zamaninasab, M., et al., 2014. Dynamically important magnetic fields near accreting supermassive black holes. Nature 510, 126–128. doi:10.1038/nature13399.

Zanni, C., et al., 2003. X-ray emission from expanding cocoons. Astron. Astrophys. 402, 949–962. doi:10.1051/0004-6361:20030302, arXiv:arXiv:astro-ph/0302275.

Zirbel, E. L., & Baum, S. A., 1995. On the FRI/FRII dichotomy in powerful radio sources – analysis of their emission-line and radio luminosities. Astrophys. J. 448, 521.